University of Southern Indiana
Pott College of Science, Engineering, and Education
Engineering Department
8600 University Boulevard
Evansville, Indiana 47712

Design and Fabrication of a Miniature Turbojet Engine and Test Bench

Jeremiah Bissey
Seth Cooper
Teddy Lashley
Mason Moore
Carson Tipton

ENGR 491 - Senior Design
Spring 2024

Approved by: Julian L. Davis 4/26/2024
Faculty Advisor: Dr. Julain Davis Date

Approved by: _____
Department Chair: Dr. Paul Kuban Date

ACKNOWLEDGEMENTS

The miniature turbojet team would like to express significant gratitude to the following people. Without them, the completion of the project would not be possible.

Dr. Brandon Field

Dr. Glen Kissel

Dr. Julian Davis

Dr. Paul Kuban

Dr. Todd Nelson

Endeavor Committee

Hanno de Coning

Jamie Curry

Justin Amos

Leo Osborne

Mariah Fulton

Meg Wagner

Abstract

Since the beginning of powered aviation, engineers have strived to enhance aircraft propulsion methods for increased efficiency and power. Traditional piston-driven, gas turbine, and electric motor engines have been the primary focus. A pivotal metric for assessing engine performance is the thrust-to-weight ratio, signifying the force generated per unit of weight. Elevated thrust-to-weight ratios yield manifold benefits to aircraft, surrounding improved climb rates, enhanced maneuverability, elevated top speeds, and extended flight times due to weight savings. Such advancements are desirable across various aviation domains, spanning military operations to hobbyist radio-controlled scale models. This study endeavors to design and fabricate a miniature turbojet engine inspired by existing models utilized in miniature radio-controlled aircraft to facilitate advanced research on various engine components. The resultant insights gathered from this miniature model are poised to serve as proof of concepts for larger-scale engines. Drawing insights from prior projects and market analyses, meticulous technical specifications were devised to ensure the competitiveness of the team's engine. Preliminary design calculations laid the foundation for the critical design phase, meticulously addressing each component. The design shows that the engine will produce 1150 N while weighing 120 N, which creates a thrust-to-weight ratio of 9.6:1. This meets the technical requirements of the team set of 1000 N and a weight of 130 N. All other technical requirements were also met by the design. The engine has yet to be test-fired but was successfully manufactured and assembled.

TABLE OF CONTENTS

INTRODUCTION 1

1 Objective and Deliverables 2

2 Identification of Subsystems 2

2.1 Compression Stage (0-3) 4

2.2 Combustion Stage (3-4) 4

2.3 Turbine Stage (4-5) 4

2.4 Exhaust Stage (5-0) 5

2.5 Electronic Control Unit 5

2.6 Test Bench 5

DESIGN 6

1 Past Projects 6

1.1 Sri Ramakrishna Engineering College 6

1.2 Universidade Da Beira Interior 6

1.3 Uppsala Universitet 7

2 Technical Requirements 8

3 Preliminary Calculations 8

3.1 Thrust Equations 8

3.2 Engine State-Points 9

4 Conceptual Design 10

4.1 Compression Design 10

4.1.1 Axial Compressor 10

4.1.2 Centrifugal Compressor 10

4.1.3 Multi-Stage Compression 11

4.1.4 Single-Stage Compression 12

4.2 Fuel System Design 12
4.3 Shaft Securing Method Design 14
4.4 Casing Material Selection 15
4.5 Turbine Thermal Barrier Coating 15
5 Critical Design 15
5.1 Compressor 16
5.2 Diffuser 17
5.3 Combustor 18
5.4 Fuel and Ignition System 26
5.5 Stator and Turbine 28
5.5.1 Thermal Barrier 29
5.6 Shaft 30
5.7 Casing 37
5.8 Nozzle 38
5.9 Electronic Control Unit 39
5.10 Test Bench 40
6 Fabrication 45
6.1 Diffuser 45
6.2 Combustor 48
6.3 Fuel and Ignition System 51
6.4 Stator and Turbine 51
6.5 Shaft 54
6.6 Casing 55
6.7 Nozzle 56
6.8 Electronic Control Unit 58

6.9 Test Bench 58
RESULTS 60
1 Testing and Results 60
2 Budget and Disposal Plan 61
3 Lessons Learn and Future Work 61
4 Conclusion 62
REFERENCES 64
APPENDIX 66
Appendix A – System Hierarchy 67
Appendix B – Proposed Schedule 70
Appendix C – Actual Schedule 71
Appendix D – Budget 72
Appendix E– Design Mass Table 76
Appendix F – Concept of Operations 77
Appendix G – FMEA's 78
Appendix H – Mechanical Block Diagram 80
Appendix I– Standards 81
Appendix J- ABET Outcome 2, Design Factor Considerations 82
Appendix K- Technical Drawings 83

List of Figures

Figure 1. Final cross-section rendering 1
Figure 2. Completed fabrication and assembly of the turbojet engine 2
Figure 3. General turbojet engine [7] 3
Figure 4. Ideal Brayton Cycle T-s Diagram for gas turbine engines [12] 3
Figure 5. Ideal Brayton Cycle p-V Diagram for gas turbine engines [12] 4
Figure 6. Universidade Da Beira Interor's 3-D engine [18] 7
Figure 7. Mass flow relation to thrust with multiple velocities 9
Figure 8. Cross-sectional view of axial compressor. Air flows from left to right, denoted by the blue arrows. Denoted by the green arrow are the rotor blades and in orange are the stator blades [3] 10
Figure 9. A centrifugal compressor. Air flow is marked with blue arrows. Note that the air flows tangentially compared to an axial compressor [3] 11
Figure 10. Maximizing net-work-output (red circle) vs single stage compression (blue circle) .. 12
Figure 11. Example of a keyway fit on a shaft 14
Figure 12. Example of an interference fit called a bonded shrink fit that uses heat [19] 14
Figure 13. 3D rendering of Holset Hx82 152mm compressor wheel 16
Figure 14. Holset Hx82 compressor wheel mass flow vs thrust production 17
Figure 15. Diffuser 3D rendering 18
Figure 16. The three most-commonly used combustor configuration types. The orange represents the combustion chamber(s) and the red represents the pressure vessel(s) [11] 19
Figure 17. Pressure loss graph for varying divergence angles [3] 21
Figure 18. A faired diffuser that has a plenum chamber on the front face of the combustor [3] . 21
Figure 19. A dump diffuser that includes a prediffuser before "dumping" the air into the combustion chamber's annulus [3] 22
Figure 20. A vortex-controlled diffuser where stream 'a' is part of the boundary layer of airflow that gets “bleeded-off” while stream ‘b’ is directed towards the combustor [3] 22
Figure 21. A graph that helps to increase a diffusers efficiency by picking a value for nondimensional length or area ratio [3] 24

Figure 22. Final rendering of the combustor using all geometric values listed above 26
Figure 23. Completed fuel ring design 27
Figure 24. ANSYS fluid domain for stator and turbine prior to simulation 28
Figure 25. ANSYS velocity results for stator and turbine flow 29
Figure 26. Shaft diagram with component sections labeled 30
Figure 27. Shaft with threaded ends 31
Figure 28. Cross-section view of angular contact bearing selected 33
Figure 29. MATLAB graphical results. Please note the units are in inches for the axis's that are unmarked 35
Figure 30. MATLAB moment graph result 35
Figure 31. Engine casing 38
Figure 32. Completed test bench foundation. Please note the rubber casters and polycarbonate shielding are not shown here 41
Figure 33. Linear guide rail system 42
Figure 34. Turbojet engine harness with threaded rods connecting the plate to the clamshell mounts 42
Figure 35. Load cell fixture 43
Figure 36. Displacement Graph of Load Cell Interface 44
Figure 37. Diffuser Facing and Profiling on the lathe 46
Figure 38. Diffuser wedge milling with 3-axis capabilities 46
Figure 39. Diffuser guide vane milling with indexer capabilities 47
Figure 40. Diffuser after milling 48
Figure 41. Special rolling technique used for rolling all parts 49
Figure 42. Rolled combustion components 49
Figure 43. Welding internal combustor components 50
Figure 44. Internal combustor components (left) external components (right) 50
Figure 45. Final combustor assembly 51
Figure 46. Stator being pocketed with the 3-axis mill 52
Figure 47. Fixture used to attach stator and turbine to indexer 53

Figure 48. Final stator and turbine as they will be assembled on shaft 53
Figure 49. First shaft on the lathe 54
Figure 50. Completed first shaft 55
Figure 51. 3D printed casing (in dark blue) 56
Figure 52. Completed casing on turbojet engine 56
Figure 53. Completed nozzle fabrication 57
Figure 54. Bolt configuration to attach the nozzle 57
Figure 55. Completed ECU setup 58
Figure 56. Fabricated test bench 59
Figure 57. Completed jet harness 60
Figure 58. Turbojet engine concept of operations 77
Figure 59. Mechanical block diagram of turbojet engine with components labeled 80

List of Tables

Table 1. Technical Requirements 8

Table 2. Characteristics for potential fuel sources [3] 13

Table 3. Key performance characteristics for the different types of combustor configurations. red, yellow, and green represent bad, average, and good respectively. 20

Table 4. Interference fit results for the compressor and turbine sections 31

Table 5. Bearing characteristics needed versus selected bearing. The data for the D6001/604/266C was supplied by an industrial engineer at Boca Bearings and confirmed on their website 32

Table 6. Bearing interference fit results 34

Table 7. MATLAB code inputs. The values appear from left to right for the shaft, compressor to turbine end 34

Table 8. Slopes of shafts for typical bearings 36

Table 9. Excel sheet results for shaft shoulder at 14.08 inches from the front end of the shaft ... 37

Table 10. Comparable miniature turbojet engine characteristics 61

Table 11. Proposed schedule for fall 2023 and spring 2024 semesters 70

Table 12. Actual schedule of spring 2024 semester 71

Table 13. Total budget for turbojet project 72

Table 14. Masses for each component based on SolidWorks models 76

Table 15. Turbojet FMEA 78

Table 16. Customer FMEA 79

Table 17. OSHA decibel standards (Table G-16) 81

Table 18. ABET design factor considerations 82

List of Symbols

Symbol	Description	Units
η_{th}	Thermal Efficiency	*Unitless*
ρ	Density	$\frac{kg}{m^3}$
$\dot{m}$	Mass flow	$\frac{kg}{s}$
A	Area	m^2
v	Velocity	$\frac{m}{s}$
C_{pr}	Compression Ratio	*Unitless*
γ	Specific Heat Ratio	*Unitless*
T	Temperature	*Degrees Celsius, °C*
η_{comp}	Compressor Efficiency	*Unitless*
T_r	Thrust	$Newtons, \frac{kg\ m}{s^2}$
R	Molar Gas Constant	$\frac{J}{mol\ K}$
P	Pressure	$Pascals, \frac{N}{m^2}$
V_m	Molar Volume	*Unitless*
MW	Molecular Weight	$\frac{g}{mol}$
η	Number of Elements	*Unitless*
f_{stoich}	Stoichiometric Ratio	*Unitless*
$\dot{W}$	Power	$Watts, \frac{kg\ m^2}{s^3}$

Design and Fabrication of a Miniature Turbojet Engine and Test Bench

INTRODUCTION

Since the beginning of powered aviation, engineers have been working to create and improve propulsion methods for aircraft. Piston-driven, gas turbine, and electric motor engines are the most common propulsion methods. There is a desire for these engines to become more efficient and powerful. A common specification for measuring engine performance is the thrust-to-weight ratio, the amount of force produced per unit of weight. When this criterion is large, the equipped aircraft benefits in many areas: climb rates increase, maneuverability improves, top speed increases, and flight time increases from weight savings. These improved aircraft aspects are highly desired in any form of aviation from military operation to hobbyist radio-controlled scale models. For this reason, the team is designing and fabricating a miniature turbojet engine. This engine will enable further research projects on various components within the engine. Successful research can then be taken from this miniature model and used as a proof of concept for larger engines. The engine will be sized based on engines that are currently being sold for miniature radio-controlled aircraft. A final rendering of the team's completed engine design is shown in Figure 1, and the completed fabrication is shown in Figure 2.

In this section, the objective and deliverables for the project are discussed. Additionally, the general gas turbine engine is described to gain insight into the thermodynamic cycle of the engine, as well as the electronics and stationary structure the engine needs to run.

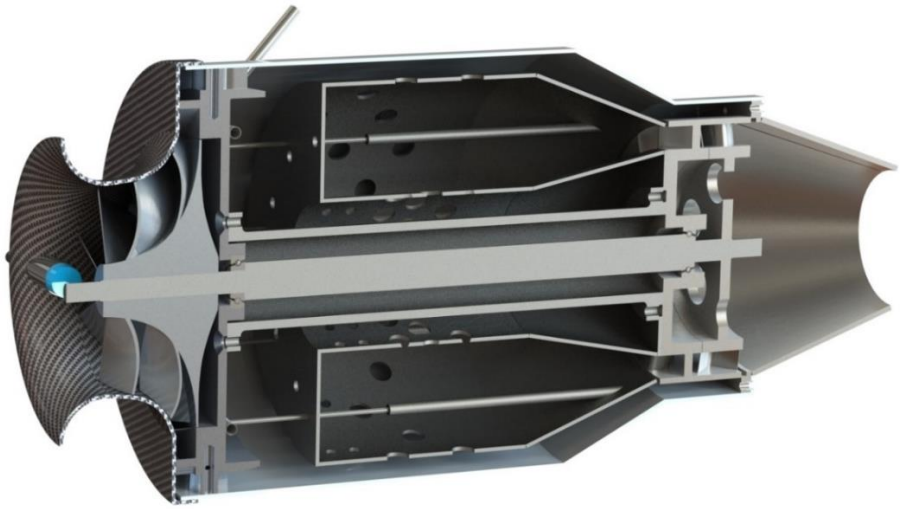

Figure 1. Final cross-section rendering

Figure 2. Completed fabrication and assembly of the turbojet engine

1 Objective and Deliverables

The objective of this project is to design and fabricate a custom test bench and miniature turbojet engine that maximizes thrust-to-weight ratio.

The deliverables for this project are the following:

- Report, presentation, and poster
- Prototyped miniature turbojet engine and test bench
- 3-dimensional models and dimension drawings for components
- Not developing an engine for mass production
- Not developing a flight-ready engine

2 Identification of Subsystems

There are many configurations of the gas turbine engine, but a typical setup is shown in Figure 3. Generally, all configurations operate using the same thermodynamic principles, in which the “Ideal Brayton Cycle” is known to closely model the gas turbine engine. The Ideal Brayton Cycle is known to have four processes, as shown in Figures 4 and 5, an isentropic compression process (0-3), a constant-pressure process (3-4) heat addition, an isentropic

expansion process (4-8), and a constant-pressure heat rejection process (8-0). For simplification purposes, the team renamed these processes into stages, the compression stage (0-3), the combustion stage (3-4), the turbine stage (4-5), and the exhaust stage (5-0) [12]. Each of these stages must work concurrently to produce the desired product which is thrust.

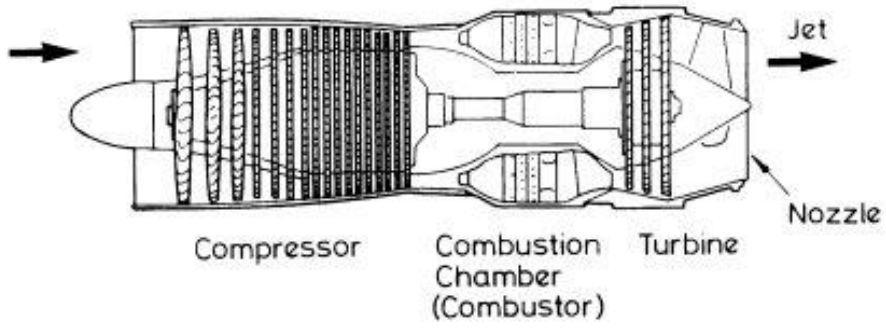

Figure 3. General turbojet engine [7]

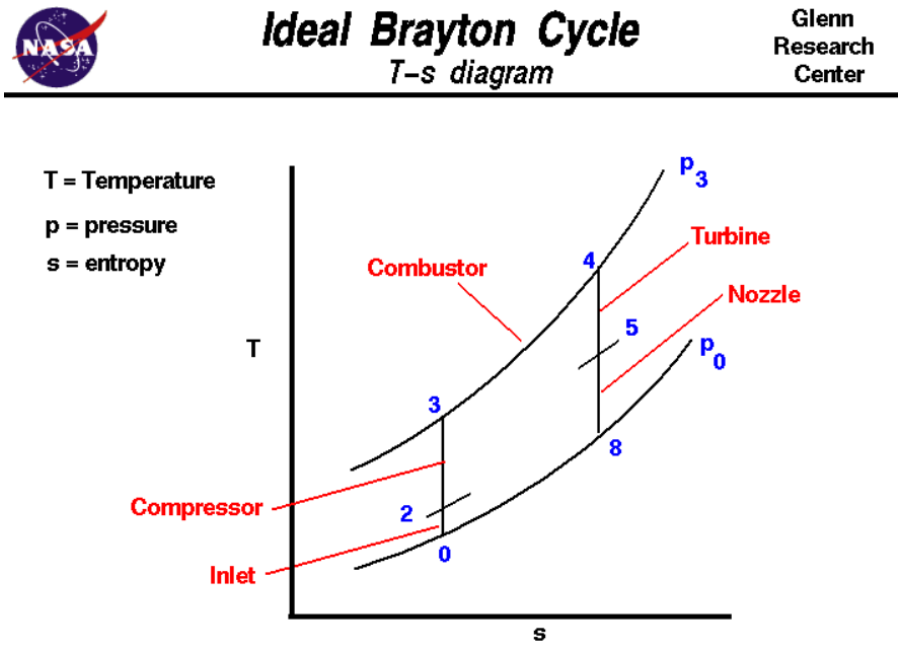

Figure 4. Ideal Brayton Cycle T-s Diagram for gas turbine engines [12]

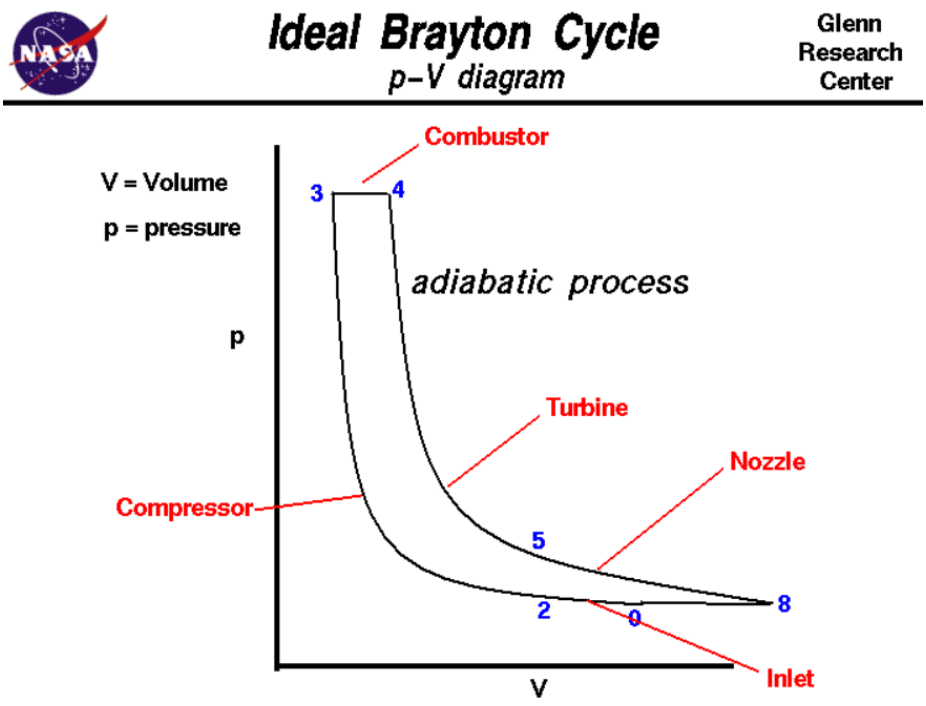

Figure 5. Ideal Brayton Cycle p-V Diagram for gas turbine engines [12]

2.1 Compression Stage (0-3)

The compression stage is the first phase within the engine. During this stage ambient air is drawn into the inlet of the engine by a compressor wheel and is then compressed and forced though a diffuser. This compression increases the energy state within the air by storing energy in the form of pressure. This prepares the air for the next stage of the engine, by changing the kinetic energy of the air into pressure.

2.2 Combustion Stage (3-4)

The combustion stage is the next phase within the engine. During this stage the pressurized air is mixed with fuel and ignited. The ignition of the air fuel mixture converts the chemical energy within the fuel to thermal energy, which increases the temperature of the air. This high temperature air begins to expand which accelerates the air into the next stage.

2.3 Turbine Stage (4-5)

The turbine stage is the next phase within the engine. During this stage hot pressurized air from combustion continues to expand from the heat addition. The high velocity air then enters the stator which accelerates the air further by reducing the fluid domain. Once the air is

accelerated it flows in the turbine, the turbine redirects the air which results in a reaction force. This reaction force is offset from the center axis of the engine, therefore producing torque. This torque is then directed into the shaft of the engine which powers the compressor. The high velocity air then flows into the next stage of the engine.

2.4 Exhaust Stage (5-0)

The exhaust (nozzle) stage is the last phase within the engine. The high velocity air flows into a nozzle which accelerates the velocity to Mach speed. This high velocity exhaust along with the amount of air mass flow creates a reaction force known as thrust. The nozzle's primary objective is to generate sufficient thrust to propel the aircraft forward.

2.5 Electronic Control Unit

To operate the engine, the engine is controlled by an electronic control unit (ECU). The ECU controls startup and ignition, throttling during operation, system monitoring, safety procedures, and shutdown. The ECU should include a temperature, pressure, engine rpm sensor along with a force transducer. The ECU is vital in the safe operation of the engine.

2.6 Test Bench

A test bench is required for stationary testing of the finished engine. The test bench allows for moving the engine when not in use, as well as housing the fuel and ECU needed to power the engine. The safety of the operator and surrounding environment during testing is of the utmost importance when considering the design of the test bench. Therefore, the design incorporated prevention to multiple failure modes the engine might encounter, like rapid unscheduled disassembly (RUD). A full list of failure modes and effect analysis (FMEAs) can be found in Appendix G.

DESIGN

In this section, past projects were reviewed to gain insight into turbojet design. From this literature review, technical requirements were set to design the team's engine towards. Preliminary calculations lead to conceptual designs that were considered. After conceptual design decisions were agreed upon, critical design was carried out on each subsystem so that fabrication of the engine was possible.

1 Past Projects

To begin the design process, the team researched past senior design projects that also designed and fabricated turbojet engines. These projects helped inform the team in many engineering design decisions and what to expect during the project, however all the projects leave room for improvement.

1.1 Sri Ramakrishna Engineering College

A team at the Sri Ramakrishna Engineering College in India designed and fabricated a micro jet engine with a thrust to weight ratio of 8:1 [2]. This team had the same goals as ours: to create an engine that is lightweight and produces significant thrust. Their report details the design of the main components of the turbojet engine, such as the combustion chamber, turbine, and shaft using equations used in their design. The team then simulated their parts in CATIA V5 to validate their design decisions. They also developed a MATLAB code that can vary different engine parameters to predict engine behavior, shown below in Figure 6.

Even though the report states that the project is designing and fabricating, the team did not display any fabricated parts. Additionally, their team's novelty of creating a new engine does not add much research to the field. Therefore, our team wanted to not only design a new engine, but also fabricate and incorporate a way to add research to the field such as differing casing material or thermal barriers on the exhaust side of the engine.

1.2 Universidade Da Beira Interior

A team at the Universidade Da Beira Interior in Portugal designed and fabricated a miniature turbojet engine [18]. This team's main goal was to create a three-dimensional design of an engine that mainly draws inspiration from previous design, specifically Thomas Kamps' *Model Jet Engines,* as well as make the report transparent so other teams can follow their work to

fabricate their own engine. The design of each subsystem went through many calculations and verification using CATIA. The finished 3-D model is shown below in Figure 6.

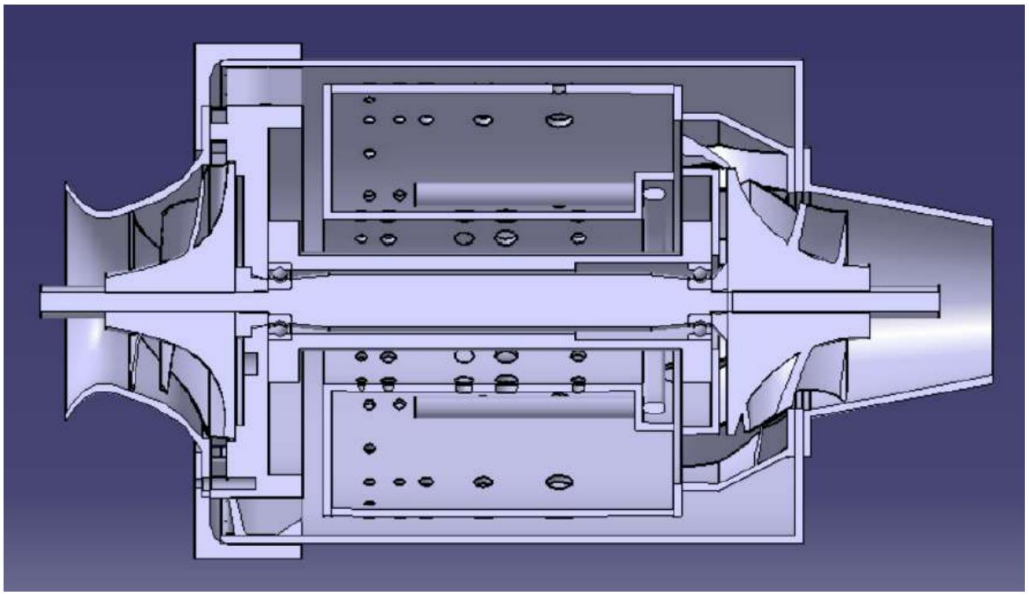

Figure 6. Universidade Da Beira Interor's 3-D engine [18]

While this team displays some fabricated components, they ran into issues with rolling, welding, and manufacturing with small dimensions. However, what was extremely impressive about this team is that they recycled scrap aluminum from an engine block to reuse through a casting process. The team noted in their future work that a test bench should be developed to properly test the engine when it is completed. Our team learned that fabrication was going to be difficult to accomplish, but with a well-rounded team determined to continue, the objective of fabrication was still upheld. Additionally, the team confirmed that a custom test bench would be needed for proper testing and storage considerations.

1.3 Uppsala Universitet

A team at Uppsala Universitet in Sweden designed and fabricated a simple, miniature turbojet engine [9]. This team began with general engine characteristic equations obtained from their research, including thrust, efficiency, and work done by the engine. Like other senior design teams, this team utilized a compressor wheel from the turbocharger of an automotive engine. This is common within design projects since the compressor is one of the most difficult components to fabricate, so most teams prefer to buy this component. During the fabrication of the other components, however, they discovered that the compressor wheel they purchased was

not compatible with the necessary RPM and compression ratio. Therefore, the engine was not completed, and testing was not accomplished. The team realized that selecting the compressor wheel was the most critical function of the design's success. From this project, the team reviewed many options for compressor wheels and selected the one that would achieve the specific goals of our engine.

2 Technical Requirements

From projects discussed in Section 1, and researching comparable-sized engines on the market, the team created benchmarks for the engine to make the team's engine competitive. These requirements are what the team designed the engine towards. Shown below in Table 1 are the five technical requirements for the engine.

The engine shall:

Table 1. Technical Requirements

1. Produce a minimum of 1100 Newtons (250 lb) of thrust at maximum RPM
2. Weigh less than 130 Newtons (29 lb)
3. Fit within 50×25×25 cm^3(20×10×10 in^3)
4. Operate continuously for at least 2 minutes
5. Operate at a temperature and pressure of 20°C and 1 atm (70°F and 14.7 psi)

3 Preliminary Calculations

3.1 Thrust Equations

Thrust is a major technical requirement for this project; therefore, it is important to understand the relationship between engine parameters and thrust capacity. To determine this, conservation of momentum can be used. A summation of forces can be performed in line with the center axis of the engine. This summation provides us with Equation 1. Once known values are input into this equation it can be determined that the two limiting factors for thrust production are air mass flow and velocity of the air exiting the rear of the engine. Mass flow is dictated based upon the compression stage; this value can be chosen based upon sizing of the compressors. The velocity on the other hand is dictated by the max operating temperature of the engine. This will be further explained in the nozzle section of the report. The max operating

temperature of many engines is 1300 Kelvin [14]. This temperature allows a theoretical exit velocity of 722.6 m/s which is then input into the equation along with the goal of 1000 Newtons of thrust. Solving for mass flow we find that the engine needs a minimum of 1.5 kg/s of mass flow to achieve the goal of 1000 Newtons of thrust as shown in Figure 7.

$$F = \dot{m}_{air} \times v_{air,out} \tag{1}$$

$$\dot{m}_{air} = 1.5 \frac{kg}{s} \tag{1a}$$

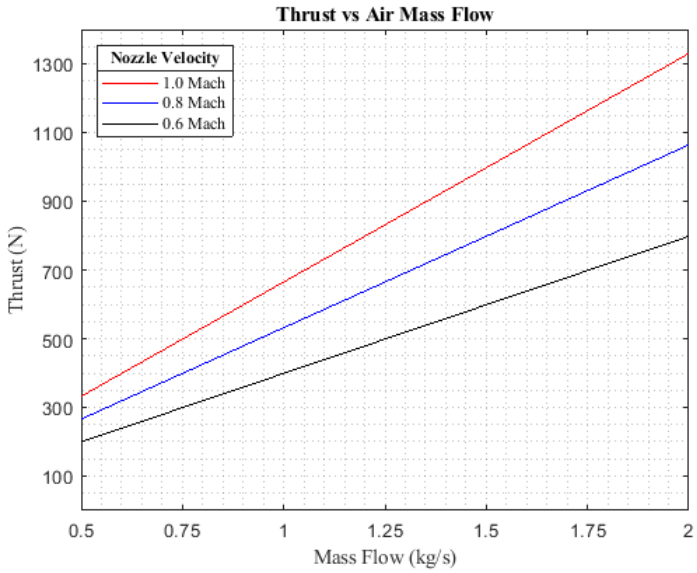

Figure 7. Mass flow relation to thrust with multiple velocities

3.2 Engine State-Points

To reduce the complexity of calculations throughout the engine, the team decided to use state points to track major engine parameters, like temperature and air speed, through the major stages. The team developed an Excel sheet to easily update parameters and equations as the values updated from research. Major inputs to the sheet were the compression ratio, which is how much pressure is added to the incoming air, airflow through the compressor, and compressor radii. Using equations found in *Jet Propulsion* [7], values for the overall thrust, work done by the compressor, and torque the turbine produces are calculated. From here, values for each of the state points in the engine can be calculated using design choices and the solved values. This sheet was essential in validating, early in the design process, that the engine would make the necessary thrust.

4 Conceptual Design

4.1 Compression Design

Highlighted throughout the report, the compression stage design is one of the most critical aspects of engine design. There were multiple conceptual designs that were researched to design the compression stage of the engine. The designs considered were the axial, centrifugal, and multiple stage centrifugal compressor, that will be discussed below.

4.1.1 Axial Compressor

One method commonly used to compress air within a gas turbine engine is to use axial compressors. Axial compressors use many sets of spinning and stationary blades to gradually compress air as shown in Figure 8. These are typically used in larger engines used on passenger jets. Axial compressors are very efficient at producing pressure and high mass flows. However, they also tend to be more complex due to the large quantity of engine components.

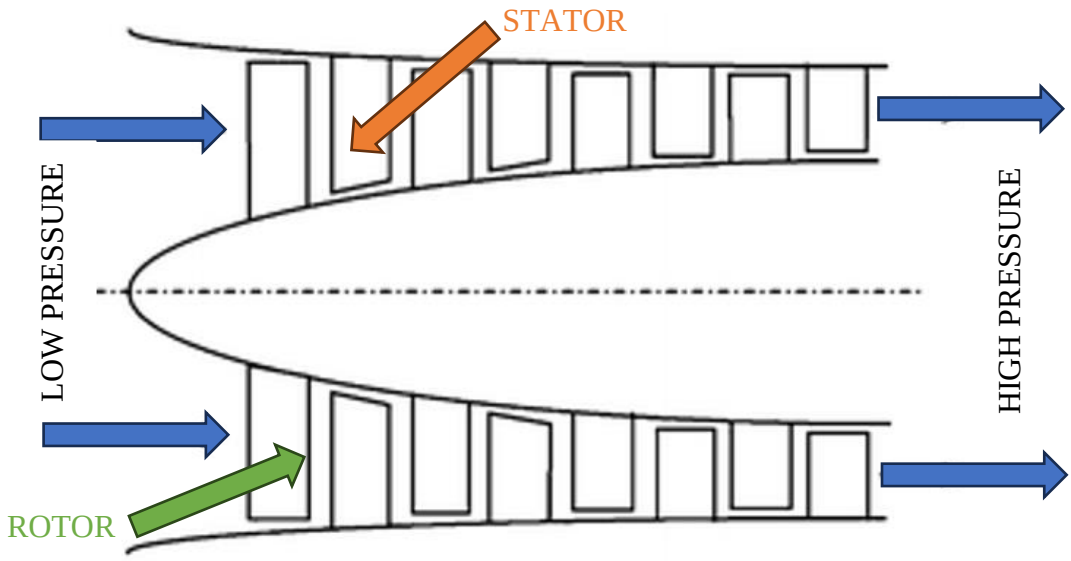

Figure 8. Cross-sectional view of axial compressor. Air flows from left to right, denoted by the blue arrows. Denoted by the green arrow are the rotor blades and in orange are the stator blades [3]

4.1.2 Centrifugal Compressor

Another method that is used to compress air within a gas turbine engine is centrifugal compression. This method uses a compressor wheel and an air diffuser to produce the pressure and flow the engine requires. This design reduced complexity but does not create the amount of pressure that the axial compressor creates. A schematic of a centrifugal compressor is shown below in Figure 9.

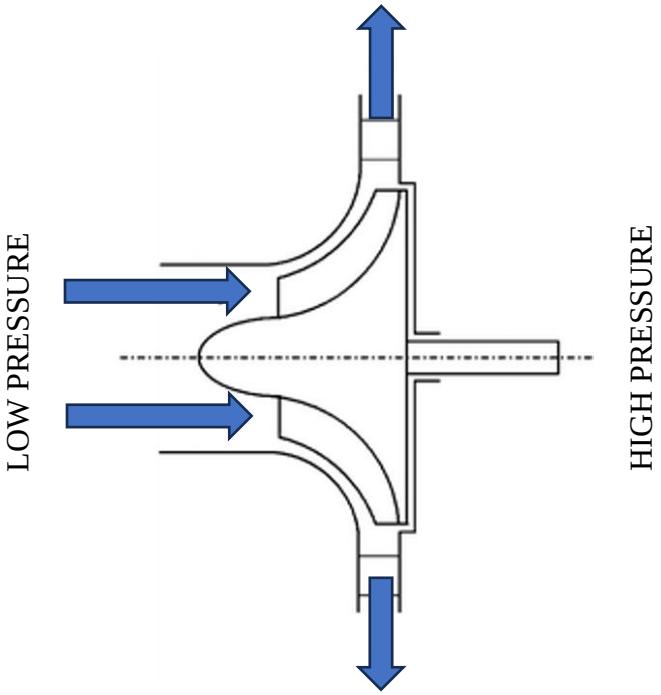

Figure 9. A centrifugal compressor. Air flow is marked with blue arrows. Note that the air flows tangentially compared to an axial compressor [3]

4.1.3 Multi-Stage Compression

The original novel idea for the engine was to use a two-stage compressor stage. This design would increase the efficiency of the engine by using two compressor wheels, allowing for a higher compression ratio. After starting preliminary calculations with this design, the thrust output the team needed could be achieved with the airflow from the compressors. Additionally, the team already acquired one the of compressor wheels needed for this design. However, the added weight from the two compressors was not worth the tradeoff of simply increasing the efficiency, which may or may not have had a large impact on thrust. After completing more calculations into this design, the team realized it was too complex and out of the project's scope. A graph, shown in Figure 10, displays the optimal operating pressure that two-stage compression (red circle) could achieve versus single-stage compression (blue circle). Therefore, a different compressor was selected.

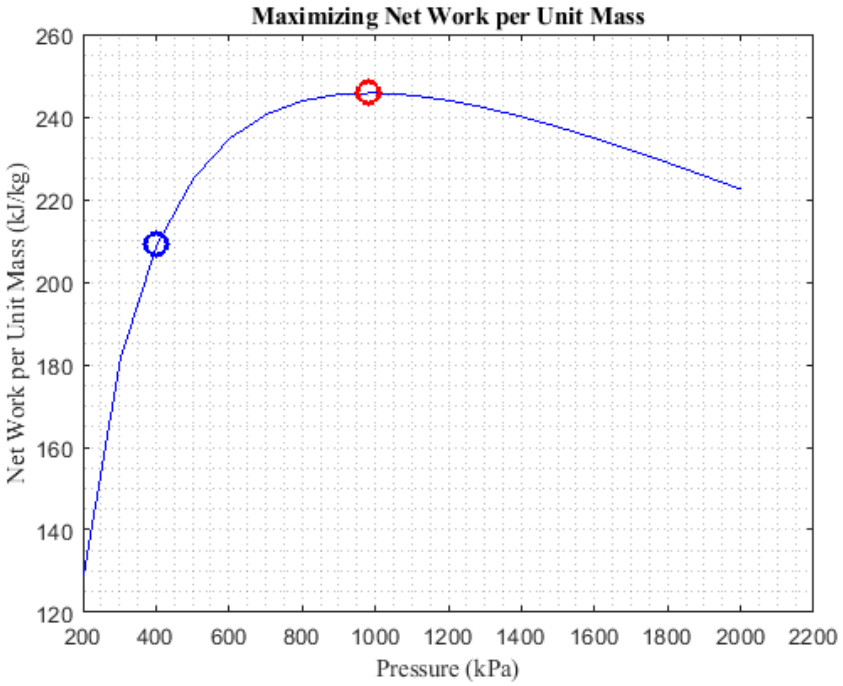

Figure 10. Maximizing net-work-output (red circle) vs single stage compression (blue circle)

4.1.4 Single-Stage Compression

After the two-stage compression design was discarded, the remaining option was to use the industry-standard single-stage compressor. The single-stage compressor, although it is less efficient, reduces the overall weight of the engine compared to the two-stage compressor. Additionally, with the right sized compressor wheel, one compressor can output the same amount of thrust as the two compressor wheels. Therefore, the one-stage compressor design was ultimately selected with the overall goal of minimizing the weight and maximizing the thrust.

4.2 Fuel System Design

The fuel system is responsible for delivering the fuel into the combustion chamber. The fuel can be delivered in a vaporized state or in an atomized state to allow for an efficient burn. Each system has its own benefits and drawbacks for the requirements of the engine. The vaporizing fuel system is comprised of a fuel ring and a set of capillary tubes that run directly through the combustion chamber. The ring allows for the fuel to be evenly distributed to the capillary tubes. The placement is to allow for the fuel to be heated up and vaporized before it enters the primary zone of the combustion chamber.

Fuel atomization can be achieved by using electronic fuel injectors. An electronic fuel injector system uses a high-pressure fuel pump to force fuel into the fuel injector. The fuel then flows through the body of the injector where it encounters a solenoid which controls the flow to nozzle. Once a signal has been sent to the solenoid it opens to allow the fuel to flow to the nozzle of the injector spraying into the combustion chamber as micro droplets. The fuel lines for fuel injectors must be a hard line to account for the pressures created by the fuel pump.

The advantage of the capillary design is that it is light weight and simple. In this case, the fuel pump does not require a high-pressure flow, only a steady flow that can be increased or decreased by a throttle. Although it is simple, it does not deliver a precise amount of fuel, as the electronic fuel injector does. The injector delivers a precise amount of fuel because nozzle sizes can be interchanged to achieve a desired air-to-fuel ratio. It also adds the complexity of an electronic control unit to signal the solenoids movement. Injectors also increase the system's weight dramatically along with the fuel pump needed to achieve the high-pressure within the fuel line.

There are also several types of fuel that can be used in a turbojet engine. Fuels that exhibit a high specific heat of combustion value such as diesel, kerosene, and petrol would be adequate for an engine of this size, along with butane and propane [18]. With these fuels being in a gaseous state, they require a larger fuel cell than that of the liquid fuel types. Shown below in Table 2 are characteristics of potential fuel sources that are being considered for the engine.

Table 2. Characteristics for potential fuel sources [3]

	Diesel	Petrol	JP1	JP4	Propane	Methanol
Density (kg/L)	.85	.76	.804	.76	.58	.79
H (MJ/kg)	42.8	42.5	43.3	42.6	46.3	19.5
Tank Capacity (ml)	880	990	920	990	1,380	2,080

4.3 Shaft Securing Method Design

The design consideration needed for the shaft is how to secure the compressor and turbine to it. This is due to the torque seen by the shaft transmitting to these components, and therefore, it needs to be fixed to the shaft's angular velocity. The two design options for securing the compressor and turbine to the shaft considered were keyways or an interference fit, shown in Figure 11 and Figure 12 below, respectively.

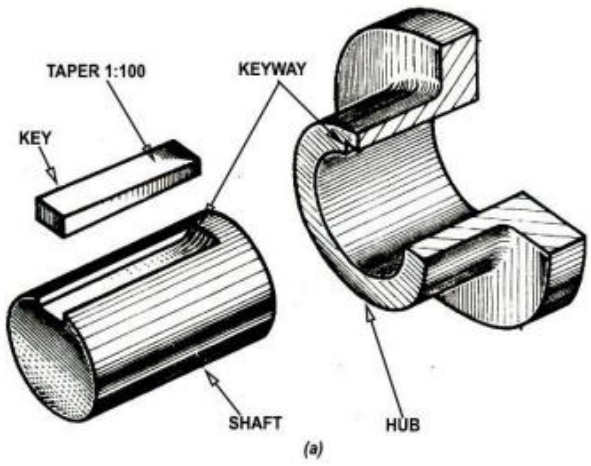

Figure 11. Example of a keyway fit on a shaft

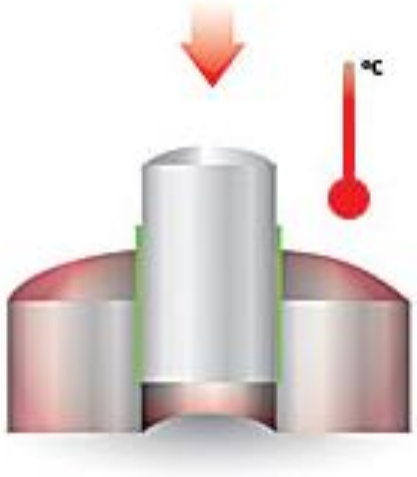

Figure 12. Example of an interference fit called a bonded shrink fit that uses heat [19]

The main advantage of keyways is that they allow for larger tolerances between the shaft and components needing to be secured. This allows for ease of manufacturing when compared to an interference fit. Interference fits need higher tolerance dimensioning during fabrication to

ensure they can handle the required torque. However, interference fits require one less part, the key, and do not introduce additional stress concentrations to the shaft. The keyway design would require a lathe and CNC to fabricate, while the interference fit can be accomplished solely on the lathe and temperature-altering methods (like heat or liquid nitrogen). Since stress concentrators are of concern for the shaft design and interference fits require only one type of machining equipment, the compressor and turbine will be secured to the shaft using interference fits.

4.4 Casing Material Selection

To minimize the weight of the engine, the team realized there could be weight savings with the casing material. Steel is commonly used on the market today, but the effects of changing to lighter materials wanted to be explored. After researching materials that would fit the requirements and weighed less than steel, two uncommon casing materials were considered: aluminum and carbon fiber.

Aluminum is a good choice for weight reduction considerations due to its relatively light weight compared to most metals. The major drawback of using aluminum compared to steel is the much lower melting temperature aluminum experiences. The team has a plan to continuously monitor the condition of the casing during testing to make sure the casing does not fail due to the high temperature the engine produces. Carbon fiber was selected as the other material due to one of the team members' vast experiences with the material and, again, it's lightweight property.

4.5 Turbine Thermal Barrier Coating

The other research topic the team wanted to explore was using a thermal barrier coating on the blades of the turbine to increase the temperature the component could handle. This would allow for a higher exhaust temperature from the combustor. This means the engine is producing more thrust with little additional weight, which significantly increases the thrust-to-weight ratio of the engine.

5 Critical Design

After preliminary calculations were completed, the team moved onto the critical design of each component using the technical requirements set forth in Section 2 to guide the design of the components.

5.1 Compressor

The team chose to use a single-stage centrifugal compressor which was chosen. During the preliminary design, it was determined that the team would need to choose a compressor that can produce a mass air flow of 1.5 kg/s to produce the desired thrust. For this reason, the team chose the Holset HX82 compressor wheel. This compressor has an inlet diameter of 110mm and an outlet diameter of 152mm. It is milled from 2618 alloy aluminum which makes it stronger than cast aluminum and lighter than alternative materials such as steel or titanium. The compressor was purchased due to the complexity of fabricating the component. The rendering of the purchased compressor wheel is shown below in Figure 13. Comparing the mass flow provided by this compressor back to Figure 7, the graph shown below in Figure 14 shows the predicted thrust production of the engine highlighted with a green circle.

Figure 13. 3D rendering of Holset Hx82 152mm compressor wheel

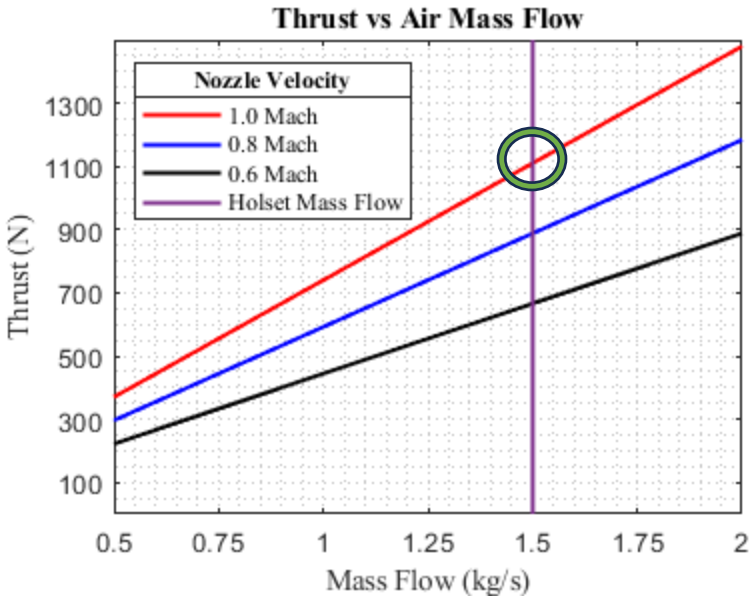

Figure 14. Holset Hx82 compressor wheel mass flow vs thrust production

5.2 Diffuser

The second component to the compression stage is the diffuser. This component is required when using a centrifugal compressor as it converts the high velocity air into pressure by using Bernoulli's principle and conservation of mass. To do this, the team altered the area of the flow from the inlet to the outlet of the diffuser. The air enters the center of the wedged fins highlighted with a green arrow in Figure 15. The wedges are angled so that the area is increased 28% from the inlet to the outlet of the diffuser. The air then needs to be turned back axially into the engine. To do this, curved fins were added to the edge of the diffuser highlighted with a red arrow in Figure 15. These fins simply act as guide vanes and do not change the pressure nor velocity magnitude. The team chose to use 6061 aluminum for this component due to the material's high strength and low relative weight. Additionally, the engine does not experience elevated temperatures at this stage and aluminum is not rated for high temperatures. To calculate the velocity of the air coming off the diffuser, Equation 2 was used below. This value will inform the airspeed coming into the combustor to size that component.

$$A_1 V_1 = A_2 V_2 \tag{2}$$

$$V_2 = 134 \frac{m}{s} \tag{2a}$$

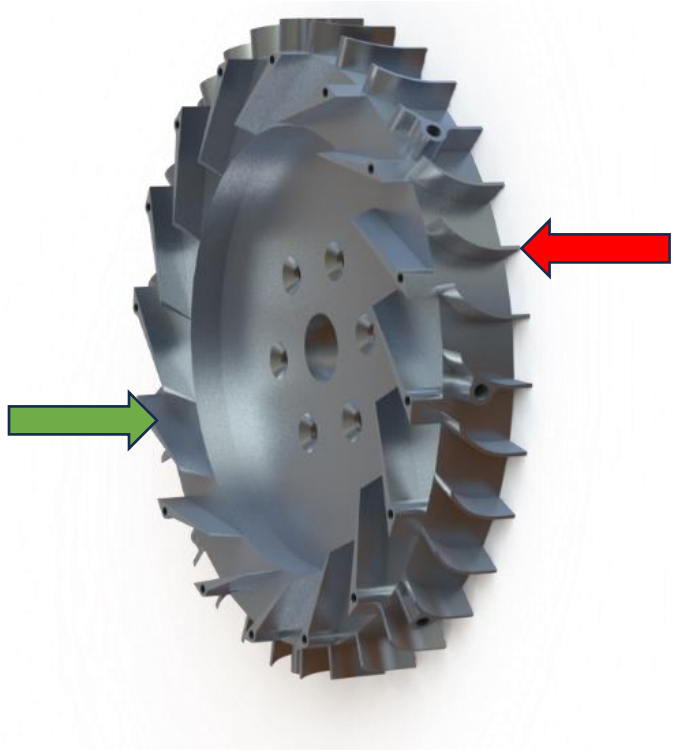

Figure 15. Diffuser 3D rendering

5.3 Combustor

To better understand a combustor performance characteristic used throughout this section, pressure loss, also known as loss coefficient, it should be noted that it is correlated with but not the inverse of combustor efficiency. One aspect of performance that can be measured is through this pressure loss value which corresponds to the geometry and inlet flow conditions of a diffuser. Loss coefficient is defined in Equation 3 below where ΔP_{diff} includes both the internal energy loss and the effects of velocity redistribution between the inlet and outlet [3]. The $\bar{q}_1$ is the average dynamic pressure at the inlet of the diffuser.

$$\lambda = \left(\Delta P_{diff}\right)\bar{q}_1 \tag{3}$$

Three main configuration types are still commonly used for a combustor design: can, can-annular (also called the tubo-annular), and annular, as shown in Figure 16 below. The key performance characteristics of these combustor types are their relative weights, ease of testing, ease of fabrication, surface area per unit volume, pressure loss, and uniformity of the exit temperature. The surface area per unit volume is important since more material exposure to hot combustion gases inside the combustor makes the combustor less adiabatic and increases air

drag, both detrimental to engine performance. Note that the surface area cannot be numerically compared since multiple factors, such as the number of combustion chambers and geometries, can vary the surface area. The pressure loss is the loss in pressure from the inlet to the exit of the combustor. The uniformity of the exit temperature is based on how uniform the exhaust from the combustor is in cross-section as it exits the combustor since hot spots are undesirable on the turbine stage.

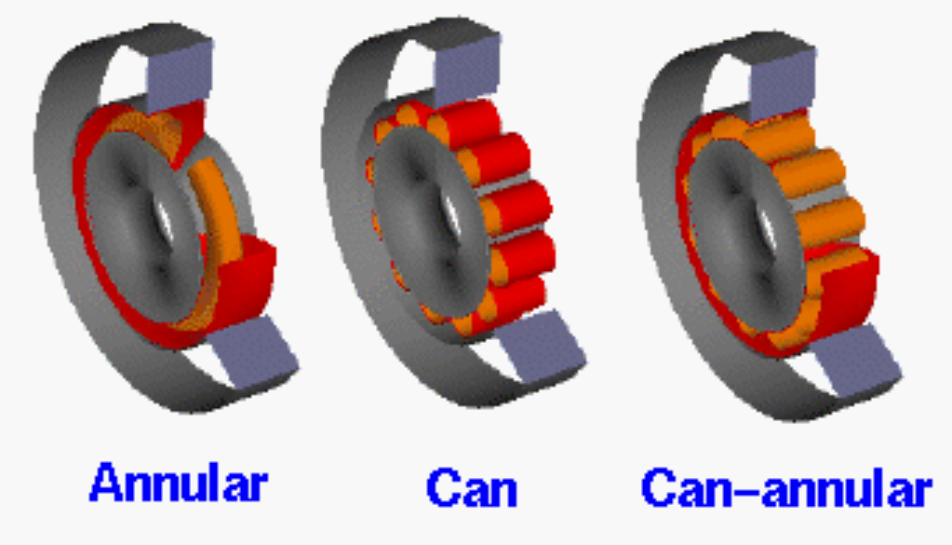

Figure 16. The three most-commonly used combustor configuration types. The orange represents the combustion chamber(s) and the red represents the pressure vessel(s) [11]

The can combustor type consists of separate cylindrical combustion chambers. The individual "cans" have their own fuel injector, igniter, liner, and pressure vessel barrier, as shown in the figure above. The can-annular combustor type also has separate cylindrical combustion chambers but no individual pressure vessels. Instead, the pressure vessel is a ring that encapsulates all the individual cylindrical combustion chambers as shown in the figure above. The final and most used type is the annular combustor. Annular combustors do not have individual combustion chambers or pressure vessels; they instead have a continuous ring-shaped combustion chamber and pressure vessel, as shown in Figure 16 above. Below are the summarized key performance characteristics of the different combustor types [3] [11].

Table 3. Key performance characteristics for the different types of combustor configurations. red, yellow, and green represent bad, average, and good respectively.

	Can	Can-Annular	Annular
Relative Weight	Heavy	Moderate	Light
Ease of Testing	Easy	Difficult	Difficult
Ease of Fabrication	Difficult	Moderate	Easy
Surface Area Per Unit Volume	High	Medium	Low
Pressure Loss	High	Medium	Low
Exit Temperature Uniformity	Bad	Average	Good

The only performance characteristic that is better for the can combustor type is its ease of testing. Since a researcher can test an individual "can" rather than a full-scale combustor. This is not a high priority for the team since this paper does not include any combustor-specific research. Since the annular combustor has reduced surface area, this allows for reduced material cost. Another valuable characteristic of the annular combustor design is that it can be shorter than the can and can-annular types, allowing for a smaller overall engine footprint [3]. Based on the desirable performance characteristics, the annular combustor will be used in this design.

Another common design choice in combustors is the type of secondary diffuser configuration. This is defined as the change in airflow area between the diffuser guide-vanes to directly before the front face of the combustor liner. A secondary diffuser, also known as a cascade diffuser, is a component that continues to slow down the high-velocity air from the compressor and diffuser before it enters the combustion chamber. Note that the secondary diffuser is a separate component from the diffuser mentioned in Section 5.2 yet has the same primary purpose of converting the kinetic energy into pressure as defined by Bernoulli's Principle.

The performance characteristics relevant to the team's design choice are the pressure loss, length, and sensitivity to inlet airflow variations. The secondary diffuser's pressure loss is the difference in pressure from the inlet to the exit. Two key parameters affect the amount of pressure loss, including friction from the diffuser walls and stall from airflow separation at the walls as illustrated in Figure 17 below [3]. This graph shows that there is an optimal point where

the pressure loss is minimized, which will be analyzed further in this section. The sensitivity to inlet airflow is the airflow's ability to stay stable at different variations in the inlet velocity profile.

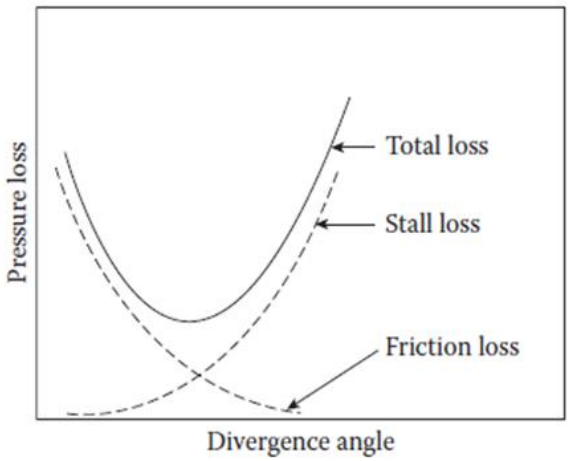

Figure 17. Pressure loss graph for varying divergence angles [3]

With these characteristics in mind, a few options for secondary diffuser types were considered. Common types of secondary diffusers for miniature jet engines include the faired, dump, and vortex-controlled diffusers. The faired diffuser, shown in Figure 18 below, includes a plenum chamber at the front of the combustor to allow for even airflow distribution. The dump diffuser includes a "prediffuser" shown in Figure 19 that increases the pressure while reducing the airflow velocity and aids airflow uniformity. The vortex-controlled diffuser, shown in Figure 20, includes an air bleed area that "bleeds off" the air boundary layer [3].

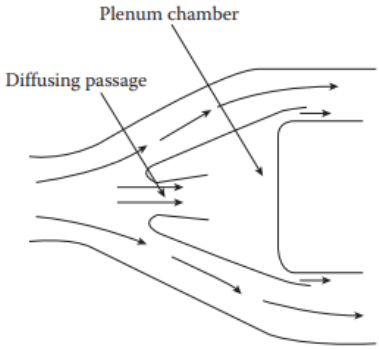

Figure 18. A faired diffuser that has a plenum chamber on the front face of the combustor [3]

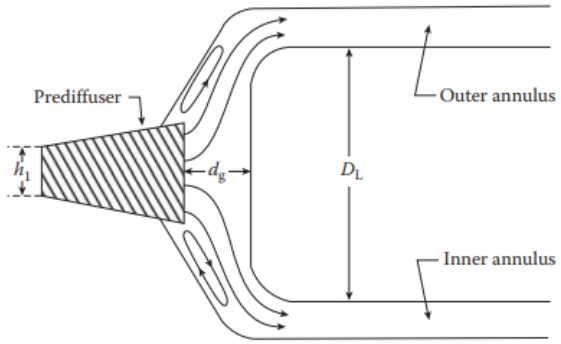

Figure 19. A dump diffuser that includes a prediffuser before "dumping" the air into the combustion chamber's annulus [3]

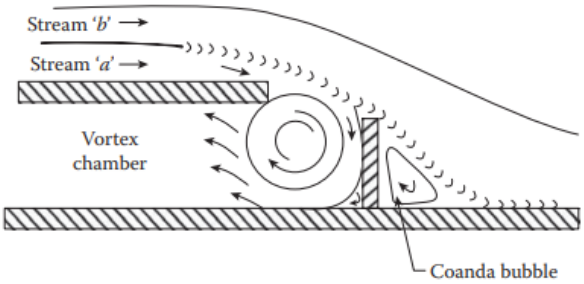

Figure 20. A vortex-controlled diffuser where stream 'a' is part of the boundary layer of airflow that gets "bleeded-off" while stream 'b' is directed towards the combustor [3]

Typical loss coefficient values range from around 0.15 for high-performance faired diffusers to around 0.45 for dump diffusers of the high liner-to-depth ratio [3]. The faired diffuser has high performance due to its low loss coefficient value of around 0.15, but due to its relatively long geometry from the plenum chamber and diffuser passage makes this diffuser type undesirable for aircraft engines due to size and weight constraints [3]. The dump diffuser and vortex-controlled diffuser are short in length compared to the faired diffuser, making them more desirable from a weight perspective. The dump diffuser is a fairly simple design but has the drawback of having around 50% higher pressure loss than the faired type [3]. The vortex-controlled design does improve the efficiency of the dump diffuser with minimal weight and size changes, but it is a far more complicated design that has not yet been fully researched with design methods to refer to. Because of this, the team decided to pick the dump diffuser type for our engine despite its inefficient design. To further affirm our design decision, note that most other turbojet engines of this size use the dump diffuser type.

Due to the complexities of designing and optimizing a novel combustor, the combustor will be based on a previous design. The literature from [20] includes the design method for a

combustor. The literature design method was picked since it has optimized design calculations for an annular combustor with a dump diffuser. Exactly the type of combustor and secondary diffuser this turbojet engine is designed for. The literature outlines most of the estimated values and equations necessary to fully design and dimension the combustor for the team's engine.

The combustor design method includes many input variables that are design choices. Due to this, Table 4 below is a list of the known and design variables relevant to the combustor design calculations. These input values were put into an Excel document that includes [20] equations that lead to the final outputs.

Table 4. Design and known variables relating to the combustor calculations

Variable	Value	Description
m_a	1.5 (kg/s)	Air mass flow rate
T_{t4}	1000 (°C)	Turbine inlet total temperature
π_B	0.9	Burner ratio
W_2/W_1	1.6	Area ratio
R	8.314 (J/mol-K)	Gas Constant
λ	0.45	Dump Diffuser Constant
k	0.7	Liner to reference area ratio
$T_{t,max}$	1100 (°C)	Maximum Allowable Turbine Inlet Temperature
$D_{L,in}$	0.08257 (m)	Inner Liner Diameter

One combustor design calculation not included in Cahya Putra's [20] paper is shown in Equation 4 below [3]. The equation was developed from empirical data from Sovran and Klomp to obtain the engine's optimal prediffuser length, L, and prediffuser inlet height, h1. Note that W_1 refers to h_1 for annular diffuser design. Using this equation and the graph in Figure 21, the team can pick an area ratio, A_{ratio}, and calculate a non-dimensional length, L/h_1, that allows for optimal diffuser effectiveness.

$$\frac{L}{h_1} = 5(A_{ratio} - 1) \tag{4}$$

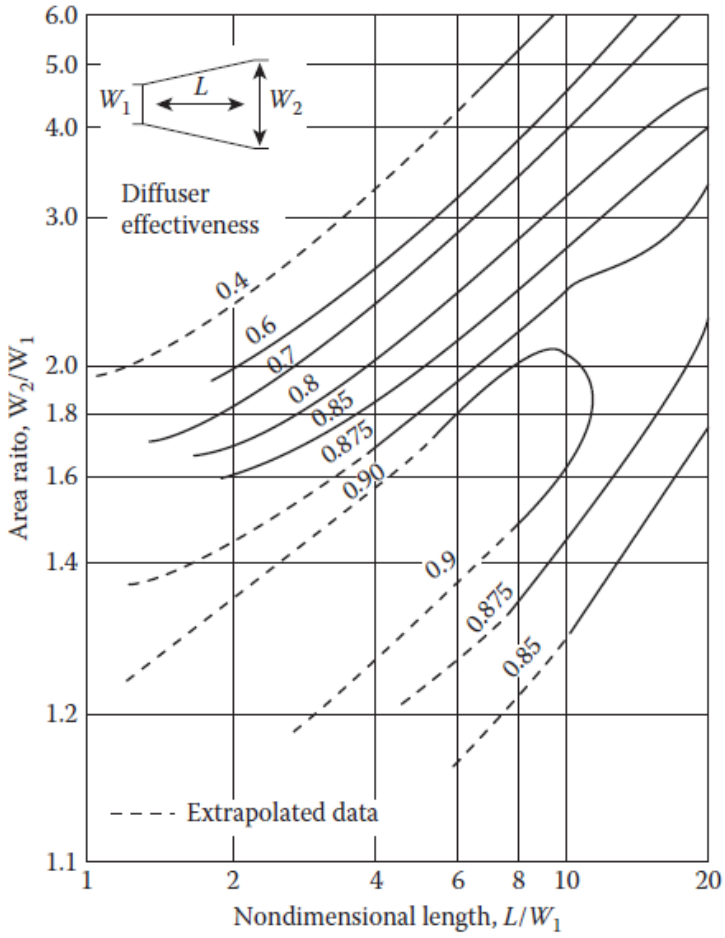

Figure 21. A graph that helps to increase a diffusers efficiency by picking a value for nondimensional length or area ratio [3]

The combustor calculations led to final values that size and dimension the combustor while being optimized for weight savings, temperature control, and flame stability. The relevant output values are listed below in Table 5.

Table 5. Output values from the combustor design method

Variable	Value	Description
N	0.0234 (m)	Prediffuser axial length
L_L	0.176 (m)	Liner Length
$d_{L,out}$	0.2052 (m)	Outer Liner Diameter
$d_{j,ax}$	6.4297 (mm)	Hole Diameter Axial Primary
n_{ax}	12	Number of Holes, Axial Primary
$d_{j,pz}$	6.4297 (mm)	Hole Diameter, Annular Primary
$n_{pz,1}$	14	Number of Holes, Annular Primary, Row 1
$n_{pz,2}$	14	Number of Holes, Annular Primary, Row 2
$d_{j,sz}$	12.792 (mm)	Hole Diameter, Annular Primary
$n_{sz,1}$	12	Number of Holes, Annular Primary, Row 1
$n_{sz,2}$	12	Number of Holes, Annular Primary, Row 2
$d_{j,dz}$	12.987 (mm)	Hole Diameter, Annular Primary
$n_{dz,1}$	6	Number of Holes, Annular Primary, Row 1

With all these final design values, the combustor was dimensioned in SolidWorks as shown in Figure 22 below. The thickness of the liner is 0.08 inches made of 4130 chromoly steel to allow for easy welding while still allowing high-temperature resistance. A stress analysis was not considered for the combustor since it is not an enclosed pressure vessel like the casing.

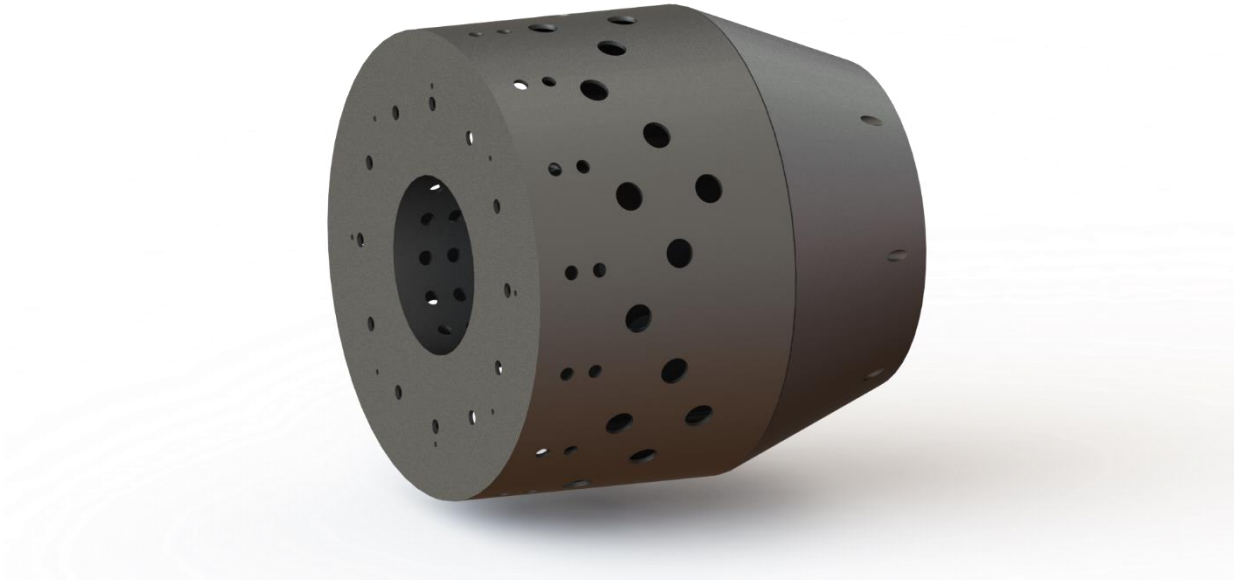

Figure 22. Final rendering of the combustor using all geometric values listed above

5.4 Fuel and Ignition System

Fuel selection plays a key role in the combustion process, kerosene has been chosen as the fuel for this engine because it is readily available at most fuel stations in the U.S. and has a higher heat of combustion value than that of methanol or petrol. The capillary and fuel ring design has been chosen because it is commonly used in engines of this size. With one of the requirements being a high thrust to weight ratio, the capillary design is lighter than the electronic fuel injector design. Because the temperature of combustion is designed to reach at least 800°C, stainless steel has been chosen for the material of the fuel ring and capillary tubes, because it is able to withstand the temperature of combustion.

Below the stoichiometric fuel ratio, shown in Equation 5, can be seen along with the mass air flow required to achieve this ratio. Note that the fuel ratio is calculated using the maximum air flow and is assumed to be a 1:1 ratio. The assumption that one mole of kerosene is being reacted with dry air where MW denotes the molecular weights of carbon, hydrogen, nitrogen, and oxygen [7] . The variable “n” denotes the number of the elements used. The final design of the fuel system is shown below in Figure 23.

$$C_{12}H_{26}C_{15}H_{32} + \frac{100.43}{2}(O_2 + 3.76N_2) \rightarrow 27CO_2 + 29H_2O + \frac{377.62}{2}N_2 \quad (5)$$

$$f_{stoich} = \frac{\dot{m}_{fuel}}{\dot{m}_{air}} = \frac{MW_C(n_C) + MW_H(n_H)}{MW_O(n_O) + MW_N(n_N)} \quad (5a)$$

$$f_{stoich} = \frac{\dot{m}_{fuel}}{\dot{m}_{air}} = .06705 \quad (5b)$$

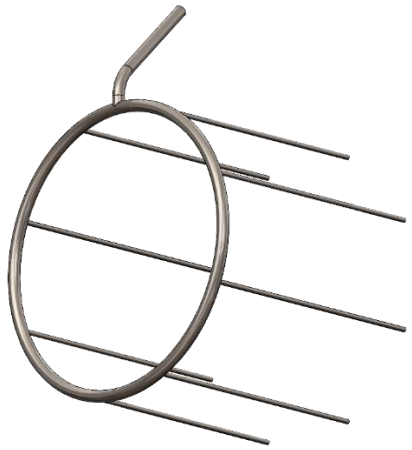

Figure 23. Completed fuel ring design

A Holley 100 GPH, gallon per hour, in-line electric fuel pump was chosen because it meets the mass flow requirements calculated above and is specifically made for kerosene. The fuel pump connects to the fuel ring via a flexible PVC fuel line, this was chosen because it is not degraded by kerosene. The flexible hose was used so the line could be flexed around the test bench's corners. The kerosene is held in an aluminum five-gallon fuel cell attached to the inlet side of the fuel pump using Army-Navy (AN) fittings and a rubber-lined steel braid hose. A glow plug will be used to ignite the kerosene. Kerosene cannot be combusted using a conventional spark plug like methanol or propane since these won't reach the necessary temperatures to ignite kerosene. A glow plug uses nichrome wire to convert electrical current into thermal energy to combust the fuel vapor.

5.5 Stator and Turbine

The stator and turbine were designed using blade profiles that were found in the Klaus Hanuke textbook [14]. The stator blades are designed to accelerate the air and redirect it 45 degrees from the axial direction. The air then enters the turbine blades which then redirects the air opposite a full 90 degrees that subsequently spins the turbine. The team determined how much torque would be required to spin the compressor to the design point of 70,000 rpm. The required torque was then used to back calculate the amount of force that each blade would be required to produce. To achieve this, the number of blades was set to 16. Using these values the amount of velocity was back calculated to produce a reaction force. ANSYS, a computational fluid dynamics software, was used to verify the velocity that would be produced by the blade profiles of the stator and turbine. The final flow domain needed for the simulation can be seen in Figure 24, and the results of the ANSYS analysis can be viewed in Figure 25.

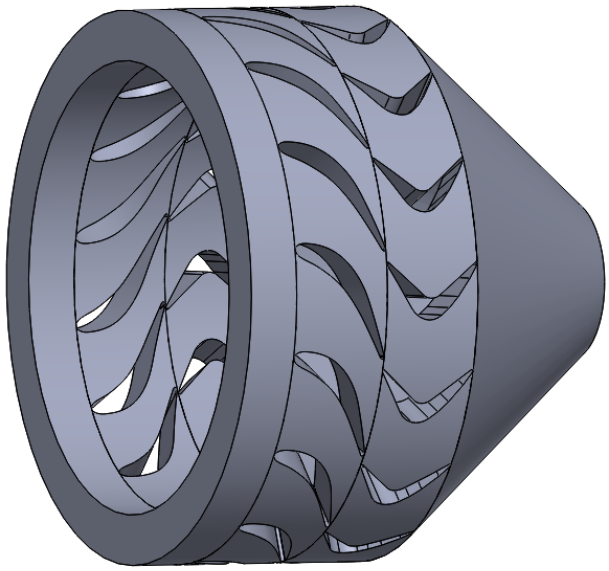

Figure 24. ANSYS fluid domain for stator and turbine prior to simulation

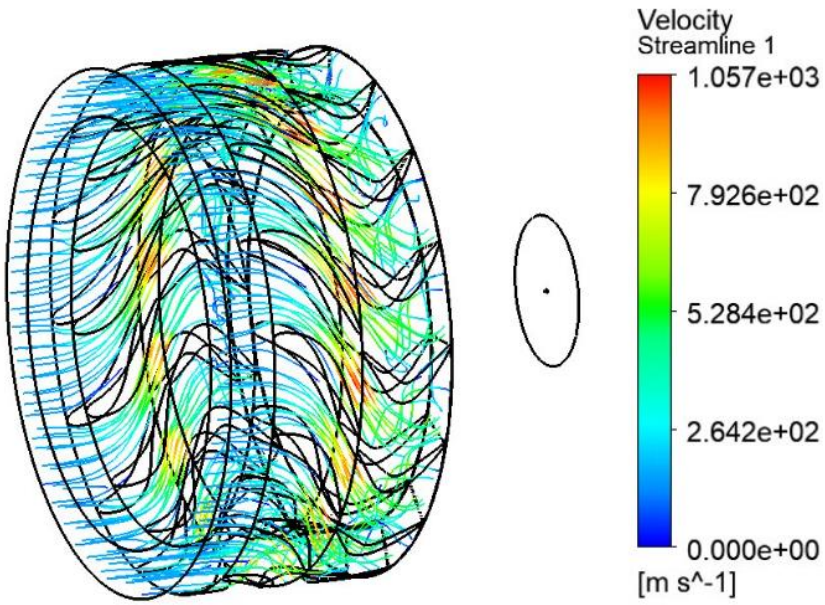

Figure 25. ANSYS velocity results for stator and turbine flow

An important factor that must be designed for is the turbine inlet temperature, which is the maximum temperature that the turbine can withstand before the material changes phases. This temperature is `based upon the austenitic transition temperature of the material that the stator and turbine are made from. Having a high turbine inlet temperature is important to attain a high exhaust gas temperature, in turn producing higher thrust. For this a high temperature material is required, the team chose 310 stainless steel, which is rated for temperatures up to 1200°C [17], where carbon steel is only rated for 800°C [17]. Although Inconel would be the best candidate for this application because it is rated for 1300°C [17], its benefits do not outweigh the cost.

5.5.1 Thermal Barrier

With the stator and turbine stage encountering the highest temperatures in the engine, a thermal barrier can be applied to ensure that material does not reach a temperature that allows the grain structure to enter the austenitic phase where the strength of the material will decrease. Adding the thermal barrier allows the engine to run at higher temperatures while maintaining the strength of the material and producing more thrust. A common type of thermal barrier is ceramic coating, where the coating is applied like paint and then baked. To ensure that the material of the turbine and stator remains below the austenitic phase, a coating with a low coefficient of heat

transfer is desired. The team chose to use the Cerakote V Series Turbine Coat ceramic coating because of its simple application process and its highest rated temperature of 985°C.

5.6 Shaft

The shaft is a rotating member responsible for transmitting power and motion, and it also provides the location and axis of rotation for all rotating parts in the engine. The shaft for the jet engine transfers torque from the turbine to the compressor. While the shaft's responsibility for transferring power is simple, many constraints must be considered when designing for this specific application due to extreme operating conditions.

The most critical parameters that need to be considered for this shaft design are the diameters, the maximum operating speed, and the maximum torque the shaft will transmit. Other considerations are the heat resistance of the shaft and maximum stress concentrations.

The shaft must axially locate the compressor, diffuser, stator, and turbine. Each of these parts will be located using shoulders for the different components. Figure 26 below shows the different segment classifications for our engine. Each component will need a separate shoulder, resulting in four locating shaft shoulders. Considering assembly, the components should be pressed onto the shaft from the ends, meaning the diameter changes should decrease from the middle to the two ends.

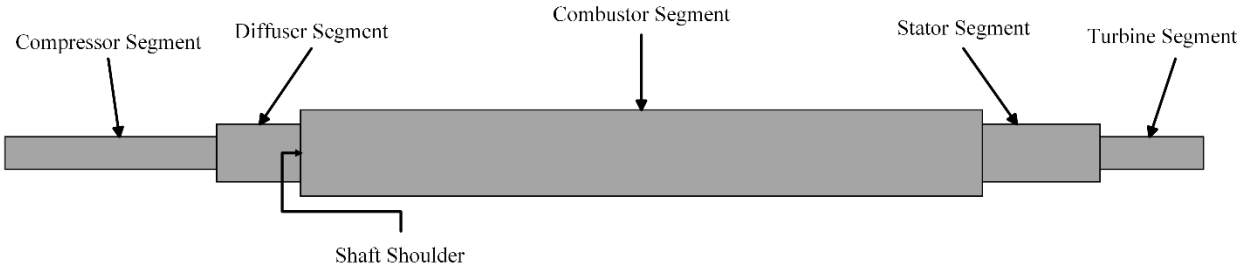

Figure 26. Shaft diagram with component sections labeled

The team needs to know key factors to calculate the diameters necessary for the compressor and turbine segment. The first is whether the interference fit will be designed based on a hole-basis or shaft-basis system. Since the hole in the compressor is not easy to bore and the shaft already needs to be lathed, this will be a hole-basis system for the compressor segment. To keep the shaft diameters symmetrical for simplicity, the turbine hole will be sized to the same inner diameter as the compressor hole. A medium drive fit will be used for the compressor and

turbine since it allows for secure torque transfer between the shaft and component without slipping [5]. This classification is H7/s6 as defined by the Preferred Mechanical Tolerances Metric ISO 286 [8]. Using a fits and tolerances calculator [19], with the nominal hole size of 11 millimeters, which is the inner diameter of the selected compressor wheel, and the H7/s6 classification, the outputs shown in Table 4 are output.

Table 4. Interference fit results for the compressor and turbine sections

	Tolerance of Shaft	Tolerance of Hole
Upper Limit Deviation (thou)	1.53547	0.70868
Lower Limit Deviation (thou)	1.10239	0
Maximum Shaft/Hole Dia. (in)	0.43462	0.43379
Minimum Shaft/Hole Dia. (in)	0.43418	0.43308
Tolerance Centre (in)	0.4344	0.43343

Since the shaft has significant torque and forces transmitted to components, threaded ends are added to the shaft to further secure components, as shown in Figure 27 below. The left-handed threaded ends will increase friction applied to the components and add a barrier to prevent components from sliding axially in the event components slip due to the torque. This redundant feature was added for its ease of fabrication, negligible weight increases, and prevalence in similar engine designs.

Figure 27. Shaft with threaded ends

Bearings must be selected since the shaft spins freely from the rest of the engine fixed to a test bench. This application requires specific bearing performance characteristics, including a minimum operational speed of 70,000 RPMs, an axial load capacity of 1000 Newtons, and a heat capacity of at least 200°C. Using the Roller-Contact Bearings chapter in Shigley's Textbook [5] and cross-referencing bearing performance characteristics from Boca Bearings, a bearing company in Florida, angular contact bearings were selected to reach all desired characteristics

while still compact. Table 5 below shows the necessary bearing characteristics and the characteristics of the angular contact bearing picked for this project.

Table 5. Bearing characteristics needed versus selected bearing. The data for the D6001/604/266C was supplied by an industrial engineer at Boca Bearings and confirmed on their website

	Bearing Characteristic Needs	D6001/604/266C
Angular Velocity (RPM)	70,000	80,000
Axial Load (N)	1,000	>1,000*
Max Operational Temperature (°C)	200	220

The angular contact bearings can only have axial loads in one direction due to a 15° angle between the raceway and rolling elements, as shown in Figure 28 below. If a load is applied in the opposite direction, the roller elements may become misaligned or separate from the raceway, inducing significant friction to the shaft or a catastrophic engine failure. To ensure the angular contact bearings do not fail in this way, the bearings are faced in opposing directions to account for axial loads in either direction.

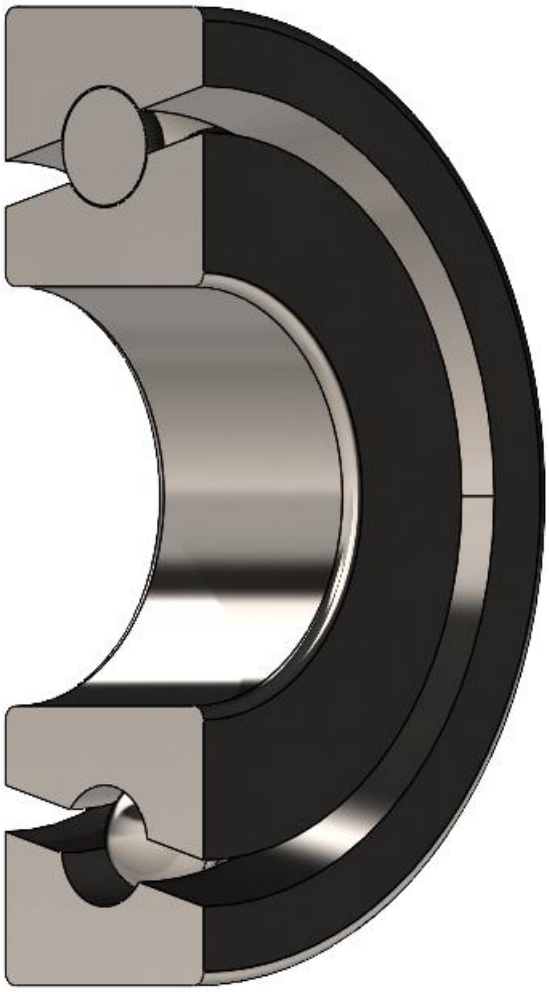

Figure 28. Cross-section view of angular contact bearing selected

The diffuser and stator segments of the shaft still need to be sized to ensure the fit on the bearings is correct. If the type of fit allows for too much clearance, then the attached components may rotate slightly misaligned from the shaft, potentially causing increases in shaft stress or contact with stationary parts. Due to this, a locational transition fit, H7/k6, is picked to ensure accurate shaft rotation. The results for this hole-basis system are shown below in Table 6 from entering the type of fit and the nominal inner diameter of bearing size of 12 millimeters.

Table 6. Bearing interference fit results

	Tolerance of Shaft	Tolerance of Hole
Upper Limit Deviation (thou)	.47245	0.70868
Lower Limit Deviation (thou)	.03937	0
Maximum Shaft/Hole Dia. (in)	0.47292	0.47316
Minimum Shaft/Hole Dia. (in)	0.47249	0.47245
Tolerance Centre (in)	0.47271	0.47281

The next step in the shaft design process is to design the shaft for the expected stresses. MATLAB software was developed in ME 466, Machine Design, to calculate the deflections for a steel stepped shaft. The code has many inputs, including shoulder diameters, forces along the shaft, and total shaft length. Table 7 below shows all input parameters necessary for this MATLAB code.

Table 7. MATLAB code inputs. The values appear from left to right for the shaft, compressor to turbine end

Types of Inputs	Shaft Values
Magnitude of Forces Applied* (lb)	1.27,2.01
Location of Forces Applied* (in)	2.421,15.083
Diameters of the Shaft* (in)	0.434, 0.473, 0.787, 0.473, 0.434
Locations of Start of Diameter Change* (in)	0, 3.25, 3.878, 14.018, 14.958
Location of the Bearings* (in)	3.721, 13.176
Length of Shaft (in)	15.958

The outputs of the MATLAB code are four graphs: one shows the half-shaft geometry to verify the diameters are correct, the second and third graphs show the total deflection and slope of the shaft, and the fourth graph displays the moment along the shaft. The deflection graph is essential in verifying that the shaft will not deflect beyond failure. The slope graph is useful in verifying that the bearings are in a proper operational range [5], shown in Table 8. The moment graph will inform custom Excel document developed in Machine Design, discussed in the next

paragraph. Figures 29 and 30 show the results below from running the numbers shown in Table 7 through the MATLAB code.

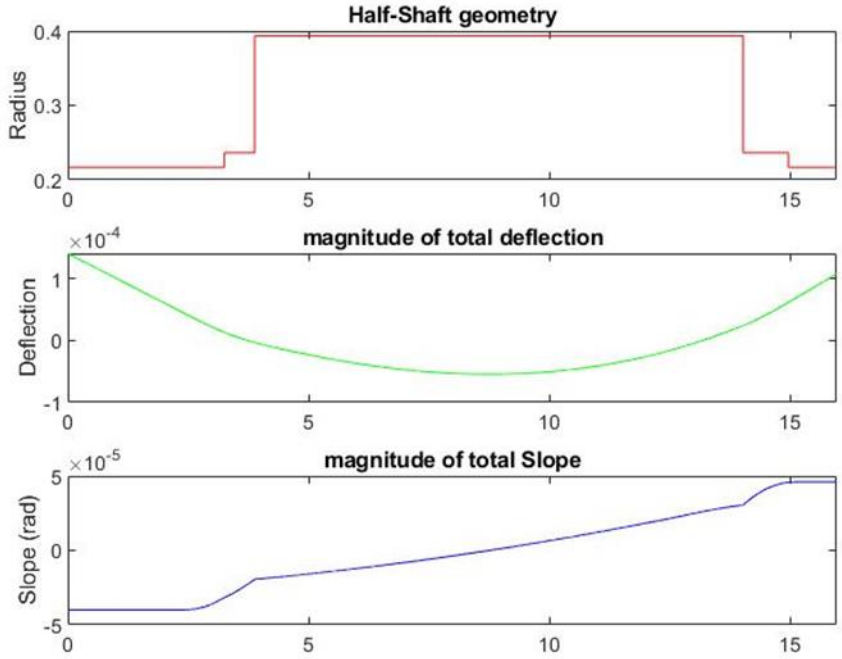

Figure 29. MATLAB graphical results. Please note the units are in inches for the axis's that are unmarked

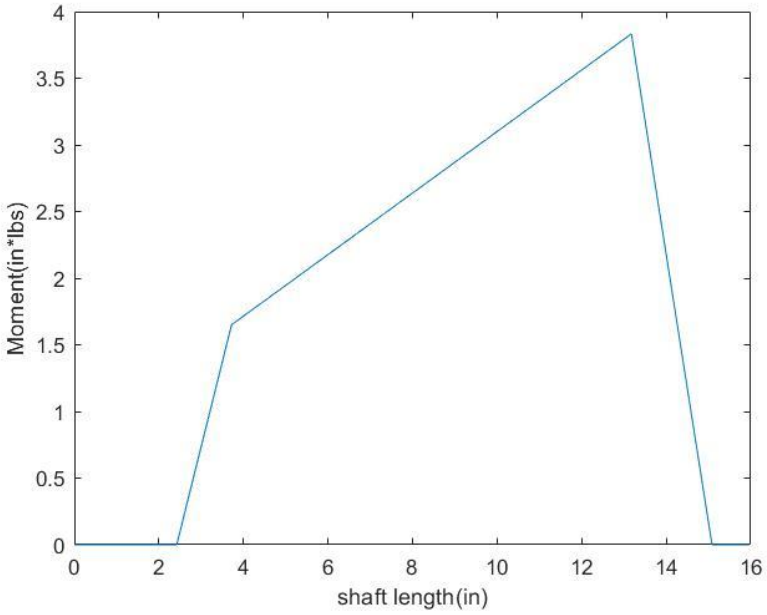

Figure 30. MATLAB moment graph result

Table 8. Slopes of shafts for typical bearings

Slopes	
Tapered roller	0.0005–0.0012 rad
Cylindrical roller	0.0008–0.0012 rad
Deep-groove ball	0.001–0.003 rad
Spherical ball	0.026–0.052 rad
Self-align ball	0.026–0.052 rad
Uncrowned spur gear	< 0.0005 rad

The other software developed in ME 466 is an Excel sheet that calculates factors of safety (FOS) for fatigue and static loads on a shaft. The inputs are the shaft radius at the desired location, the torque and moment at that location, and material properties. After the diameters were verified to not cause critical deflection, material selection was needed to begin the FOS calculations. The material for the shaft was originally selected as AISI 1040 hot-rolled steel. This material was selected for its relative strength and heat-resistance; however, its major quality was its machinability, since the shaft requires lathing. This material was moved on from, though, due to the low FOS that resulted from the loading conditions necessary for the desired thrust production. Therefore, a stronger material was needed to achieve higher FOS.

The final material selected was AISI 4140 steel, known as Chromoly steel. This steel fits the need for a higher strength, while not compromising the heat-resistant properties. The drawback of this steel is that it is harder to machine, making the fabrication process more difficult. The FOS was computed at the shoulders of the shaft since those are critical locations for stress concentrations. The desired results for the FOS are above 2 for each shoulder to ensure that failure will not occur during testing. Shown below in Table 9 are the results from one of the shaft shoulders.

Table 9. Excel sheet results for shaft shoulder at 14.08 inches from the front end of the shaft

Goodman FOS	3.356
Gerber FOS	3.429
Static Yield FOS	2.932

5.7 Casing

The casing wraps around the entirety of the engine to act as a barrier for airflow and houses all components within. The team designed three different casings, each with different materials. Carbon fiber, stainless steel, and aluminum would each be used in different test runs of the engine to determine which material decreased the most weight without overheating or rupturing during testing. Carbon fiber is one of the design decisions because of its high strength and extremely low density. The carbon fiber in this design is Hexcel AS4 and has a yield strength of 4501 MPa and density of 1.79 g/cm^3 [17]. The second material chosen for the casing is 310 stainless steel due to its high strength, excellent heat resistance, but it does have a high density. 310 stainless steel has a yield strength of 275 MPa and density of 8.00 g/cm^3 [17]. The final material planned for the casing is 6061-T6 aluminum due to its moderate strength, but lower density compared to steel. This aluminum has a yield strength of 276 MPa and density of 2.7 g/cm^3 [17]. If any of these materials held up just as well as the others but weighed less, then this would overall improve the thrust-to-weight ratio that the team is looking at reducing. The casing was designed as shown below in Figure 31 due to the custom shape of this turbojet engine.

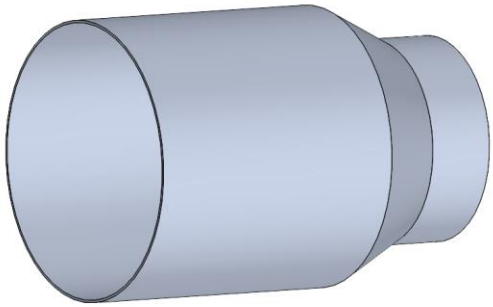

Figure 31. Engine casing

Due to the engine's properties during testing, the casing can be treated as a thin wall pressure vessel with open ends, and calculations were done to determine the minimum thickness. The thickness equation is referenced below in Equation 6. The inner diameter of the engine is d_i, the yield strength of each material is σ_{max}, and the internal pressure while the engine is running is P_2. P_2 and d_i are 202,650 Pascals and 0.225 meters, respectively, and stay constant between all three materials. The pressure is determined by doubling atmospheric pressure due to the air inside the engine being compressed by a factor of two. The inner diameter of the engine is 8.875 inches which translates to 0.225 meters.

$$t = \frac{d_i}{\frac{\sigma_{max}}{P_2} - 1} \tag{6}$$

Starting with the 4140-steel casing, the yield strength is 415 Megapascals. After putting this into the equation, a thickness of 0.00011 meters is found which converts to 0.0043 inches. The next casing material is 6061-O Aluminum. The yield strength of this aluminum is 55.2 Megapascals. This gives a material thickness of 0.00083 meters which converts to 0.0327 inches. The last casing material is HexTow AS4 carbon fiber. With the yield strength being 4501 Megapascals, this gives a casing thickness of 0.0000101 meters which translates to 0.000398 inches. With the thicknesses sized, materials were ordered based upon the closest standard thickness sizes.

5.8 Nozzle

The nozzle of the engine is the last component the hot exhaust air encounters before releasing into the atmosphere. This component needs to be able to handle high temperatures and air speeds close to the speed of sound. Therefore, 4140 Chromoly steel was selected, since it has

many other applications in our project and can sufficiently handle the same heat the combustor is experiencing. There are two primary nozzle designs that are common with miniature turbojet engines: divergent and convergent. Divergent nozzles are used on engines where the speed of the air coming out of the engine is supersonic, meaning the speed is faster than the speed of sound. Convergent nozzles are used when the speed is less than the speed of sound. For the scope of this project, a convergent nozzle was selected and designed.

5.9 Electronic Control Unit

The electronic control unit is used to operate the engine. The team decided to use an Arduino Mega 2560 microcontroller. This board allows the team to use both analog and digital sensors to monitor the engine along with using pulse width modulation (PWM) to control and throttle the engine. A custom MATLAB program was written to collect and process any data from the engine.

The engine is throttled through by altering the volumetric fuel flow of the fuel pump. To achieve this a potentiometer was used and an analog pin on the Arduino was used to read the voltage to determine the potentiometer position. This input was normalized to the board voltage to determine a throttle percentage, from 0% to 100%. The microcontroller then outputs a pulse width modulation with a duty cycle identical to the throttle. This PWM pin is connected to a mosfet that acts as a switch to vary the power to the pump. This was used because the pump runs off a 12 VDC system with a max amperage of 30 amps. The microcontroller is only rated at 5 VDC and has a lower amp rating. Using this mosfet allowed the team to separate the two power systems while still controlling this higher power system from the microcontroller. The team decided that there was no need for feedback within the throttle of the engine, rather the operator will monitor and change the throttle as needed.

The ECU also needed to collect data from the engine. To do this thermistors, manifold absolute pressure sensors (MAP), proximity sensors, and force transducers were used. Thermistors were used to collect temperature data from the engine. Thermistors were placed in areas of interest, inlet temperature, diffuser outlet temperature, turbine inlet temperature, and nozzle exit temperature. MAP sensors were placed at the inlet, diffuser outlet, and turbine inlet. The proximity sensor was used to determine engine RPM. This was done by placing it within the inlet and allowing the sensor to read the compressor wheel as it spins. Each time a blade passes

the proximity switch a pulse is sent to the Arduino. This is collected along with the time the pulse occurred. By taking the difference in time between two reading and the number of blades, the team can determine the angular velocity of the engine. The force transducer was placed between the engine and the test bench; this is further explained within the test bench section.

The ECU has built safety protocols to shut the engine down in the event of malfunction or other emergencies. The main safety protocol is implemented within the control program of the engine. This protocol used the data from the sensors on the engine, temperatures and pressures are compared to a set value to determine the health of the engine. If any temperature or pressure is out of range of the set values the engine will not start up and if they exceed the values during operation the engine will shut down. This is the automatic safety protocol; it is always checking the health of the system. The second, or manual, safety system is the emergency stop (E-Stop) buttons. These are large red buttons that can be pressed by operators or bystanders in the event of malfunction or emergency. The E-Stop buttons will cut all power to the engine when actuated. The E-Stop buttons are also monitored by the control program to determine if the button has been actuated. If the control program determines that the button has been actuated the control program will shut down power to the system. E-Stop is on both the controller and on the test bench to allow anyone to stop the engine at any point in time. An electrical block diagram can be found in Appendix H.

5.10 Test Bench

The team also designed a test bench for testing our engine. From initial literature review, a report from Worcester Polytechnic [1] used aluminum extrusion to secure the engine and a test bench to easily move the engine around. This source provided great insight into a typical test bench design, and the team used this to design our own test bench due to our custom engine size and ECU components. Our test bench was fully designed and modeled in SolidWorks due to the availability and familiarity of this software on USIs campus.

To begin the design process, angle iron legs with a structural steel baseplate on top were picked as the foundation of the test bench for strength and rigidity. On the bottom of each angle iron leg, rubber castor wheels are bolted to allow the entire test bench to easily move while the engine is shut down. Plywood shelves are added between the angle iron to house all external engine components such as the ECU, fuel cell, and gauges. Steel cross bars were welded on the

angle iron to provide more stability. Polycarbonate shielding was attached outside the operating area to ensure the safety of the user. On top of the baseplate, 25 mm x 25 mm aluminum extrusion is mounted for ease of engine fixturing and locating. This size of extrusion was picked due to its high yield strength to handle the thrust loads while also being the cheapest option from the manufacturer, 80/20. The overall foundation of the test bench can be seen in Figure 32.

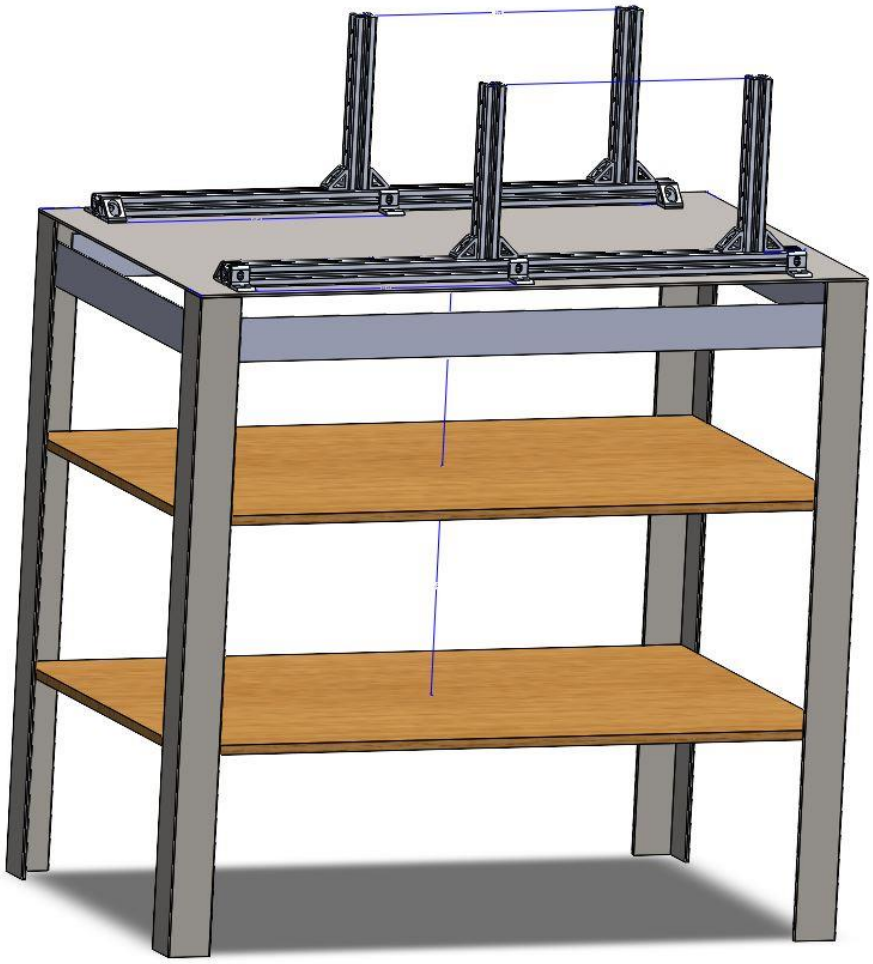

Figure 32. Completed test bench foundation. Please note the rubber casters and polycarbonate shielding are not shown here

Attached to the aluminum extrusion is a linear guide rail system as seen in Figure 33. This system allows for the engine to have one degree of freedom to move axially in the x-direction. To fasten the engine to the rail system, clamshell mounts manufactured from 1/8” medium-carbon steel are clamped around the engine and applied to the bearing mounts on the rail. High-strength steel 1/2" threaded rods are welded to the clamshell mounts and extended past the engine to connect a 1/4” 4140 steel plate that engages with the load cell. This design was inspired by Chattanooga State Community College and The University of Tennessee at

Chattanooga [22]. An image of the engine harness design is shown below in Figure 34. The load cell used is a Revere Transducers 363 S-Type Load Cell rated for 500 lb which is an equivalent of 2224.11 N. An S-type load cell was chosen due to its simplicity of assembly, reasonable price, load rating of 500 lb., and is already widely used in typical test bench designs. This load cell is mounted to a 1/4” thick 4140 steel plate and supports 25mm × 25mm 80/20 aluminum extrusion at the left end of the test bench. This load cell assembly can be seen in Figure 35.

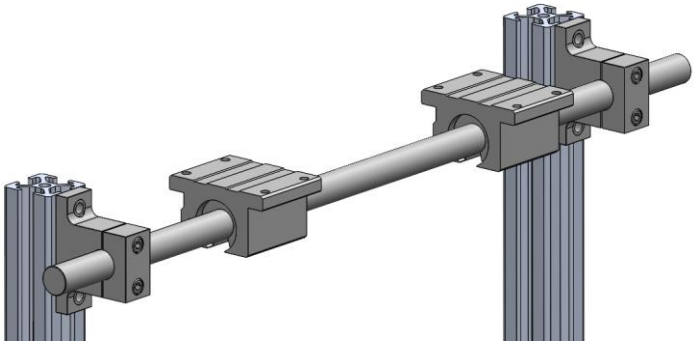

Figure 33. Linear guide rail system

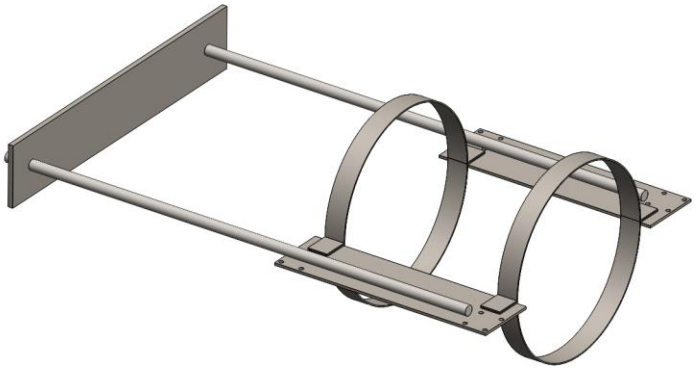

Figure 34. Turbojet engine harness with threaded rods connecting the plate to the clamshell mounts

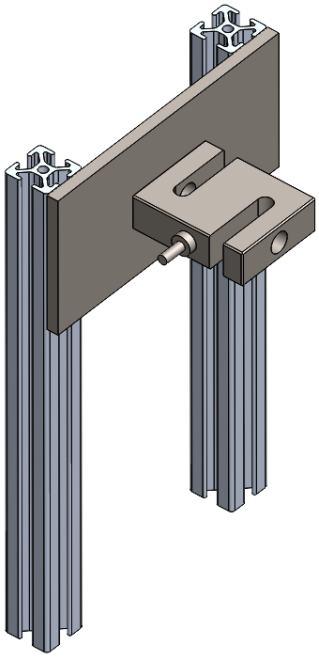

Figure 35. Load cell fixture

To validate the test bench design, Finite Element Analysis (FEA) using SolidWorks was conducted on the load cell assembly, aluminum extrusions, threaded rods, and clamshell mounts. The FEA for the load cell assembly can be seen below in Figure 36. This image showcases the Von Mises Stress graph. The max stress is 200 MPa which is below the 4140-steel yield stress of 415 MPa. This allows for a factor of safety of 2.08. The max deflection the plate will experience is 7.08 mm. This displacement is very minimal and not a concern with the design. The FEA for the aluminum extrusion can also be seen below in Figure 36. The max stress is 85 MPa which is below the 6105-T5 aluminum yield stress of 241 MPa. This allows for a factor of safety of 2.84. The max deflection the extrusion will experience is 3.5 mm. This displacement is also small enough to not raise concern.

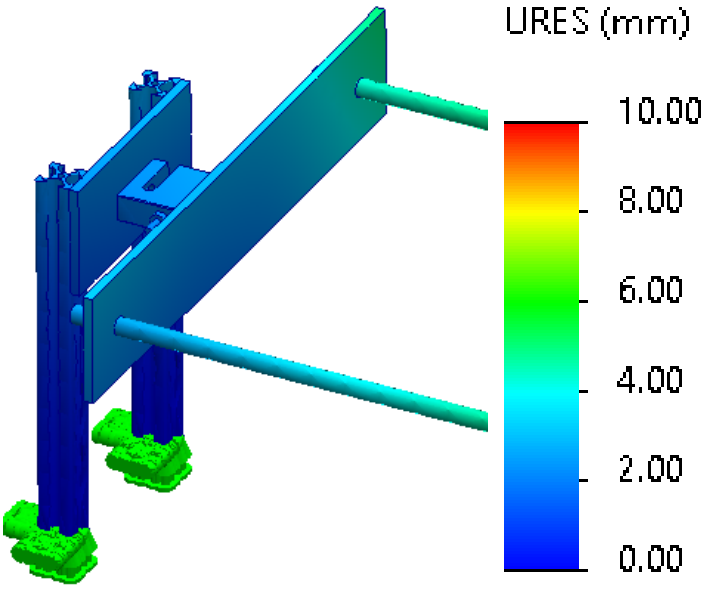

Figure 36. Displacement Graph of Load Cell Interface

The threaded rods will experience axial compression when the engine is running, so a stress calculation was done below. There are two threaded rods being compressed, so the force input into the equation was 500 N. The diameter of each rod is ½ inch, and was converted to 0.0127 m.

$$\sigma = \frac{F}{A} \tag{7}$$

$$\sigma = \frac{500\ N}{\pi\left(\frac{0.0127\ m}{2}\right)^2} \tag{7a}$$

$$\sigma = 3{,}947{,}050\ Pa = 3.947\ MPa \tag{7b}$$

The tensile yield strength of these threaded rods is 350 MPa which is well above the stress it would experience while the engine is running. This gives a factor of safety of 89 as shown below in Equation (8).

$$FoS = \frac{350\ MPa}{3.947\ MPa} \tag{8}$$

These threaded rods also need to account for buckling due to their length and slenderness. The critical force required for buckling to occur was calculated below. The end conditions are fixed-fixed, and the material of the rods are 1018 Low Carbon Steel.

$$F_{cr} = \frac{\pi^2 EI}{(kL)^2} \tag{9}$$

$$F_{cr} = 27.81\ kN \tag{9a}$$

The critical force required for buckling is 27.81 kN which is well above the 500 N of force each threaded rod will experience during testing. With this value found, a factor of safety was calculated below for each rod. The factor of safety for the threaded rods in buckling is 55.62.

$$FoS = \frac{F_{cr}}{F_{expected}} \tag{10}$$

$$FoS = \frac{27810\ N}{500\ N} = 55.62 \tag{10a}$$

6 Fabrication

6.1 Diffuser

The manufacturing process for the diffuser began by cutting a disk from round aluminum stock that was nine inches in diameter and two inches thick. This was done by using a horizontal metal band saw allowing the team to achieve a thickness that was roughly accurate to the dimensions. The disk was then milled, using a lathe, to face the piece shown in Figure 37. The surface finish needs to be flat for accurate measuring and to allow proper fixturing. The disk can then be moved to a 3-axis milling machine as illustrated in Figure 38 below. A 3-axis mill operates in the xyz-plane where the working table and the saddle of the machine moves the part in the xy-plane, and the cutting tool moves in the z-axis. This machine allows for the wedges and the bolts holes of the diffuser to be cut with high dimensional accuracy. The fins of the diffuser were cut using the same 3-axis machine with a manual indexer that allowed for rotary motion, as shown in Figure 39. A program was written in the xy-plane to cut the profile of each blade. The total depth of the blades was half an inch, these where cut in three equal depth passes. Once a single blade was milled the indexer was rotated 11.25 degrees and another blade was cut. This was done 32 times to mill each blade. After these blades were cut there was still left over material between blades, the indexer was manually turned, and the excess material was milled manually. Once completed the part will need to be deburred to ensure that handling of the part will not cause harm to the user. To do this, the team filed each edge and sanded each part, with the final part shown in Figure 40.

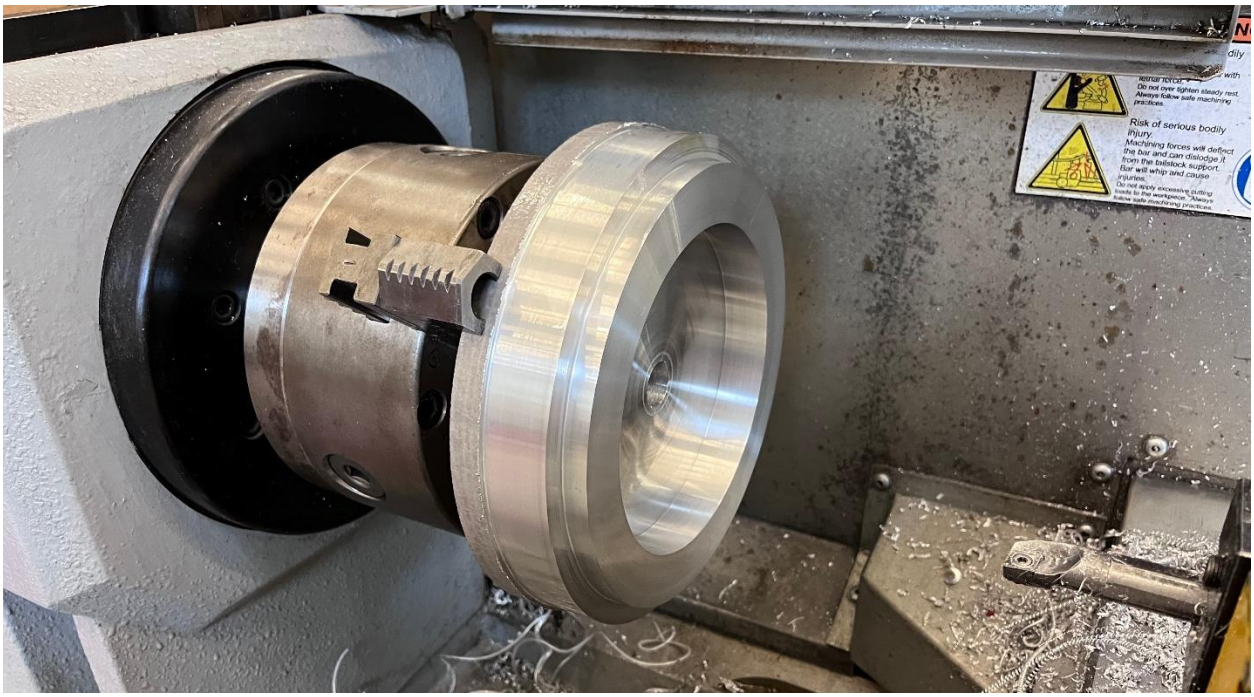

Figure 37. Diffuser Facing and Profiling on the lathe

Figure 38. Diffuser wedge milling with 3-axis capabilities

Figure 39. Diffuser guide vane milling with indexer capabilities

Figure 40. Diffuser after milling

6.2 Combustor

The combustor was cut from a flat sheet of steel using a water jet. The flat sheets were then rolled using a hand powered roller seen in Figure 41. Each part of the combustor had to be rolled separately and in multiple steps to ensure that the sheet was not being warped or flattened. The conical shapes were also rolled using the same machine and a rubber mallet had to be used to ensure the largest radius of the piece entered the machine orthogonally. If the largest radius did not enter orthogonally the edges would not line up and the piece could not be welded. Once all the pieces of the combustor were rolled, it was the welded using a Lincoln tig welder. The final combustor is shown in Figure 42 through Figure 45.

Figure 41. Special rolling technique used for rolling all parts

Figure 42. Rolled combustion components

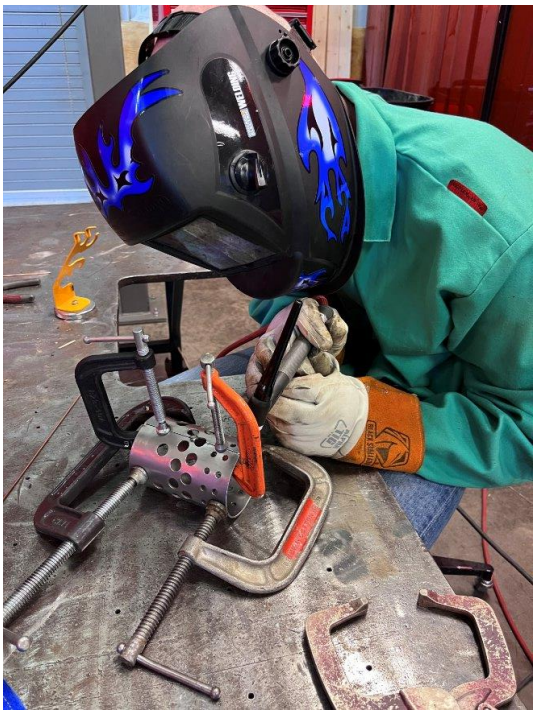

Figure 43. Welding internal combustor components

Figure 44. Internal combustor components (left) external components (right)

Figure 45. Final combustor assembly

6.3 Fuel and Ignition System

The stainless-steel tubing for the fuel ring was bent using a custom 3D-printed tool that was a quarter of the final circumference. This tool allowed the team to bend the ring to the correct diameter with the least amount of warping. Holes were then drilled where the capillary tubes would extend from the fuel ring. Finally, the capillary tubes were cut to the correct length and attached to the fuel ring using high-temperature JB weld. The final assembly was not photographed before being assembled into the combustor, so the team cannot show it in this report.

6.4 Stator and Turbine

Firstly, due to machining concerns and time considerations, mild 1018 steel was purchased from McMaster-Carr for the stator and turbine. This steel is easier to machine than tough 310 stainless that the components were designed for. This means that the turbine and stator can see less heat from the combustor, but this fabrication decision was necessary in the completion of the engine.

The stator and turbine were made in a very similar manner to the diffuser. Each was faced and centered using the lathe. However, the team did not profile the hubs of these components on the lathe, instead the team milled each hub on the 3-axis mill, as shown below in Figure 46. This allowed for swifter production of both the components. These components were both designed with a hole pattern centered within their hubs. This allowed the team to fixture the component into the indexer and avoid milling into the indexer, as shown in Figure 47, and highlighted with a blue arrow. Once this was complete the blades on the outside were milled in three equal depth steps. Each blade was cut with a single program and manual indexed to the next blade position. All excess material was cut with manual indexing and manual milling. The stator and turbine were both placed in a deburring tumbler with abrasive material to break all edges. The final stator and turbine are shown in series in Figure 48.

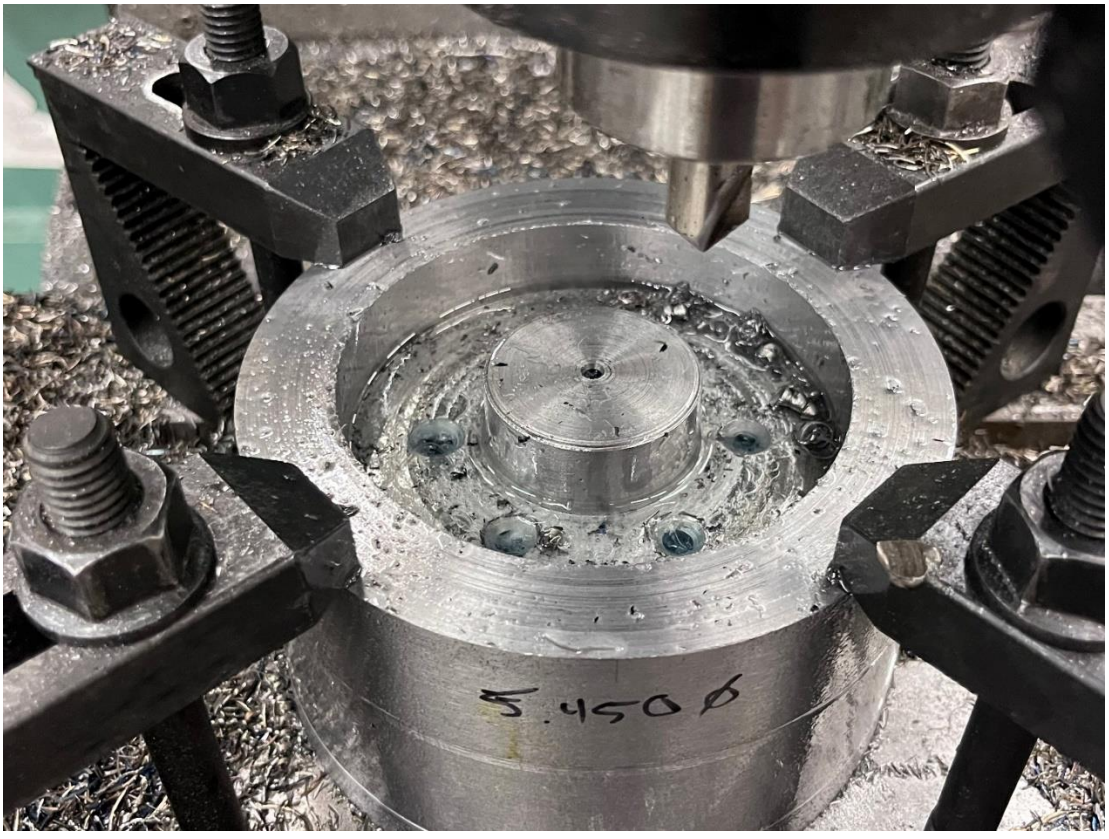

Figure 46. Stator being pocketed with the 3-axis mill

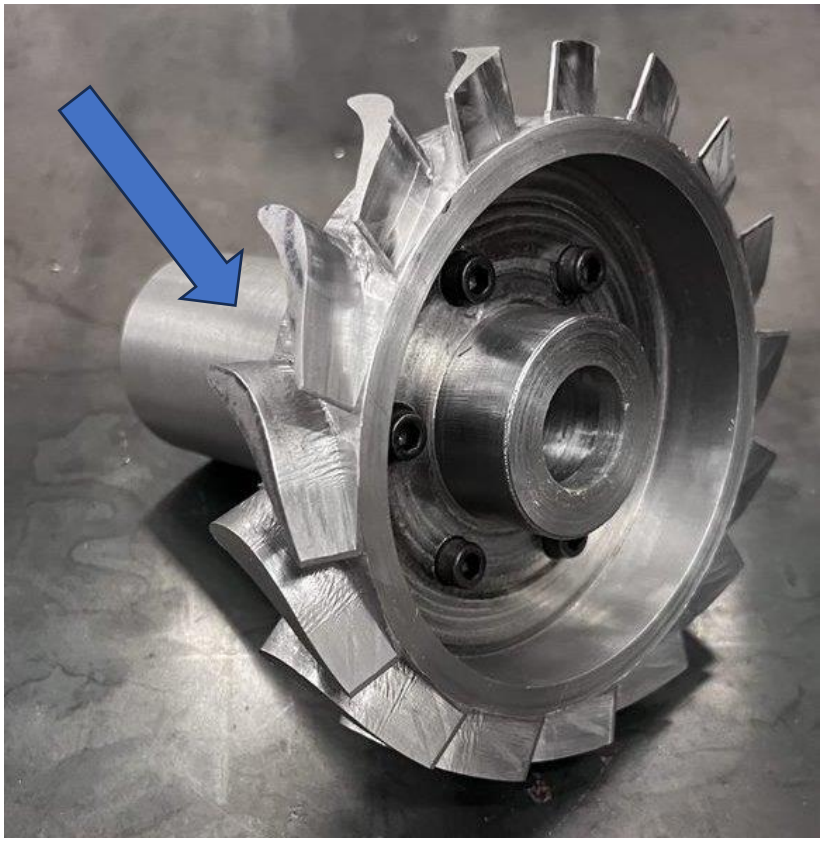

Figure 47. Fixture used to attach stator and turbine to indexer

Figure 48. Final stator and turbine as they will be assembled on shaft

6.5 Shaft

The shaft was fabricated using the lathe shown below in Figure 49. The diameters of the shaft were lathed to the correct dimensions with tolerances. The first shaft that was lathed was not used since it did not include proper tolerances or fittings for the compressor and diffuser, leaving them to wobble slightly. Additionally, the team realized that Chromoly is more difficult to machine than we expected. The surface finish on the first shaft was much rougher than allowed. The threaded ends were also lathed on either end of the shaft using an M10×1 left-handed die. The first lathed shaft is shown below in Figure 50.

Figure 49. First shaft on the lathe

Figure 50. Completed first shaft

Therefore, a second shaft was lathed to correct the tolerance issue. Since the team had more experience lathing Chromoly, the second iteration was lathed quicker and more precisely due to the need of higher tolerances for the press fits. Additionally, to achieve the designed press fits, the compressor and turbine were heated in the AECs furnaces to expand their inner hole diameter, then attached to the shaft. As the components cooled, the team verified that the components fit tightly on the shaft with no wobble. The team originally planned on using liquid nitrogen to cool the shaft, but we ran out of time to borrow more from USI's chemistry department. Again, the team did not photograph the second shaft before attaching all the components, but it looks very similar to the first iteration with minor changes described in this paragraph.

6.6 Casing

The casing was cut from the waterjet into four pieces. The only casing material manufactured was from stainless steel but plans for the aluminum and carbon fiber casings to be manufactured are in place. After water jetting, the pieces were rolled to their size and welded together. Much work was needed to shave down the interior of the casing walls to ensure the engine interior would fit. A slight slot was cut out of the casing walls to allow the fuel line to install correctly. An image of the 3D printed casing is shown in Figure 51, highlighted with an

orange arrow. Again, the team forgot to photograph just the casing, but it can be seen on the outside of the jet engine, as shown in Figure 52, highlighted with an orange arrow.

Figure 51. 3D printed casing (in dark blue)

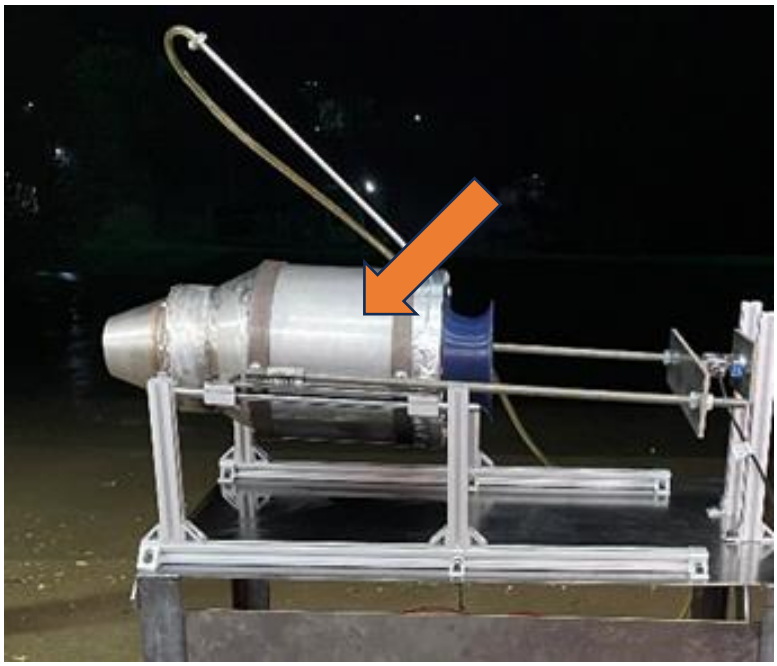

Figure 52. Completed casing on turbojet engine

6.7 Nozzle

The nozzle was cut from the waterjet and rolled to the correct size. It was then welded together with the nozzle flange to attach to the casing. An image of the completed nozzle is

shown below in Figure 53. Bolts were welded to the rear flange connected to the casing to fit the holes on the nozzle flange, which is shown below in Figure 54, highlighted with an orange box.

Figure 53. Completed nozzle fabrication

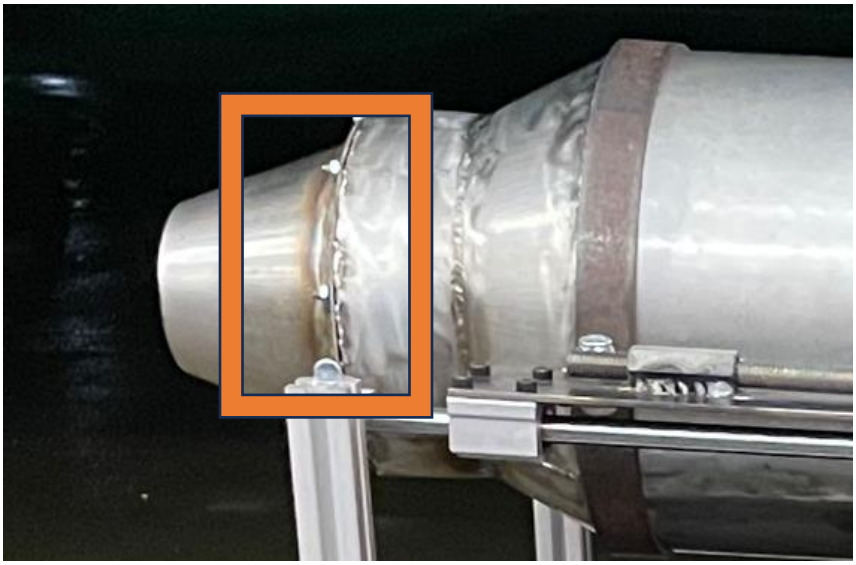

Figure 54. Bolt configuration to attach the nozzle

6.8 Electronic Control Unit

The electronic control unit consisted of many components, many of which were purchased. These components were all attached to the test bench then wired together. The base components of the ECU as attached to the test bench are shown below in Figure 55.

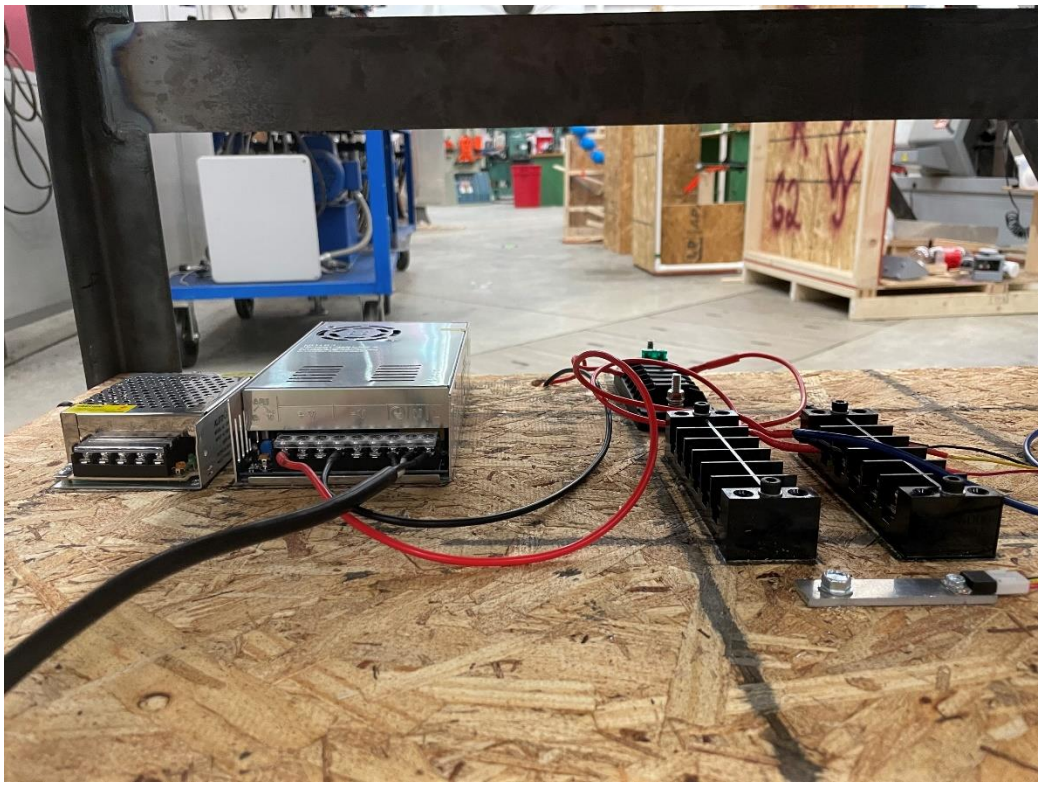

Figure 55. Completed ECU setup

6.9 Test Bench

The completed test bench is shown below in Figure 56, highlighted with the blue arrow. The angle iron legs were welded to the sheet metal baseplate. The main manufacturing method used was fasteners. The aluminum extrusion, plywood shelving, aluminum short-side cross bars, casters, and floor brackets were all secured to the test bench using various sized bolts, washers, and nuts from the AEC. Standard drills and the drill press were used to cut the holes for the fasteners. Additionally, the long-side straight bars were welded to the inside of the angle iron

legs. The ECU and fuel pump were secured to the plywood with additional fasteners, as well as the ECU being raised slightly to keep it balanced during operation.

Figure 56. Fabricated test bench

The completed engine fixture is shown below in Figure 57, highlighted by the orange arrow. The clamshell mounts were rolled, and holes cut out for the fasteners. The clamshell mounts were attached to steel sheet metal, which connected to the linear guide rail system. To engage the loadcell, long nuts were welded to the sheet metal to connect the threaded rods to the engine. The threaded rods are attached to the long ¼-in thick steel plate to engage the load cell (not pictured). The loadcell was attached to another ¼-in thick metal using a custom fastener supplied by the load cell's manufacturer.

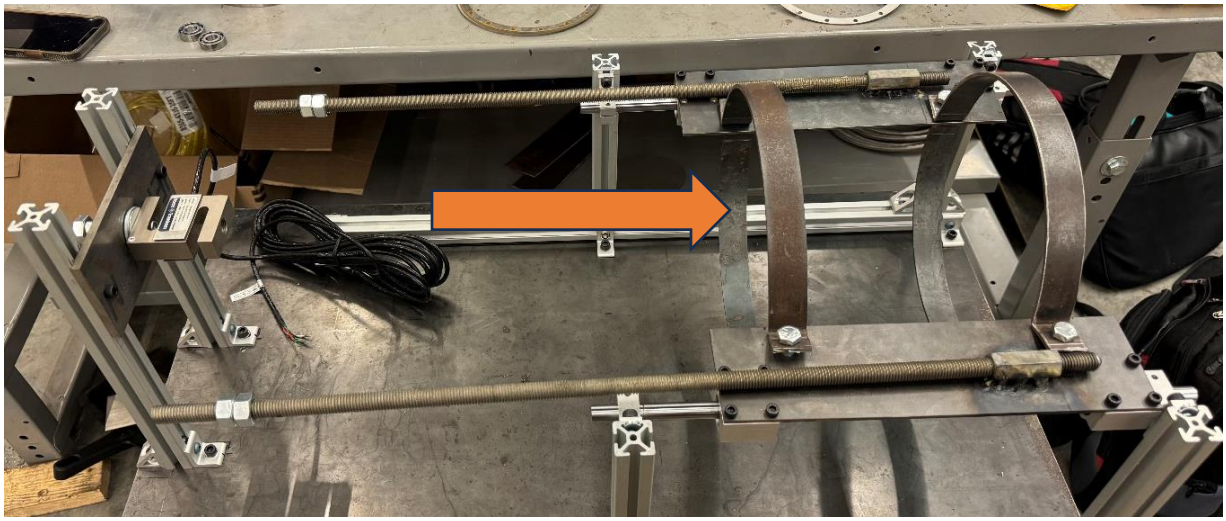

Figure 57. Completed jet harness

RESULTS

In this section, the results of the design and fabrication are outlined, as well as the budget, disposal plan, lessons learned, future work, and the conclusion of the project.

1 Testing and Results

After the team fabricated and assembled the engine, there was little time for testing. However, the engine was not able to run and sustain thrust. As mentioned before, the team is planning on conducting further research into alternating casing materials for weight saving properties. Additionally, the team has plans in place to at least leave proof of concept testing for applying Cerakote on the turbine and stator. This will be carried out using the 310 stainless steel sheet, the same used for the casing, and applying Cerakote to the sheet to see how much better or worse it can handle incoming heat.

The result of the design of the engine was that it met the technical requirements set for the engine. The engine was designed to achieve 1150 Newtons of thrust, weighs around 120 Newtons, and fits exactly within the 50×25×25 cm^3 footprint. Additionally, the engine is designed to run for more than two minutes and operate at a temperature and pressure of 20°C and 1 atm. The team's engine was compared to two typical engines on the market to compare benchmark characteristics, as shown in Table 10.

Table 10. Comparable miniature turbojet engine characteristics

Specification	SHX-1200N [23]	JetCat P1000-PRO [21]	Our Engine
Footprint ()	50×20×20	44×23×23	50×25×25
Thrust (N)	1000	1100	1150
Weight (N)	91	108	120
Thrust-to-Weight Ratio	11:1	10:1	9.6:1

2 Budget and Disposal Plan

The budget for the project is shown in Table 13 in Appendix D. The team applied for and was granted extra money through USI's Endeavor Grant, and we will present the findings of our research at the Endeavor Symposium next April. Since the team used money from the engineering department, the engine will be donated to USI to aid in educating students about jet engines. Additionally, dimensional drawings of each component will be included in the deliverables, as mentioned in Section 1 of the Introduction, so that if a part were to break or need replaced, the University has the information available needed to get the engine running again.

3 Lessons Learn and Future Work

As shown throughout the report, this project was a large undertaking. The team realized from past senior design projects that fabrication was the challenging aspect, and to leave sufficient time to achieve this stage of the project. From the schedule, which is shown in Tables 11 and 12 in Appendix B and C, the team originally scheduled more than a month for fabrication and testing, with buffers, to complete the project at a reasonable time. However, fabrication still took longer than expected due to the inherent complexity of the major components and needing

outside help from professional machinists. Manufacturing plans should have been in place well before the spring semester started to achieve the completion of the project within a reasonable period.

After the completion of the project, the team learned many things about the engineering design process to prepare for our careers. Firstly, the team experienced what many projects before us experienced: challenges during the fabrication process. With our reliance on machinists whose time is limited and lead time for needed tooling, the fabrication process got behind quickly. This was also due to the critical design taking longer than expected. The team ran into interfacing challenges and trouble working through equations to size components. These two setbacks combined led to significant delays that were difficult to overcome.

Despite the challenges and setbacks, the team stuck together to try to complete the project. Effective communication was key to achieving deadlines in a timely manner, as well as realistic expectations for work needed to be completed over the week and weekend. Although the project was challenging, the experience the team gained will be invaluable in the future.

There are many components and designs that can be improved upon in the future work of this project. First, the test bench could be designed to allow for more ease of adjusting lengths and widths if the engine itself changed dimensions. The aluminum extrusion the team utilizes already has good maneuverability, but adjusting the engine fixture clamshell mounts to be customizable to different radii of engines will allow for an easier testing experience. Additionally, a variable sized exhaust nozzle could be implemented to further increase thrust production. A nozzle, possibly compliant, that expands or retracts according to changes in RPM would be more efficient in expelling the air to the atmosphere and therefore producing even more thrust at potentially the same or less weight. Finally, the two-stage compression design that the team considered early in the preliminary design could be developed further. Due to the overarching scope of our project, the design of the two-stage compression could be a project on its own to determine its feasibility in a miniature engine.

4 Conclusion

Enhancing aircraft propulsion methods have been ongoing since the emergence of powered aviation, focusing primarily on traditional piston-driven, gas turbine, and electric motor engines. The thrust-to-weight ratio has proved a pivotal metric for assessing the engine’s

performance, offering numerous benefits such as improved maneuverability, top speeds, and flight times. This report aimed to contribute to this field by designing and fabricating a miniature turbojet engine inspired by existing miniature engine models used in radio-controlled aircraft. Through technical specifications and thorough design calculations, the team achieved a thrust-to-weight ratio of 9.6:1, meeting the most critical technical requirement. While the engine has yet to undergo testing, its successful manufacturing and assembly mark a significant step forward toward research for the specific engine, with potential implications for large-scale and more efficient engines.

REFERENCES

[1] Almazan, Alexander, et al. *Small Jet Engine Test Fixure, Design and Fabrication*. Worcester: Worcester Polytechnic Institute, 2023.

[2] Ananthan, Adithya and Thomas Renald. *DESIGN AND FABRICATION OF MICRO JET ENGINE OF T/W OF 8:1*. June 2021. <https://www.researchgate.net/publication/354167778_DESIGN_AND_FABRICATION_OF_MICRO_JET_ENGINE_OF_TW_OF_81>.

[3] Ballal, Dilip and Arthur Lefebvre. *Gas Turbine Combustion*. Boca Raton: Taylor and Francis Group, 2010. Book.

[4] Benson, Tom. *Ideal Brayton Cycle*. 13 May 2021. Article. 3 April 2024.

[5] Budynas, Richard and Keith Nisbett. "Shafts and Shaft Components." Budynas, Richard and Keith Nisbett. *Shigley's Mechanical Engineering Design*. New York: McGraw-Hill, 2020. 373-420. Textbook.

[6] Cengel, Yunus, John Cimbala and Afshin Ghajar. *Fundamentals of Thermal-Fluid Sciences*. McGraw Hill, 2021.

[7] Cumpsty, Nicolas. *Jet Propulsion: A Simple Guide to the Aerodynamic and Thermodynamic Design and Performance of Jet Engines.* Cambridge University Press, 1997.

e, Engineer's. n.d.

[8] Engineers Edge. *Preferred Mechanical Tolerances Metric ISO 286*. 2024. Website. 18 March 2024.

[9] Fahlström, Simon and Rikard Pihl-Roos. *Design and Construction of a Simple Turbojet Engine*. Uppsala: Uppsala University, 2016.

[10] Farohki, Saeed. *Aircraft Propulsion*. John Wiley & Sons, Incorporated, 2014.

[11] Hall, Nancy. *Combustor - Burner*. 13 May 2021. Article. 22 April 2024.

[12] —. *National Aeronautics and Space Administration*. 13 May 2021. Diagram.

[13] "HexTow AS4 Data Sheet." 2023. *HEXCEL*. PDF. 5 4 2024.

[14] Hünecke, Klaus. *Jet Engines: Fundamentals of Theory, Design, and Operation* . Airlife, 2017.

[15] Lakshminarayanan, P.A. and Yogesh Aghav. *Modeling Diesel Combustion*. Singapore: Springer, 2022.

[16] Lescarbeau, Doug and Rob Dunkel. *Increasing Strength and Reliability of Interference Fits*. 1 October 2013. 25 April 2024.

[17] *MatWeb*. n.d. 23 4 2024.

[18] Pereira, Rui Gonçalo Gonçalves Esteves. "Design and Manufacture of a mini-turbojet." 2020. *uBibliorum.* <https://ubibliorum.ubi.pt/bitstream/10400.6/10627/1/7410_16026.pdf>.

[19] Pferd. *Fits and Tolerances Calculator*. 2024. Website. 18 March 2024.

[20] Putra, Cahya. "Design and Analysis of Annular Combustion Chamber for a Micro Turbojet Engine." *ResearchGate* (2020).

[21] Quellwerke, JetCat. *JetCat P1000-Pro*. n.d. 13 April 2024.

[22] Val deOlloqui, Chuck Margraves. *Developing A Jet Test System on a Shoestring Budget: An Application of Project-Based Learning*. 2019. 25 4 2024.

[23] Website, China Defence. *100kg Thrust Turbojet Engine SXH-1200N(Low Cost)*. n.d. 17 April 2024.

APPENDIX

Appendix A – System Hierarchy

Appendix B – Proposed Schedule

Appendix C – Actual Schedule

Appendix D – Budget

Appendix E – Design Mass Table

Appendix F – Concept of Operations

Appendix G – FMEA's

Appendix H – Mechanical Block Diagram

Appendix I – Standards

Appendix J – ABET Outcome 2, Design Factor Considerations

Appendix K – Technical Drawings

Appendix A – System Hierarchy

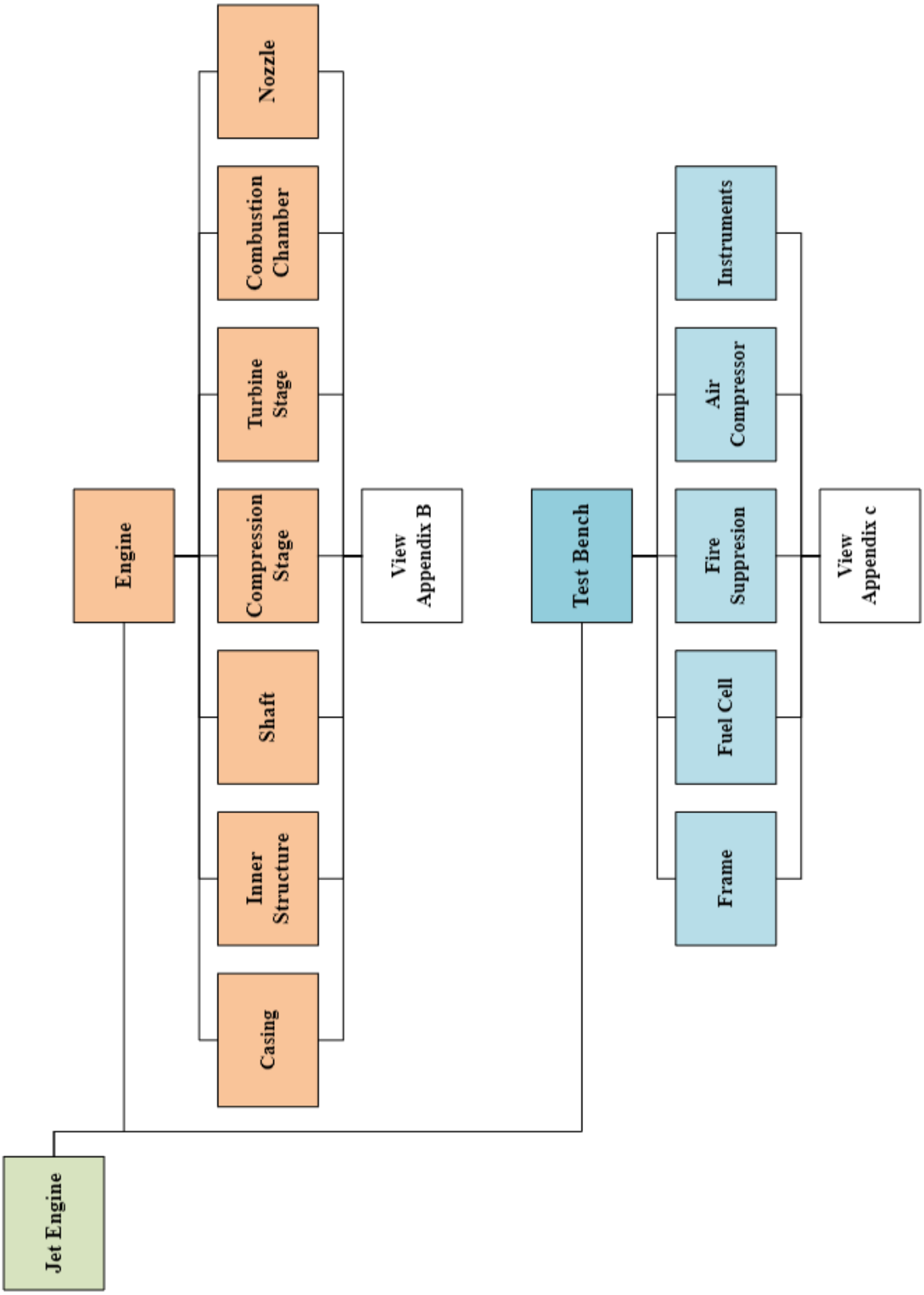

Appendix A – System Hierarchy Continued

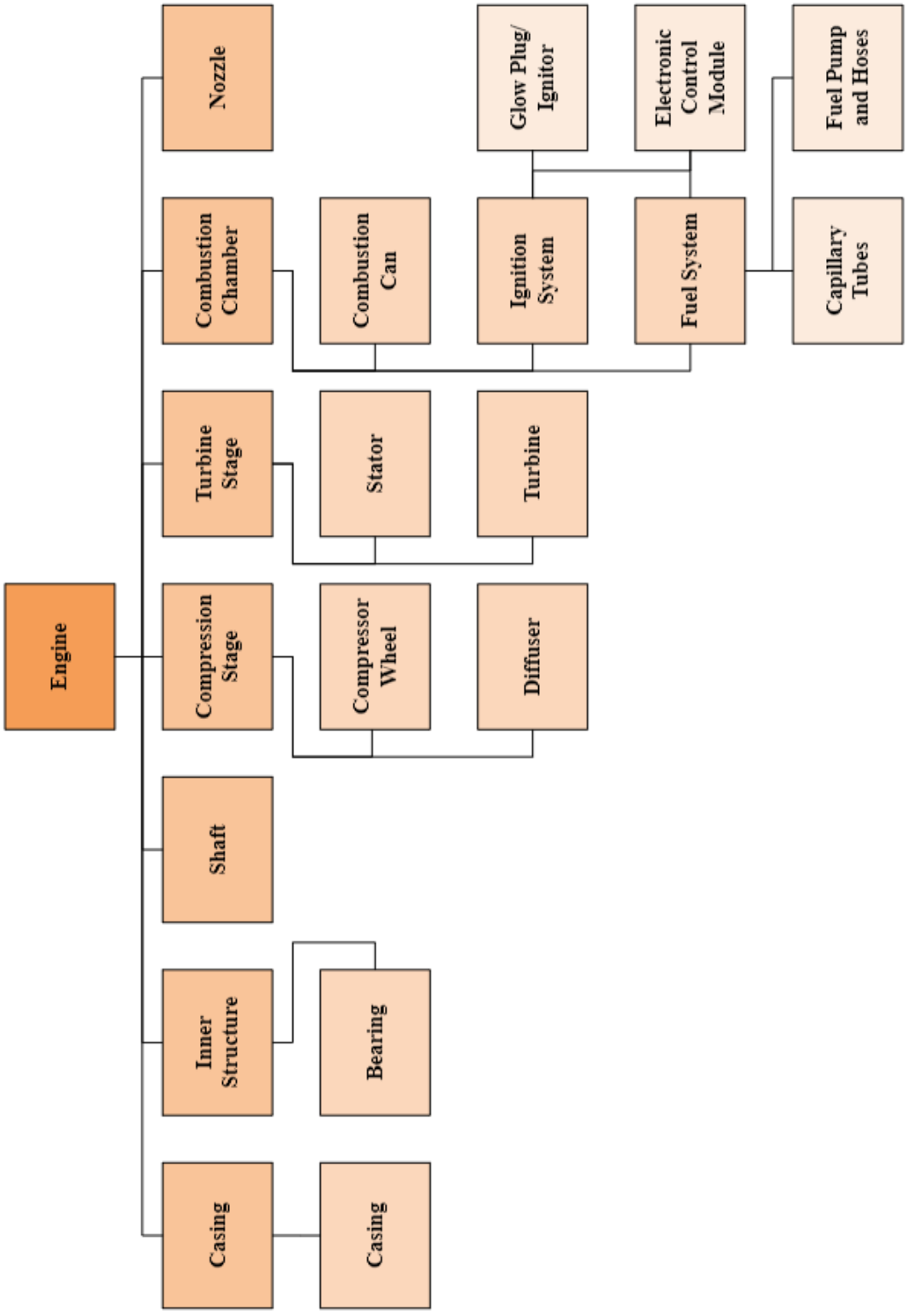

Appendix A – System Hierarchy Continued

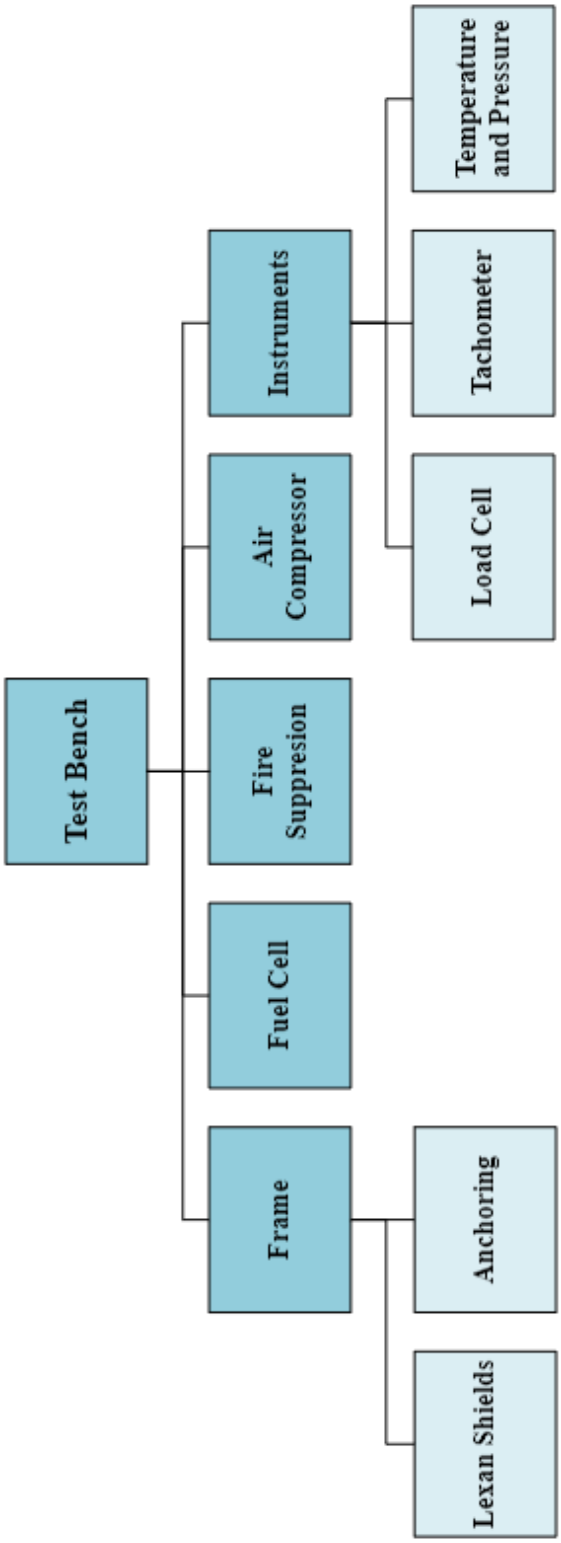

Appendix B – Proposed Schedule

Table 11. Proposed schedule for fall 2023 and spring 2024 semesters

Fall 2023 Semester	**Date**
Final Draft of Senior Design Proposal	10/06/2023
Assign Components to Team Members	10/06/2023
3 Design Concepts	10/11/2023
Senior Design Proposal Oral Presentations	10/16/2023
Preliminary Design Review Oral Presentation	11/13/2023
Begin Solid Modeling Components	11/20/2023
Ethics and Professionalism Discussion	11/27/2023
Systems Engineering Quiz	11/29/2023
Agreed Upon Preliminary Design	11/30/2023
Engineering Economics Module and Quiz	12/01/2023
Pre-Senior Design Report	12/07/2023
Spring 2024 Semester	**Date**
Begin Fabricating Engine	01/06/2024
Arrange Weekly Meetings with Faculty Advisor	01/08/2024
Critical Design Review	02/08/2024
Submit Order for Parts	02/09/2024
Initial Testing of Components and Engine	03/11/2024
Complete Fabrication and Testing of Engine	03/22/2024
Design Presentation Reviews Complete	03/29/2024
Final Test Run and Remanufacturing (if needed)	04/01/2023
Check Grammar and Punctuation at Writer's Room	04/03/2024
Draft Due to Advisor	04/05/2024
Practice for Senior Design Presentation	04/12/2024
Senior Design Presentation	04/19/2024
Senior Design Poster Session	04/25/2024
Final Report and Shared Drive Due to Advisor	04/26/2024
Final Report submitted to SOAR	05/03/2024

Appendix C – Actual Schedule

Table 12. Actual schedule of spring 2024 semester

Spring 2024 Semester	Date
Set up weekly meeting with advisor	1/08/2024
Endeavor Grant application submitted	02/05/2024
Critical design review	2/18/2024
First bill of materials submitted	02/20/2024
Begin engine fabrication	02/23/2024
Second bill of materials submitted	03/11/2024
Design presentation review	03/26/2024
Third bill of materials submitted	04/01/2024
Report draft to advisor	04/05/2024
Poster due to OneDrive	04/12/2024
Senior design presentations	04/19/2024
Senior design poster night	04/25/2024
Final report and flash drive due to advisor	04/26/2024
Final report submitted to SOAR	04/26/2024

Appendix D – Budget

Table 13. Total budget for turbojet project

Items	Quantity	Unit Price	Total Price
Easy-to-Weld 4130 Alloy Steel Rod, 3-inch dia. By 1 ft. long	1	$177.96	$177.96
Easy-to-Weld 4130 Alloy Steel Sheet, 36 inches by 36 inches by 0.0800 inch	1	$173.23	$173.23
K-Type Thermocouple PK-1000 Temperature Sensor High Temperature	2	$39.99	$79.98
Taiss LJC18A3-H-Z/BY Proximity Switch 1-10mm Distance Measuring Capacitance Proximity Sensor Switch PNP NO	2	$11.99	$23.98
Arduino Mega 2560	1	$48.00	$48.00
Gravity: Air Pressure Sensor (15-700kPa) - I2C - MPX5700AP	4	$64.90	$259.60
Firma 85A Brushless Smart ESC / 4000Kv Sensorless Motor Combo	1	$104.99	$104.99
OS Engines A3 Glow Hot Plug	2	$14.00	$28.00
316 Stainless Steel Tubing 0.1" OD, 0.009" Wall Thickness, 3 ft Long	2	$46.17	$92.34
Easy-to-Weld 4130 Alloy Steel Round Tube, 6 ft long	1	$33.07	$33.07
Smooth-Bore Seamless 316 Stainless Steel Tubing	1	$61.76	$61.76
309 Stainless Steel Sheet Metal 24" x 24" 0.059" thick	2	$210.89	$421.78
12 mm inner diameter, 28 mm outer diameter, 8 mm width Angular Contact Bearings for Shaft	2	$186.51	$373.02
Multipurpose 4140 alloy steel rod; 1.5 inch diameter 6 feet long	1	$164.27	$164.27
2Pcs 12mm x 400mm (0.472 x 15.74 inches) Vigorous Linear Motion Rods	1	$14.99	$14.99
4PCS SK12 Aluminum Linear Motion Rail Clamping Rod Rail Guide Support for 12mm Diameter Shaft	1	$12.49	$12.49
SCS12UU Linear Ball Bearing Aluminum Slide Block, ID 12mm Linear Motion Ball Bearings CNC Slide Bushing	1	$18.73	$18.73
25Pcs M8 304 Stainless Steel Rigid Pipe Strap	1	$5.99	$5.99

Appendix C – Budget Continued

High-Strength Steel Threaded Rod	2	$10.18	$20.36
4 feet, 8 feet 7/16 inch thick plywood sheet for shelving to house electrical components and fuel cell	1	$14.90	$14.90
REVERE 363 S-TYPE LOAD CELL	1	$208.00	$208.00
700 mm long, 25 mm x 25 mm aluminum extrusion	2	$11.19	$22.38
300 mm long, 25 mm x 25 mm aluminum extrusion	2	$6.39	$12.78
200 mm long, 25 mm x 25 mm aluminum extrusion	4	$5.19	$20.76
Gussets	12	$5.90	$70.80
Brackets	8	$5.32	$42.56
Bolts and T-nuts for connecting gussets and brackets	40	$0.72	$28.80
2x2x3/16 inch, 30 inches long steel angle iron	4	$15.30	$61.20
310S Steel 6" Dia 1.5" Thick (SRB 310 6" x 1-1/2")	2	$187.25	$374.50
Ceratkote Coating for thermal barrier (Quart-32oz)	1	$168.00	$168.00
Holley 100 GPH In-Line Electric Fuel Pumps 12-170	1	$179.90	$179.90
DC 12V 50A 600W Power Supply Adapter Transformer Switch AC 110V / 220V	1	$39.41	$39.41
G2 Powerstage Air Bundle: 3S 2200mAh LiPo Battery / S120 Charger, SPMXPSA200	1	$44.98	$44.98
APIELE (Pack of 2)22mm 2 Position Selector Switch Momentary	1	$15.49	$15.49
DaierTek Red 12V LED Lighted Toggle Switch	1	$9.99	$9.99
APIELE 22mm NC Red Mushroom Emergency Stop Push Button	2	$9.99	$19.98
uxcell 6 Positions Dual Rows 600V 60A Wire Barrier Block Terminal Strip	2	$9.49	$18.98
6 Way Fuse Block Blade Fuse Box with Negative Bus, 6 Circuit Fuse Holder Fuse Block	2	$11.99	$23.98

Appendix C – Budget Continued

ZIPCCI 80 Pcs Standard Car Fuse, Fuses Assortment kit (80Standard	1	$7.99	$7.99
12 Gauge Wire Combo 6 Pack 12V 100'FT per Roll	1	$41.99	$41.99
5 Gallon fuel cell w/ fuel lines and fittings included	1	$104.89	$104.89
Fuel fitting for fuel pump	1	$11.77	$11.77
eSUN PLA+ Filament 1.75mm 1KG (U-Dark Blue)	1	$22.99	$22.99
eSUN PLA+ Filament 1.75mm 1KG (I-fire Engine Red)	1	$22.99	$22.99
eSUN PLA+ Filament 1.75mm 1KG (D-black)	1	$22.99	$22.99
eSUN PLA+ Filament 1.75mm 1KG (S-Green)	1	$22.99	$22.99
eSUN PLA+ Filament 1.75mm 1KG (N-Orange)	1	$22.99	$22.99
SPACEKEEPER Workbench Casters kit 660 Lbs - Retractable Casters Heavy Duty Bench Caster Wheels 4 Pack	1	$27.39	$27.39
Multipurpose 6061 Aluminum Sheet 0.08" Thick, 36" x 36"	1	$143.28	$143.28
Fuel line for fuel ring 25ft soft pvc fuel line	1	$21.25	$21.25
Corner Machine Bracket with 2 Mounting Slots, 316 Stainless Steel, 3" x 2" x 2"	4	$13.29	$53.16
Easy-to-Weld 4130 Alloy Steel 6" x 36" x 1/4"	1	$89.66	$89.66
High-Temperature 309/310 Stainless Steel Bar 1/4" Thick, 2" Wide	1	$103.89	$103.89
High-Temperature 309/310 Stainless Steel Sheet 0.12" Thick 12" x 12"	1	$96.11	$96.11
Fuel fitting for fuel pump	1	$14.00	$14.00
316 Stainless Steel, M10 x 1 mm Thread Size	4	$8.60	$34.40
Rod, 3-1/8" Diameter 3' Long	1	$163.52	$163.52
Heat Shrink Tubing Kit	1	$13.99	$13.99

Appendix C – Budget Continued

Insulated Wire Electrical Connectors with Wire Crimping Tool	1	$18.68	$18.68
316 Stainless Steel Tubing 5/16" OD, 0.035" Wall Thickness 6' Length	1	$60.00	$60.00
Zinc-Plated Steel Coupling Nut Extra-Long, 5/16"-18 Thread Size	2	$1.00	$2.00
- 6 AN Orb male to 5/16 hose barb	1	$11.77	$11.77
1/2 " diameter, 5 - 1/2" long steel stud anchor for concrete	4	$3.75	$15.00
12 mm inner diameter, 28 mm outer diameter, 8 mm width Angular Contact Bearings for Shaft	1	$186.51	$186.51
1/4"NPT Brass Electric Solenoid Valve Normally Closed	1	$15.69	$15.69
Hydraulic Check Valve	1	$9.90	$9.90
		Total Price	$4,853.72

Appendix E– Design Mass Table

Table 14. Masses for each component based on SolidWorks models

ITEM NO.	DESCRIPTION	QTY.	Component Mass (kg)	Mass (kg)	Weight (N)
1	Stator	1	1.17	1.17	11.43
2	Turbine	1	0.92	0.92	9.05
3	Combustion Chamber	1	3.37	3.37	33.06
4	Holset Hx82 152mm	1	0.57	0.57	5.59
5	Inner Structure	1	1.61	1.61	15.79
6	Angular Contact Bearing	2	0.03	0.05	0.52
7	Engine Shaft	1	0.75	0.75	7.32
8	Stator Housing	1	0.58	0.58	5.70
9	Fuel Ring and Capillary Tubes	1	0.04	0.04	0.36
10	Rear Flange	1	0.11	0.11	1.12
11	Casing	1	0.85	0.85	8.34
12	Inlet	1	0.24	0.24	2.38
13	Nozzle	1	0.92	0.92	8.99
14	Compressor Diffuser	1	1.14	1.14	11.15
			Total (kg) :	12.31	120.79

Appendix F – Concept of Operations

- Preheat Engine
- Increase Shaft and attached component's RPM
- Inject Fuel
- Throttle Engine

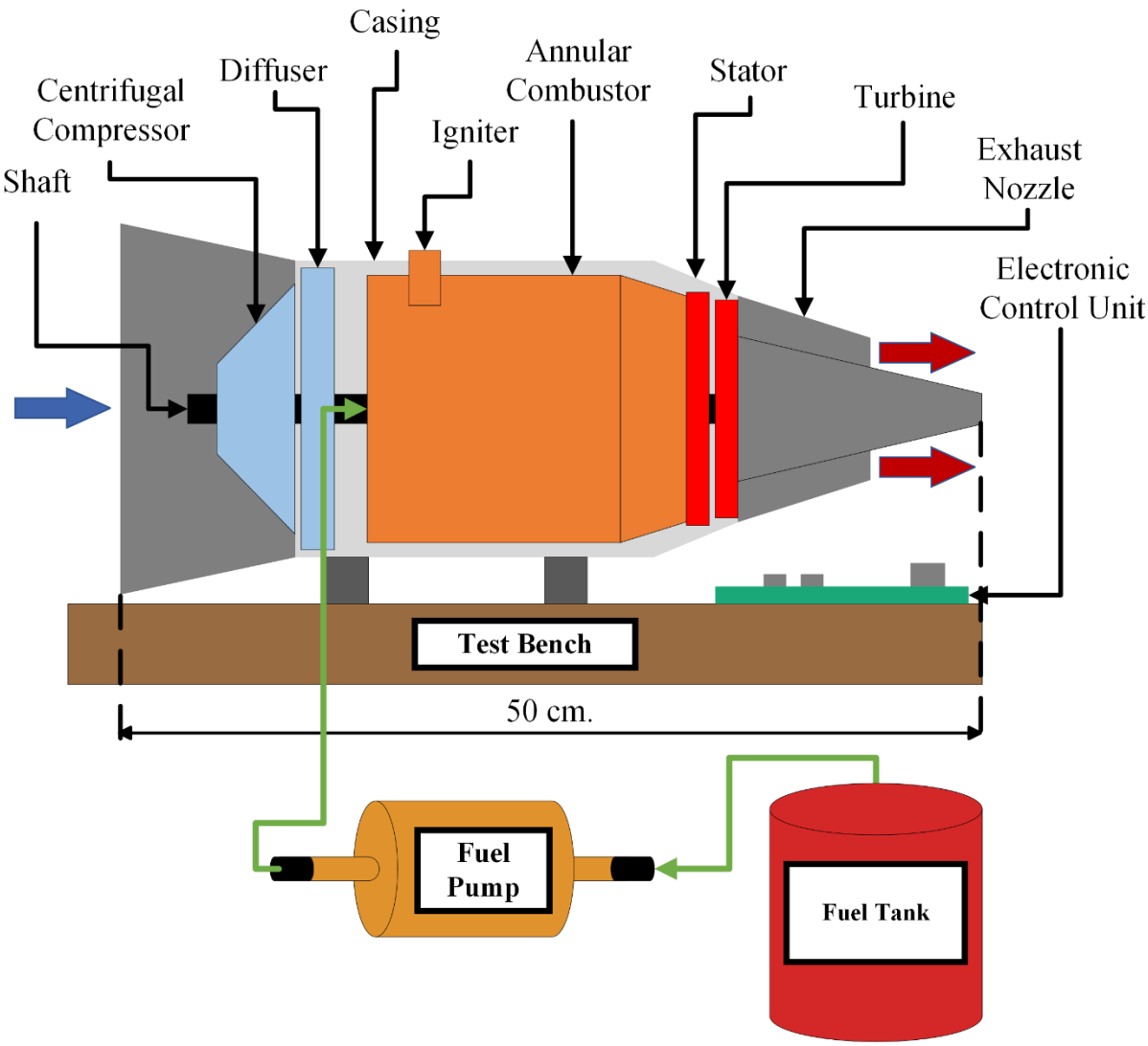

Figure 58. Turbojet engine concept of operations

Appendix G – FMEA's

Table 15. Turbojet FMEA

Item	Failure Modes	Cause of Failure	Possible Effects	Probability (of failure mode)	Severity (of failure mode)	Possible action to reduce failure rate or effects
Centrifugal Compressor	1. Compression ratio not enough	1. Low RPM, too small, single-stage design	1. Won't sustain thrust	1. Med.	1. High	1. Determine a sufficient compression through calc.
	2. Wobble	2. Weight distribution, asymmetric design	2. Shaft or compressor breaking during a test	2. High	2. High	2. Dremel and lathe techniques
Igniter	Does not cause combustion	Insufficient arc temperature, faulty placement	Continuous combustion won't be sustained, lower thrust output	1. High	High	Consider igniter placement carefully; more preliminary research into igniter placement, type, and temperature
Test Bed	1. Jet engine becomes loose or breaks free from the test bed	1. Fasteners are not tight, not secured, not of adequate dimensions for the	1. Damage to jet engine, surroundings, or to the team	1. Low	1. High	1. Ensure factors of safety are met from the requirements in fastener design choices
	2. Faulty thrust readings	2. Improper approach for this characteristic, faulty calibration on equipment	2. Misunderstand jet engine capabilities	2. Med.	2. Low	2. Preliminary research into testbed designs, reduce friction
Bearings	1. Melt/Burn, Crack	1. Engine gets too hot	1. Engine cycle halts or tears itself	1. Med.	1. High	1. Get ceramic gasket and high heat rated bearings
	2. Expands outside allowable tolerances	2. Thermal expansion from high temperatures	2. More friction, reduced rpms	2. Med.	2. Med.	2. Allow higher tolerances, cool the engine
Combustion Chamber	1. No combustion	1. Faulty air holes	1. Engine won't run	1. Med.	1. High	1. Calculate air hole placement and sizing correctly
	2. Melts	2. Low melting temp. material, too hot	2. Broken combustion chamber, catastrophic explosion	2. Low	2. High	2. Choose high-temp material, add a cooling system

Table 16. Customer FMEA

Item	Failure Modes	Cause of Failure	Possible Effects	Probability (of failure mode)	Severity (of failure mode)	Possible action to reduce failure rate or effects
Fuel Injection System	1. Fuel does not ignite properly	1. Wrong fuel used or ECU to injector timing issue	1. Engine may not run efficiently or at all	1. Med.	1. Med.	1. Clearly label fuel the engine can use in user instructions and provide instructions for ECU inputs
	2. Improper fuel flow	2. Pump with wrong fuel flow rating or improper throttle placement	2. Engine will not run	2. Low	2. High	2. Clearly label the fuel flow rating necessary
	3. Surge	3. Improper injector timing	3. Temperatures may rise above limit, compression ratio will drop significantly, and/or hot exhaust may exit	3. Med.	3. High	3. Include a cutoff switch to the fuel pump and provide clear ECU input instructions
Test Bed	1. Engine breaks free from fasteners	1. Deviating from proper test bed setup procedures	1. Harm to user and/or engine	1. Low	1. High	1. Provide setup procedures and the test bed intended for this specific engine
	2. Test bed flips	2. Forgetting to weigh or bolt the test bed down	2. Harm to user and/or engine	2. Low	2. High	2. Add a label on the outside casing asking if the test bed is secured
Turbine or Compressor	1. RUD or Rapid Unscheduled Disassembly	1. Lose internal pieces or external objects pulled into the inlet	1. Upon impact, high speed fragments of the unintended object or engine components will rapidly deconstruct	1. Med.	2. High	1. Repeat in the user instructions to conduct tests in a large open space with no loose parts in a provided caution area and give clear instructions on building the engine properly
Nozzle Exhaust	1. Combustion or burning of unintended people or objects	1. Wrongful placement of self or items within the caution area	1. Severe burns of self or burned objects	1. Low	2. High	1. Caution users to stay to the sides of the jet engine at a certain distance behind a safety shield and keep all objects the same distance and direction away during tests

Appendix H – Mechanical Block Diagram

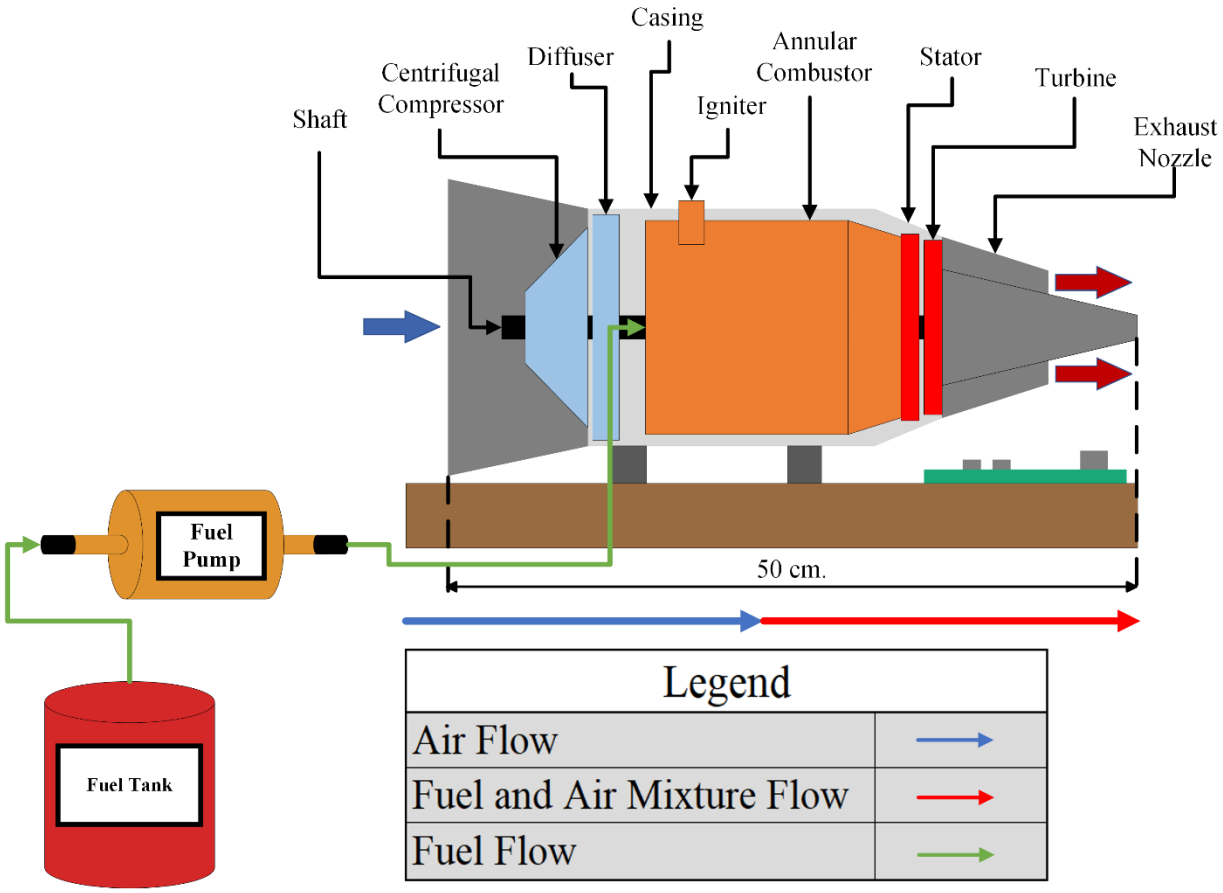

Figure 59. Mechanical block diagram of turbojet engine with components labeled

Appendix I– Standards

From the Federal Aviation Administration Code of Federal Regulations Part 33- Airworthiness Standards: Aircraft Engines

14 CFR 33.15. Materials: The suitability and durability of materials used in the engine must—

(a) Be established on the basis of experience or tests; and

(b) Conform to approved specifications (such as industry or military specifications) that ensure their strength and other properties assumed in the design data.

14 CFR 33.17(a). Fire Protection: The design and construction of the engine and the materials used must minimize the probability of the occurrence and spread of fire during normal operation and failure conditions and must minimize the effect of such a fire. In addition, the design and construction of turbine engines must minimize the probability of an internal fire that could result in structural failure or other hazardous effects.

From OSHA 1910.95(b)(1):

When employees are subjected to sound exceeding those listed in Table G-16, or Table 17 in this report, feasible administrative or engineering controls shall be utilized. If such controls fail to reduce sound levels within the levels of Table G-16, personal protective equipment shall be provided and used to reduce sound levels within the levels of the table.

Table 17. OSHA decibel standards (Table G-16)

Duration per day, hours	Sound level dBA slow response
8	90
6	92
4	95
3	97
2	100
1½	102
1	105
½	110
¼ or less	115

Appendix J- ABET Outcome 2, Design Factor Considerations

ABET Outcome 2 states "An ability to apply engineering design to produce solutions that meet specified needs with consideration of public health safety, and welfare, as well as global, cultural, social, environmental, and economic factors." ABET also requires that design projects reference appropriate professional standards, such as IEEE, ATSM, etc. These design considerations and professional standards are referenced in Table 18.

Table 18. ABET design factor considerations

Design Factor	Page number, or reason not applicable
Public health, safety, and welfare	Pg. 5, 80
Global	Pg. iii, 1
Cultural	Non-Applicable; no cultural implications
Social	Non-Applicable; no social implications
Environmental	Non-Applicable; under emissions level
Economic	Pg. 60, 69-74
Ethical & Professional	Pg. 80
Reference for Standards	Pg. 80

Appendix K- Technical Drawings

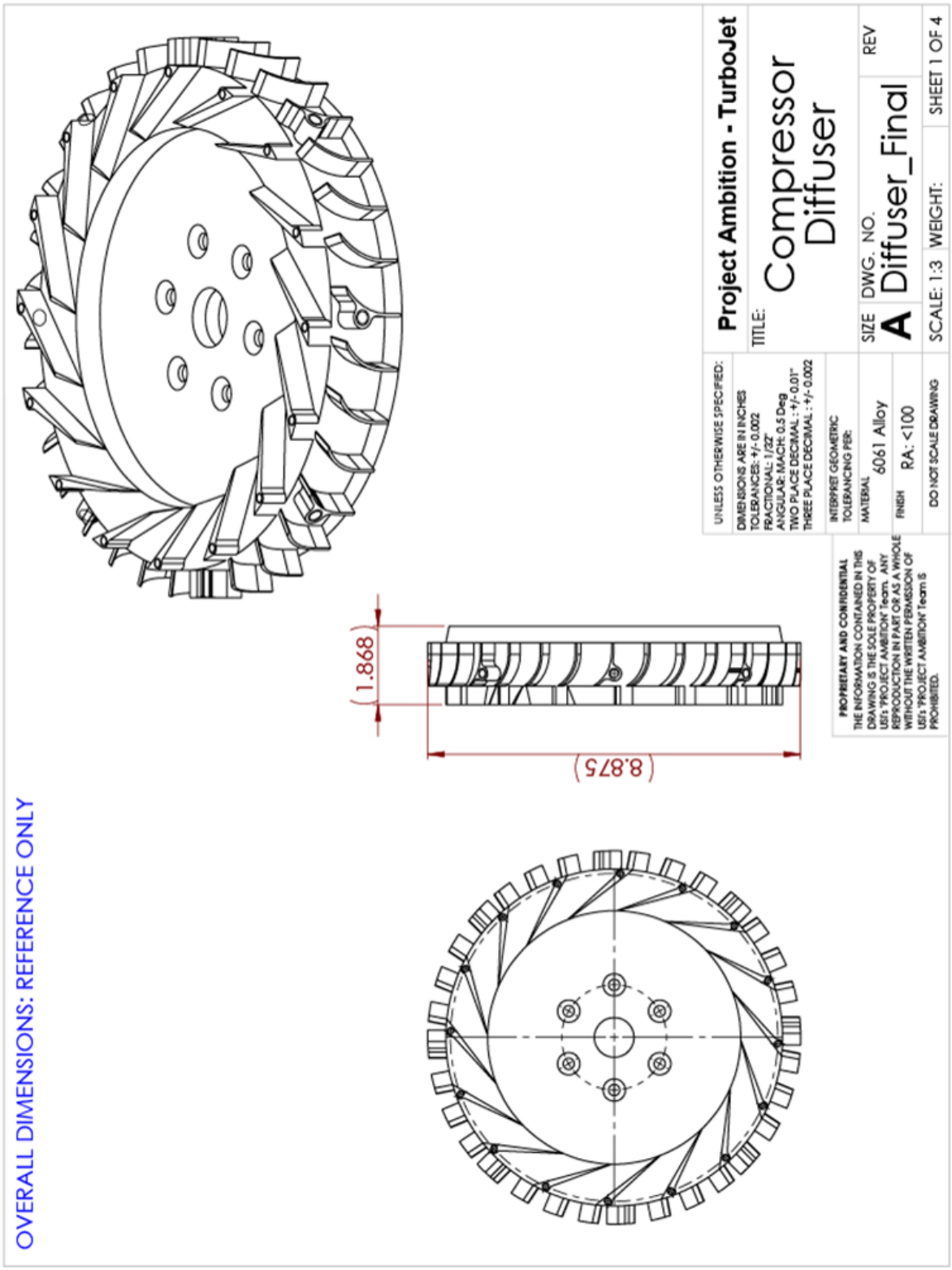

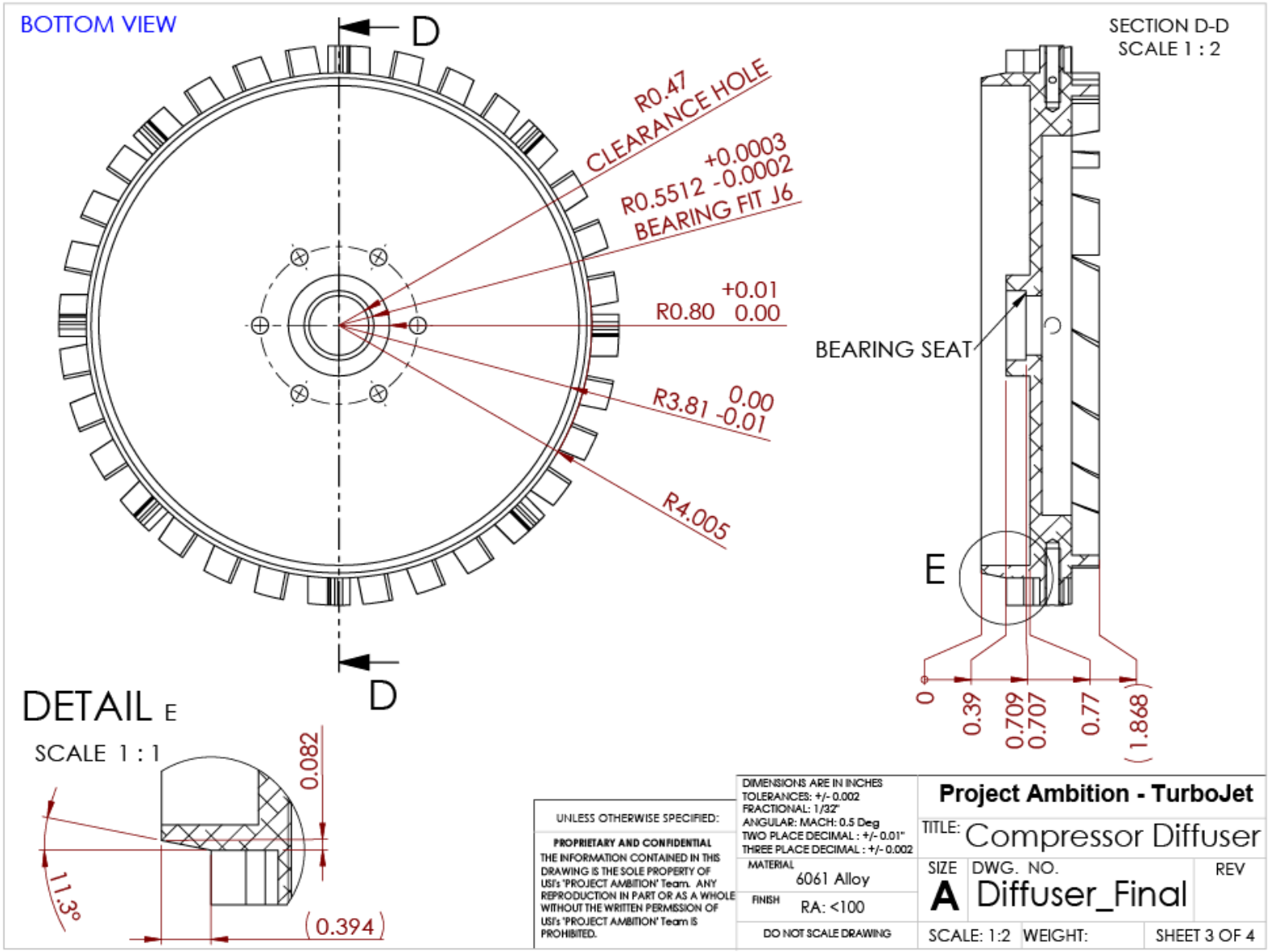
BOTTOM VIEW
D
R0.47
CLEARANCE HOLE
R0.5512 +0.0003 -0.0002
BEARING FIT J6
R0.80 +0.01 0.00
R3.81 0.00 -0.01
R4.005
D
SECTION D-D
SCALE 1 : 2
BEARING SEAT
E
0
0.39
0.709
0.707
0.77
(1.868)
DETAIL E
SCALE 1 : 1
0.082
11.3°
(0.394)
UNLESS OTHERWISE SPECIFIED:
PROPRIETARY AND CONFIDENTIAL
THE INFORMATION CONTAINED IN THIS DRAWING IS THE SOLE PROPERTY OF USI's 'PROJECT AMBITION' Team. ANY REPRODUCTION IN PART OR AS A WHOLE WITHOUT THE WRITTEN PERMISSION OF USI's 'PROJECT AMBITION' Team IS PROHIBITED.
DIMENSIONS ARE IN INCHES
TOLERANCES: +/- 0.002
FRACTIONAL: 1/32"
ANGULAR: MACH: 0.5 Deg
TWO PLACE DECIMAL : +/- 0.01"
THREE PLACE DECIMAL : +/- 0.002
MATERIAL 6061 Alloy
FINISH RA: <100
DO NOT SCALE DRAWING
Project Ambition - TurboJet
TITLE: Compressor Diffuser
SIZE A
DWG. NO. Diffuser_Final
REV
SCALE: 1:2
WEIGHT:
SHEET 3 OF 4

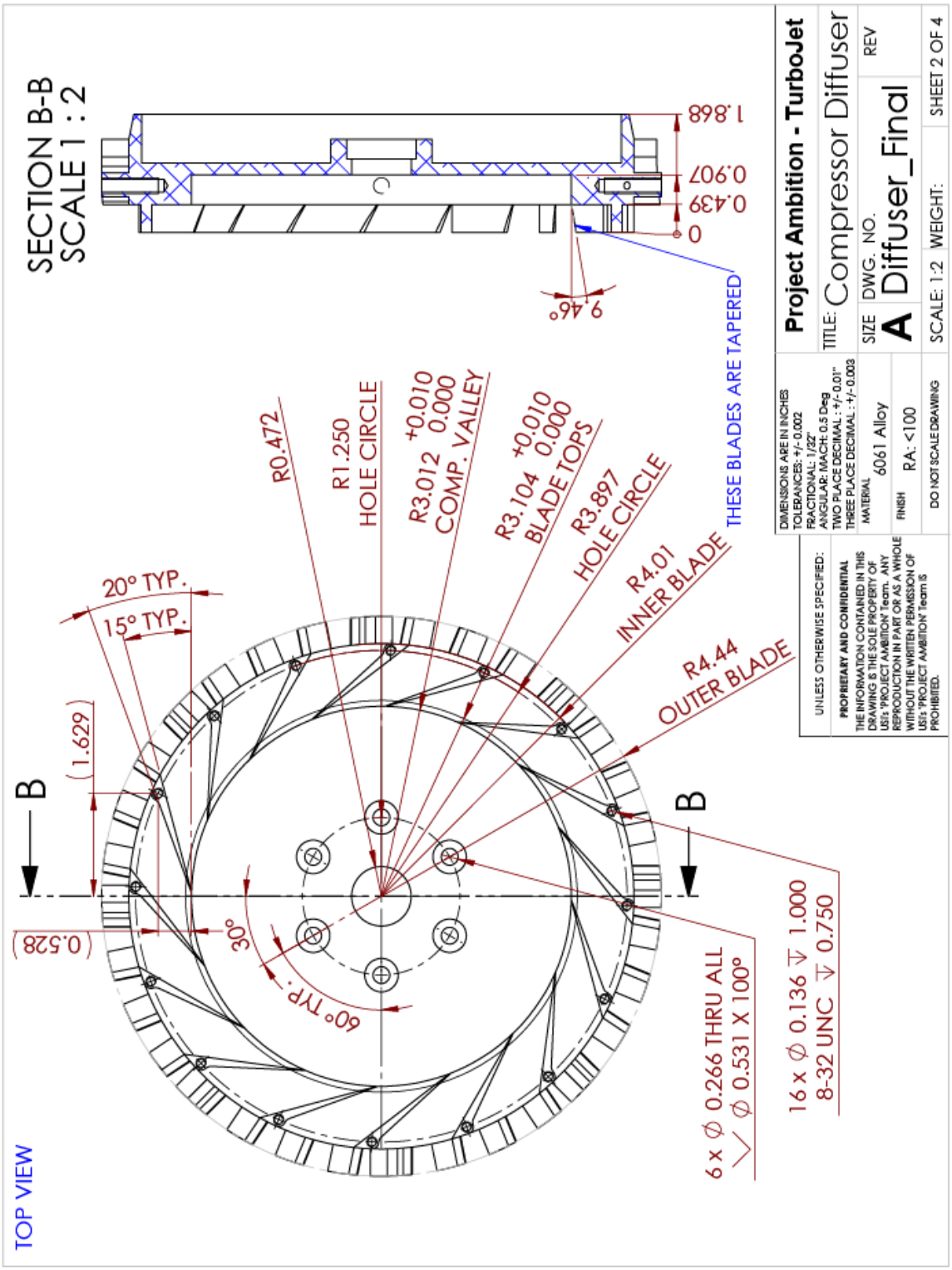
SECTION B-B
SCALE 1 : 2
1.868
0.907
0.439
0
9.46°
THESE BLADES ARE TAPERED
TOP VIEW
B
B
(1.629)
(0.528)
20° TYP.
15° TYP.
30°
60° TYP.
R0.472
R1.250
HOLE CIRCLE
R3.012 +0.010 0.000
COMP. VALLEY
R3.104 +0.010 0.000
BLADE TOPS
R3.897
HOLE CIRCLE
R4.01
INNER BLADE
R4.44
OUTER BLADE
6 x ⌀ 0.266 THRU ALL
⌵ ⌀ 0.531 X 100°
16 x ⌀ 0.136 ⩛ 1.000
8-32 UNC ⩛ 0.750
UNLESS OTHERWISE SPECIFIED:
PROPRIETARY AND CONFIDENTIAL
THE INFORMATION CONTAINED IN THIS DRAWING IS THE SOLE PROPERTY OF <Insert Company Name here>. ANY REPRODUCTION IN PART OR AS A WHOLE WITHOUT THE WRITTEN PERMISSION OF <Insert Company Name here> IS PROHIBITED.
DIMENSIONS ARE IN INCHES
TOLERANCES: +/- 0.002
FRACTIONAL: 1/32"
ANGULAR: MACH: 0.5 Deg
TWO PLACE DECIMAL: +/- 0.01"
THREE PLACE DECIMAL: +/- 0.003
MATERIAL 6061 Alloy
FINISH RA: <100
DO NOT SCALE DRAWING
Project Ambition - TurboJet
TITLE: Compressor Diffuser
SIZE A
DWG. NO. Diffuser_Final
REV
SCALE: 1:2
WEIGHT:
SHEET 2 OF 4

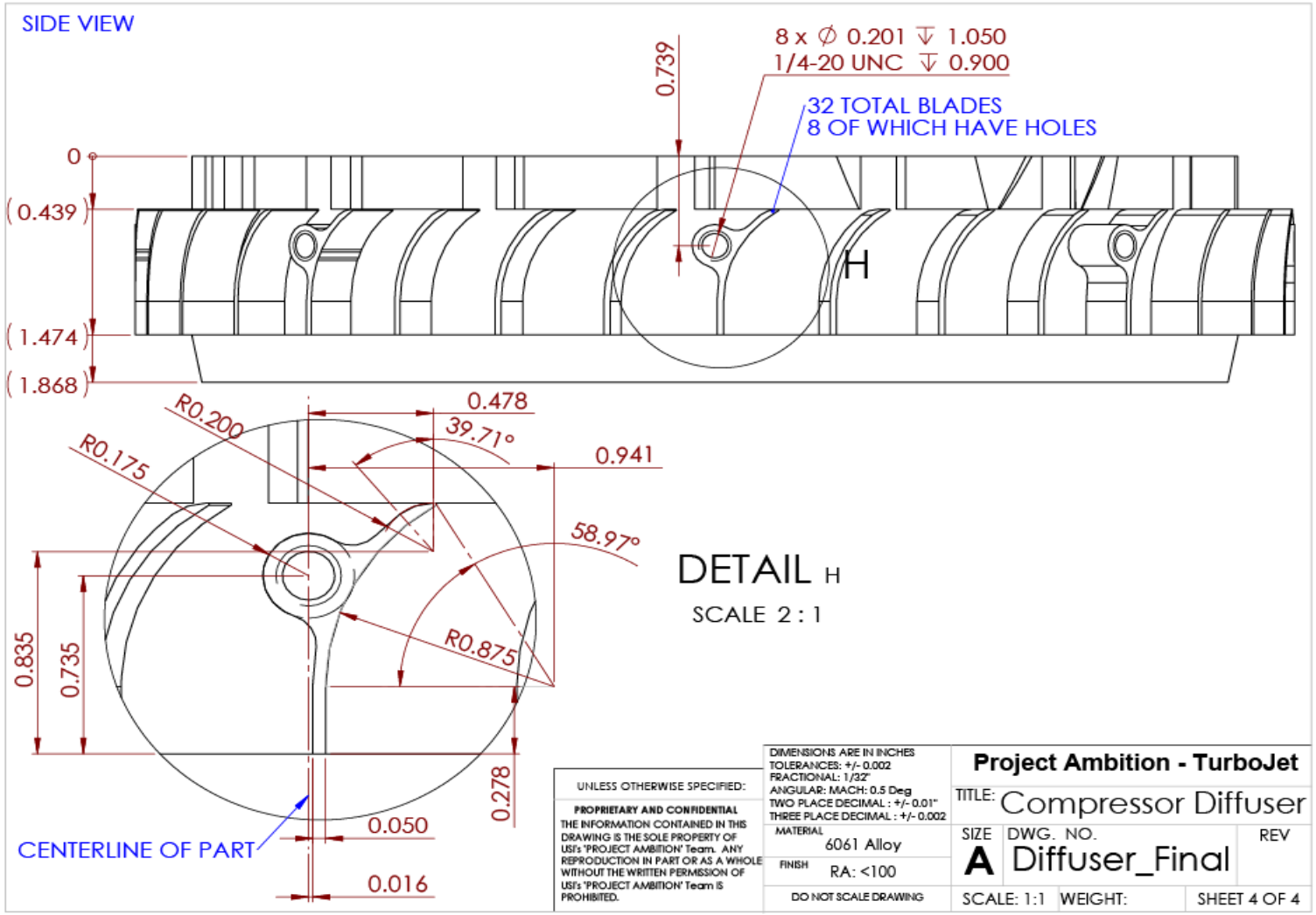
SIDE VIEW
8 x ∅ 0.201 ↧ 1.050
1/4-20 UNC ↧ 0.900
0.739
32 TOTAL BLADES
8 OF WHICH HAVE HOLES
0
0.439
1.474
1.868
H
R0.200
R0.175
0.478
39.71°
0.941
58.97°
R0.875
0.835
0.735
0.278
0.050
0.016
CENTERLINE OF PART
DETAIL H
SCALE 2 : 1
UNLESS OTHERWISE SPECIFIED:
PROPRIETARY AND CONFIDENTIAL
THE INFORMATION CONTAINED IN THIS DRAWING IS THE SOLE PROPERTY OF USI's 'PROJECT AMBITION' Team. ANY REPRODUCTION IN PART OR AS A WHOLE WITHOUT THE WRITTEN PERMISSION OF USI's 'PROJECT AMBITION' Team IS PROHIBITED.
DIMENSIONS ARE IN INCHES
TOLERANCES: +/- 0.002
FRACTIONAL: 1/32"
ANGULAR: MACH: 0.5 Deg
TWO PLACE DECIMAL : +/- 0.01"
THREE PLACE DECIMAL : +/- 0.002
MATERIAL
6061 Alloy
FINISH
RA: <100
DO NOT SCALE DRAWING
Project Ambition - TurboJet
TITLE: Compressor Diffuser
SIZE
A
DWG. NO.
Diffuser_Final
REV
SCALE: 1:1
WEIGHT:
SHEET 4 OF 4

OVERALL DIMENSIONS: REFERENCE ONLY

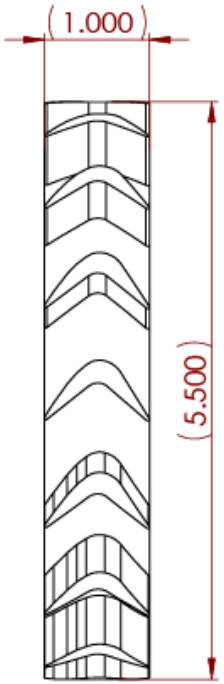

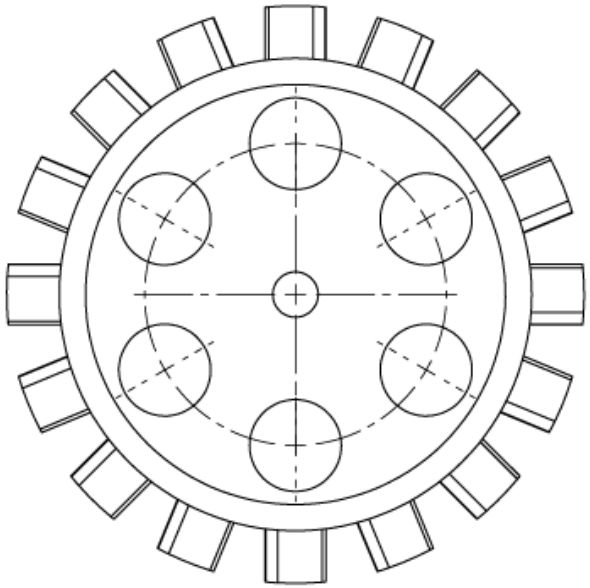

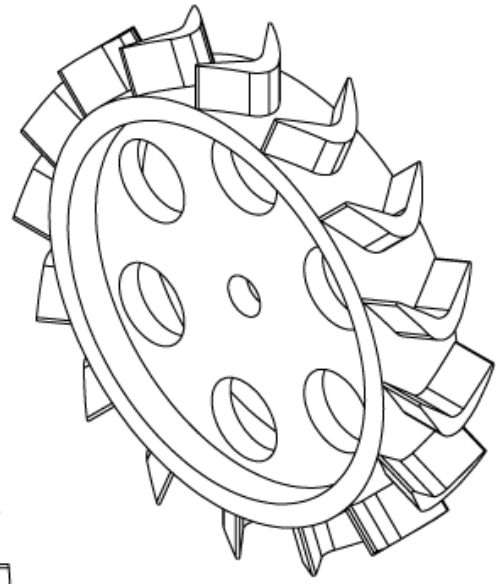

UNLESS OTHERWISE SPECIFIED: **PROPRIETARY AND CONFIDENTIAL** THE INFORMATION CONTAINED IN THIS DRAWING IS THE SOLE PROPERTY OF USI's 'PROJECT AMBITION' Team. ANY REPRODUCTION IN PART OR AS A WHOLE WITHOUT THE WRITTEN PERMISSION OF USI's 'PROJECT AMBITION' Team IS PROHIBITED.	DIMENSIONS ARE IN INCHES TOLERANCES: +/- 0.002 FRACTIONAL: 1/32" ANGULAR: MACH: 0.5 Deg TWO PLACE DECIMAL : +/- 0.01" THREE PLACE DECIMAL : +/- 0.002 MATERIAL: 310 STAINLESS STEEL FINISH: RA: <100 DO NOT SCALE DRAWING	**Project Ambition - TurboJet** TITLE: TURBINE WHEEL SIZE: A DWG. NO.: Turbine REV SCALE: 2:3 WEIGHT: SHEET 1 OF 3

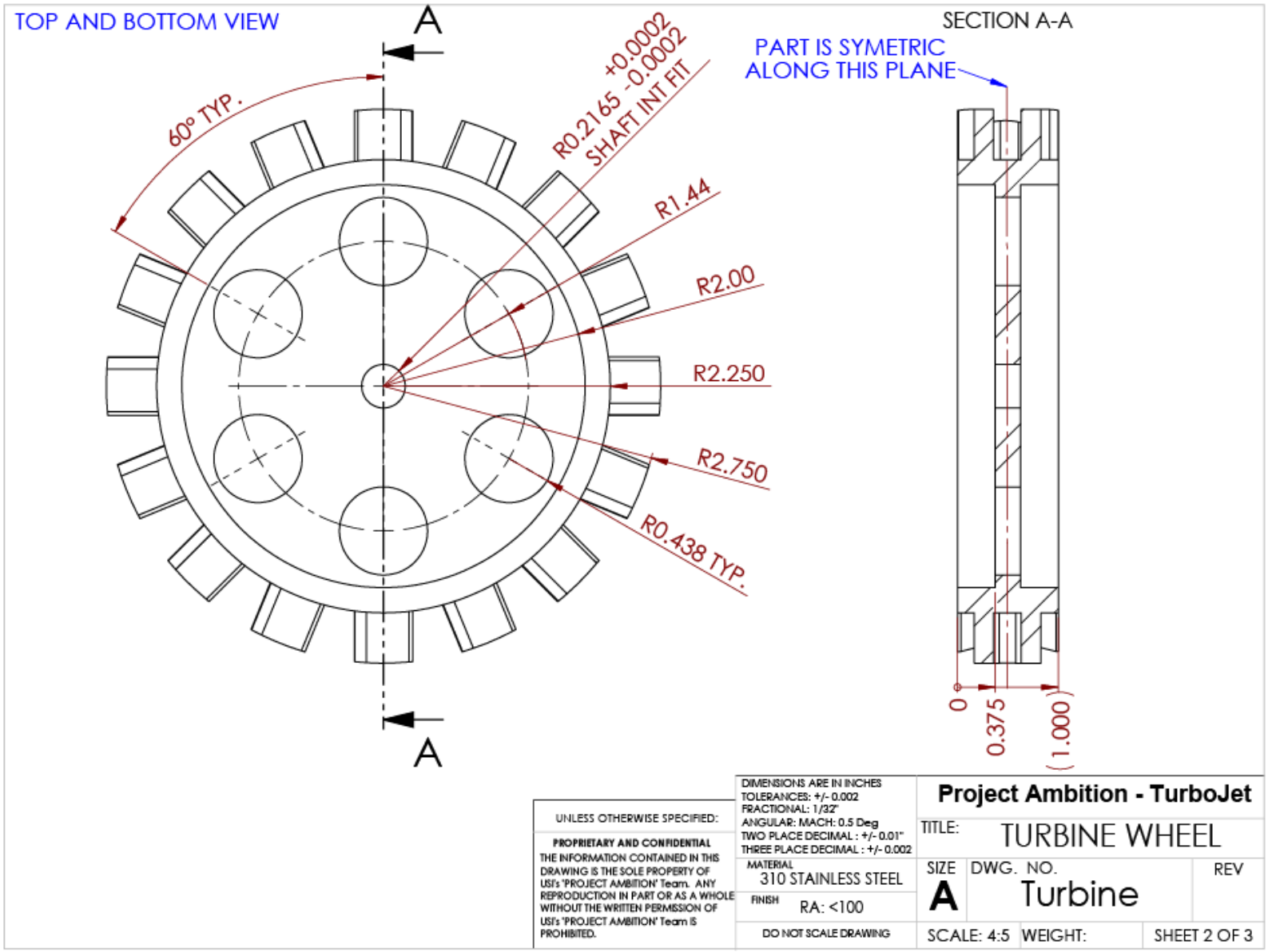
TOP AND BOTTOM VIEW
A
A
60° TYP.
R0.2165 +0.0002 -0.0002
SHAFT INT FIT
R1.44
R2.00
R2.250
R2.750
R0.438 TYP.
SECTION A-A
PART IS SYMETRIC
ALONG THIS PLANE
0
0.375
(1.000)
UNLESS OTHERWISE SPECIFIED:
PROPRIETARY AND CONFIDENTIAL
THE INFORMATION CONTAINED IN THIS DRAWING IS THE SOLE PROPERTY OF USI's 'PROJECT AMBITION' Team. ANY REPRODUCTION IN PART OR AS A WHOLE WITHOUT THE WRITTEN PERMISSION OF USI's 'PROJECT AMBITION' Team IS PROHIBITED.
DIMENSIONS ARE IN INCHES
TOLERANCES: +/- 0.002
FRACTIONAL: 1/32"
ANGULAR: MACH: 0.5 Deg
TWO PLACE DECIMAL : +/- 0.01"
THREE PLACE DECIMAL : +/- 0.002
MATERIAL
310 STAINLESS STEEL
FINISH
RA: <100
DO NOT SCALE DRAWING
Project Ambition - TurboJet
TITLE:
TURBINE WHEEL
SIZE
A
DWG. NO.
Turbine
REV
SCALE: 4:5
WEIGHT:
SHEET 2 OF 3

BLADE VIEW

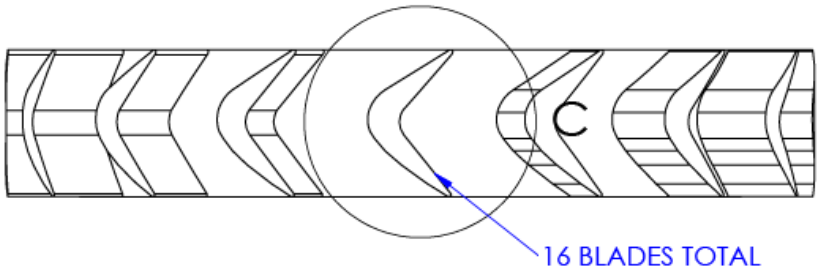

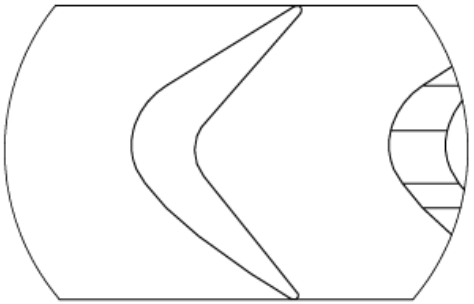

DETAIL C

SCALE 2 : 1

UNLESS OTHERWISE SPECIFIED:

PROPRIETARY AND CONFIDENTIAL

THE INFORMATION CONTAINED IN THIS DRAWING IS THE SOLE PROPERTY OF USI's 'PROJECT AMBITION' Team. ANY REPRODUCTION IN PART OR AS A WHOLE WITHOUT THE WRITTEN PERMISSION OF USI's 'PROJECT AMBITION' Team IS PROHIBITED.

DIMENSIONS ARE IN INCHES
TOLERANCES: +/- 0.002
FRACTIONAL: 1/32"
ANGULAR: MACH: 0.5 Deg
TWO PLACE DECIMAL : +/- 0.01"
THREE PLACE DECIMAL : +/- 0.002

MATERIAL: 310 STAINLESS STEEL

FINISH: RA: <100

DO NOT SCALE DRAWING

Project Ambition - TurboJet

TITLE: TURBINE WHEEL

SIZE	DWG. NO.	REV
A	Turbine	

SCALE: 1:1	WEIGHT:	SHEET 3 OF 3

OVERALL DIMENSIONS: REFERENCE ONLY

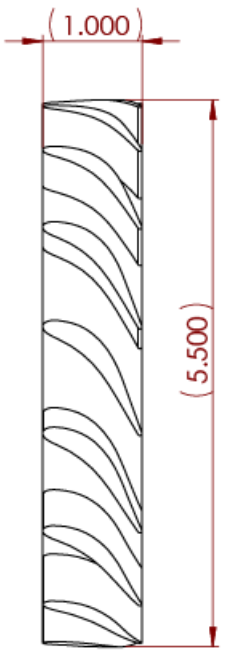

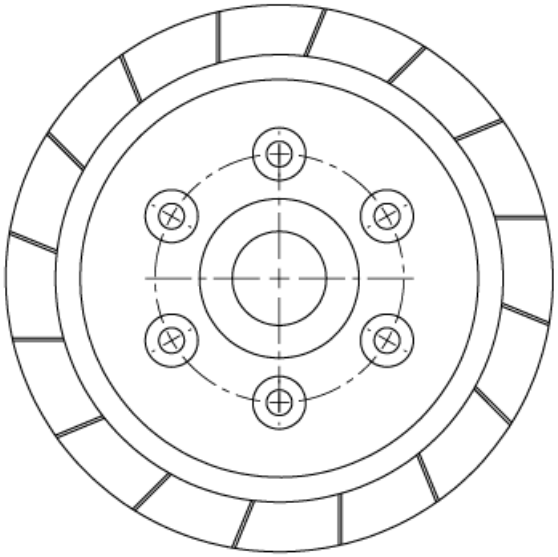

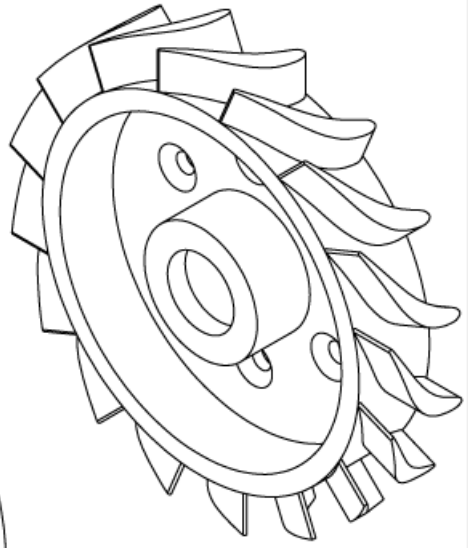

UNLESS OTHERWISE SPECIFIED:	DIMENSIONS ARE IN INCHES TOLERANCES: +/- 0.002 FRACTIONAL: 1/32" ANGULAR: MACH: 0.5 Deg TWO PLACE DECIMAL : +/- 0.01" THREE PLACE DECIMAL : +/- 0.002	**Project Ambition - TurboJet**	
PROPRIETARY AND CONFIDENTIAL THE INFORMATION CONTAINED IN THIS DRAWING IS THE SOLE PROPERTY OF USI's 'PROJECT AMBITION' Team. ANY REPRODUCTION IN PART OR AS A WHOLE WITHOUT THE WRITTEN PERMISSION OF USI's 'PROJECT AMBITION' Team IS PROHIBITED.	MATERIAL 310 STAINLESS STEEL	TITLE: Stator	
	FINISH RA: <100	SIZE **A** DWG. NO. Stator	REV
	DO NOT SCALE DRAWING	SCALE: 2:3 WEIGHT:	SHEET 1 OF 4

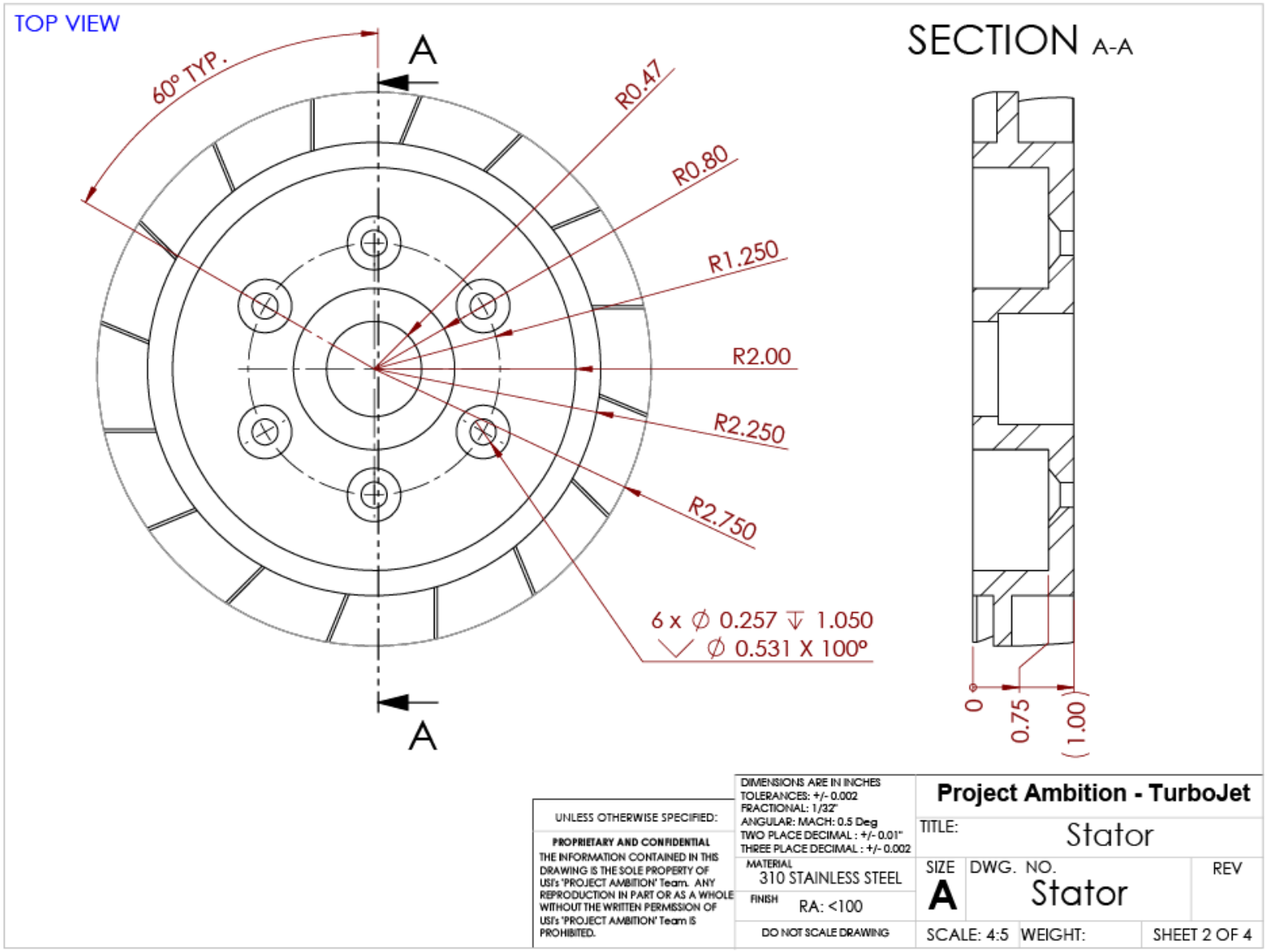
TOP VIEW
60° TYP.
A
A
R0.47
R0.80
R1.250
R2.00
R2.250
R2.750
6 x ∅ 0.257 ↧ 1.050
⌵ ∅ 0.531 X 100°
SECTION A-A
0
0.75
(1.00)
UNLESS OTHERWISE SPECIFIED:
PROPRIETARY AND CONFIDENTIAL
THE INFORMATION CONTAINED IN THIS DRAWING IS THE SOLE PROPERTY OF USI's 'PROJECT AMBITION' Team. ANY REPRODUCTION IN PART OR AS A WHOLE WITHOUT THE WRITTEN PERMISSION OF USI's 'PROJECT AMBITION' Team IS PROHIBITED.
DIMENSIONS ARE IN INCHES
TOLERANCES: +/- 0.002
FRACTIONAL: 1/32"
ANGULAR: MACH: 0.5 Deg
TWO PLACE DECIMAL : +/- 0.01"
THREE PLACE DECIMAL : +/- 0.002
MATERIAL
310 STAINLESS STEEL
FINISH
RA: <100
DO NOT SCALE DRAWING
Project Ambition - TurboJet
TITLE:
Stator
SIZE
A
DWG. NO.
Stator
REV
SCALE: 4:5
WEIGHT:
SHEET 2 OF 4

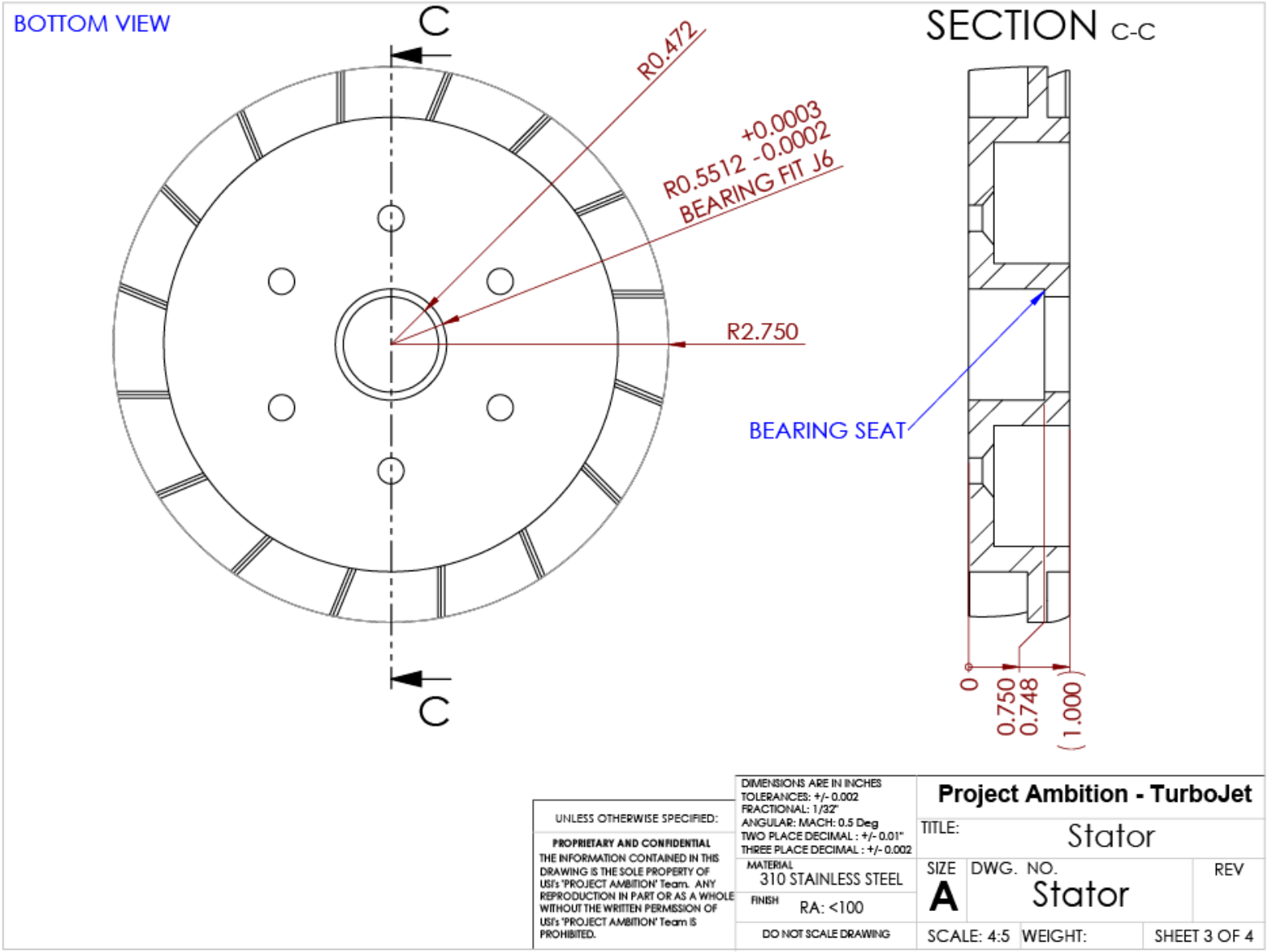
BOTTOM VIEW
C
C
R0.472
+0.0003
R0.5512 -0.0002
BEARING FIT J6
R2.750
SECTION C-C
BEARING SEAT
0
0.750
0.748
(1.000)
UNLESS OTHERWISE SPECIFIED:
PROPRIETARY AND CONFIDENTIAL
THE INFORMATION CONTAINED IN THIS DRAWING IS THE SOLE PROPERTY OF USI's 'PROJECT AMBITION' Team. ANY REPRODUCTION IN PART OR AS A WHOLE WITHOUT THE WRITTEN PERMISSION OF USI's 'PROJECT AMBITION' Team IS PROHIBITED.
DIMENSIONS ARE IN INCHES
TOLERANCES: +/- 0.002
FRACTIONAL: 1/32"
ANGULAR: MACH: 0.5 Deg
TWO PLACE DECIMAL : +/- 0.01"
THREE PLACE DECIMAL : +/- 0.002
MATERIAL
310 STAINLESS STEEL
FINISH
RA: <100
DO NOT SCALE DRAWING
Project Ambition - TurboJet
TITLE:
Stator
SIZE
A
DWG. NO.
Stator
REV
SCALE: 4:5
WEIGHT:
SHEET 3 OF 4

BOTTOM VIEW

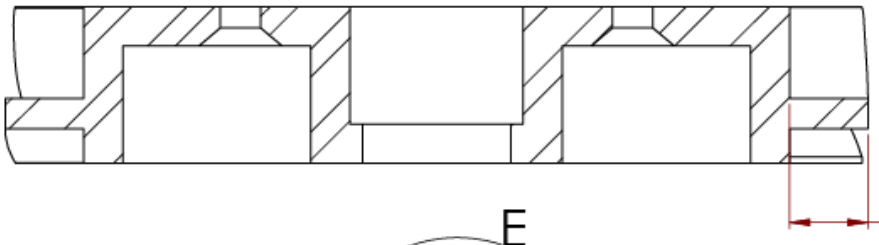

SECTION E-E

0.500

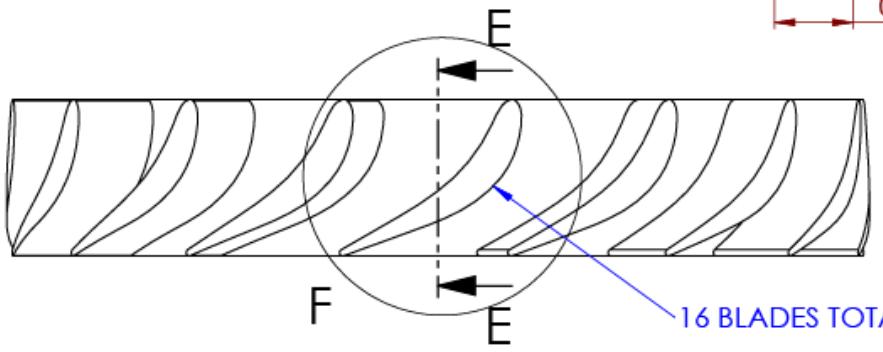

CENTERLINE

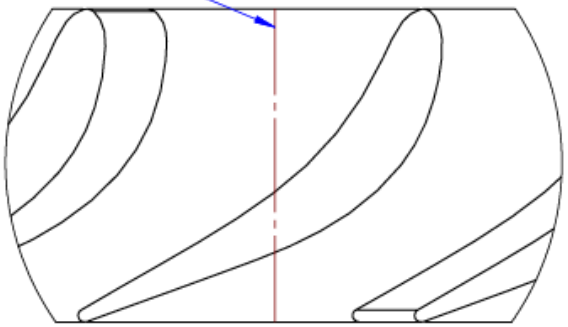

DETAIL F

SCALE 2 : 1

UNLESS OTHERWISE SPECIFIED:	DIMENSIONS ARE IN INCHES TOLERANCES: +/- 0.002 FRACTIONAL: 1/32" ANGULAR: MACH: 0.5 Deg TWO PLACE DECIMAL : +/- 0.01" THREE PLACE DECIMAL : +/- 0.002	**Project Ambition - TurboJet**	
PROPRIETARY AND CONFIDENTIAL THE INFORMATION CONTAINED IN THIS DRAWING IS THE SOLE PROPERTY OF USI's 'PROJECT AMBITION' Team. ANY REPRODUCTION IN PART OR AS A WHOLE WITHOUT THE WRITTEN PERMISSION OF USI's 'PROJECT AMBITION' Team IS PROHIBITED.	MATERIAL 310 STAINLESS STEEL	TITLE: Stator	
	FINISH RA: <100	SIZE A	DWG. NO. Stator
	DO NOT SCALE DRAWING	SCALE: 1:1	WEIGHT:
		SHEET 4 OF 4	REV

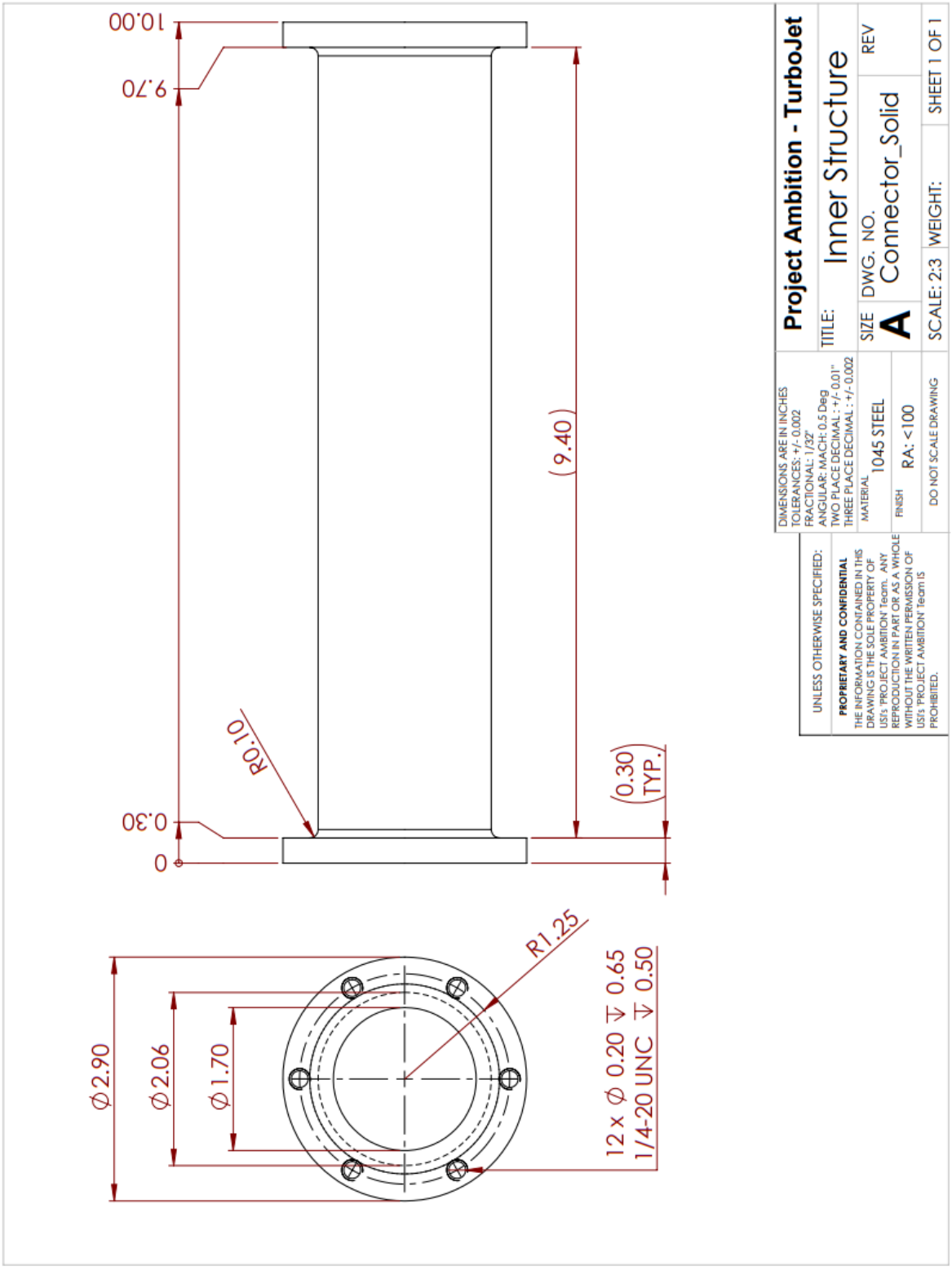
10.00
9.70
(9.40)
R0.10
0.30
0
(0.30 TYP.)
R1.25
Ø2.90
Ø2.06
Ø1.70
12 x Ø 0.20 ↧ 0.65
1/4-20 UNC ↧ 0.50
DIMENSIONS ARE IN INCHES
TOLERANCES: +/- 0.002
FRACTIONAL: 1/32"
ANGULAR: MACH: 0.5 Deg
TWO PLACE DECIMAL: +/- 0.01"
THREE PLACE DECIMAL: +/- 0.002
UNLESS OTHERWISE SPECIFIED:
PROPRIETARY AND CONFIDENTIAL
THE INFORMATION CONTAINED IN THIS DRAWING IS THE SOLE PROPERTY OF USI's 'PROJECT AMBITION' Team. ANY REPRODUCTION IN PART OR AS A WHOLE WITHOUT THE WRITTEN PERMISSION OF USI's 'PROJECT AMBITION' Team IS PROHIBITED.
MATERIAL
1045 STEEL
FINISH
RA: <100
DO NOT SCALE DRAWING
Project Ambition - TurboJet
TITLE:
Inner Structure
SIZE
A
DWG. NO.
Connector_Solid
REV
SCALE: 2:3
WEIGHT:
SHEET 1 OF 1

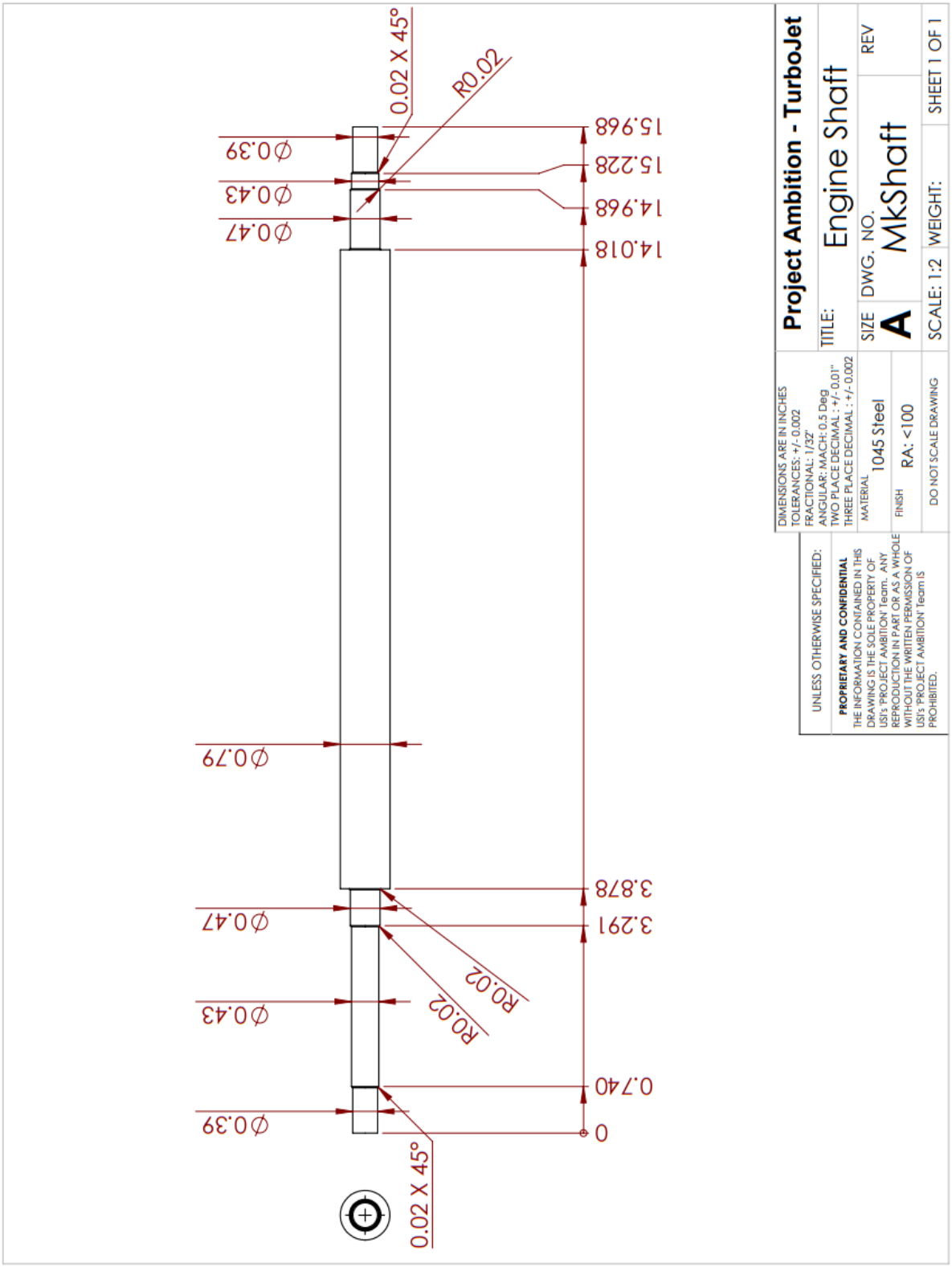
Project Ambition - TurboJet
TITLE: Engine Shaft
SIZE A
DWG. NO. MkShaft
REV
SCALE: 1:2
WEIGHT:
SHEET 1 OF 1
DIMENSIONS ARE IN INCHES
TOLERANCES: +/- 0.002
FRACTIONAL: 1/32"
ANGULAR: MACH: 0.5 Deg
TWO PLACE DECIMAL : +/- 0.01"
THREE PLACE DECIMAL : +/- 0.002
MATERIAL 1045 Steel
FINISH RA: <100
DO NOT SCALE DRAWING
UNLESS OTHERWISE SPECIFIED:
PROPRIETARY AND CONFIDENTIAL
THE INFORMATION CONTAINED IN THIS DRAWING IS THE SOLE PROPERTY OF USI's 'PROJECT AMBITION' Team. ANY REPRODUCTION IN PART OR AS A WHOLE WITHOUT THE WRITTEN PERMISSION OF USI's 'PROJECT AMBITION' Team IS PROHIBITED.
0.02 X 45°
R0.02
15.968
15.228
14.968
14.018
3.878
3.291
0.740
0
Ø0.39
Ø0.43
Ø0.47
Ø0.79
R0.02
R0.02
Ø0.47
Ø0.43
Ø0.39
0.02 X 45°